ICSSC TR-8

DEPARTMENT OF THE INTERIOR
U.S. GEOLOGICAL SURVEY

Tsunamis: Hazard Definition and Effects on Facilities

A DRAFT TECHNICAL REPORT OF SUBCOMMITTEE 3,
"EVALUATION OF SITE HAZARDS,"
A PART OF THE INTERAGENCY COMMITTEE ON SEISMIC SAFETY IN CONSTRUCTION

SUBCOMMITTEE CHAIRMAN - WALTER W. HAYS
U.S. GEOLOGICAL SURVEY
RESTON, VIRGINIA 22092

Prepared for use by:
Interagency Committee on Seismic Safety in Construction (ICSSC)

OPEN-FILE REPORT 85-533

(ICSSC TR-8)

COMPILED BY
JOYCE A. COSTELLO

Reston, Virginia

1985

FOREWORD

This draft technical report, "Tsunamis--Hazard Definition and Effects on Facilities" was developed within Subcommittee 3, Evaluation of Site Hazards, a part of the Interagency Committee on Seismic Safety in Construction (ICSSC). The report was started by former Subcommittee 8, "Tsunamis and Flood Waves," chaired by James Houston. When the ICSSC was reorganized in 1983, Subcommittee 3 took on the responsibility of tsunamis. This is the fifth report of Subcommittee 3; the other four addressed surface faulting, earthquake-induced ground failure, design of large dams, and the technical issues that arise in the evaluation of earthquake hazards. The membership of the two Subcommittees during the preparation of this report are given below with members of Subcommittee 8 noted with an asterisk:

S. T. Algermissen	U.S. Geological Survey
*Fred E. Canfield	Army Corps of Engineers
*Frank P. Dall	Department of Housing and Urban Development
John M. Ferritto	Naval Civil Engineering Laboratory
*John R. Filson	U.S. Geological Survey
*Myron Flieged	Nuclear Regulatory Commission
*John French	U.S. Coast Guard
*Michael Gaus	National Science Foundation
Julius G. Hansen	Department of Labor
Walter W. Hays	U.S. Geological Survey
*Daniel S. Haynosch	Department of Navy
Larkin S. Hobbs	Veterans Administration
*James R. Houston	Army Corps of Engineers
Guan S. Hsiung	General Services Administration
D. Earl Jones, Jr.	Department of Housing and Urban Development
*Mike W. Kim	Department of Navy
Henry F. Kravitz	Department of Labor
Ellis L. Krinitzsky	Army Corps of Engineers
Richard D. McConnell	Veterans Administration
James F. Lander	National Oceanic and Atmospheric Administration
*Harold G. Loomis	National Oceanic and Atmospheric Administration
Peter V. Patterson	Department of Agriculture
David M. Perkins	U.S. Geological Survey
Leon Reiter	Nuclear Regulatory Commission
Lawrence Salomone	National Bureau of Standards
*M. G. Spaeth	National Oceanic and Atmospheric Administration
Kuppusmay Thirumalai	National Science Foundation
*Frank Tsai	Federal Emergency Management Agency
Davis E. White	Department of Housing and Urban Development

Subcommittee 3 has recommended that this draft technical report be submitted to all concerned agencies with the request that they test its implementation through use in planning, design, contract administration, and quality control, either on a trial or real basis during 1985 and 1986. Following the trial implementation, the Subcommittee 3 plans to review the draft report, revise it as necessary, and then recommend its adoption by the Interagency Committee as a manual of standard practice for use in developing design and construction standards against tsunami, seiche, and flood wave threats. Comments on this draft are welcomed and should be forwarded to the Chairman, Walter W. Hays.

PUBLICATIONS OF SUBCOMMITTEE 3

INTERAGENCY COMMITTEE ON

SEISMIC SAFETY IN CONSTRUCTION

M. G. Bonilla, 1982, Evaluation of Potential Surface Faulting and Other Tectonic Deformation, U.S. Geological Survey Open-file Report 82-732 (ICSSC TR-2).

John M. Ferritto, 1982, Evaluation of Earthquake-Induced Ground Failure, U.S. Geological Survey Open-file Report 82-880 (ICSSC TR-3).

E. L. Krinitzsky and W. F. Marcuson III, 1983, Considerations in Selecting Earthquake Motions for the Engineering Design of Large Dams, U.S. Geological Survey Open-file Report 83-636 (ICSSC TR-4).

Walter W. Hays, 1985, An Introduction to Technical Issues in the Evaluation of Seismic Hazards for Earthquake-resistant Design, U.S. Geological Survey Open-file Report 85-371 (ICSSC TR-6).

CONTENTS

PAGE

FIGURES

PAGE

TABLES

ABSTRACT

This report describes the tsunami threat in the United States and its territories and possessions and the kinds of physical effects that a tsunami can have on facilities. The report is intended for use by engineers who require the forcing function produced by these hydrodynamic phenomena for structural design purposes and by emergency managers and planners who desire to reduce the potential risk that these phenomena present to life and property. Chapter 1 presents an account of the historical tsunami hazard in the United States and describes important physical characteristics of tsunamis. Numerical and hydraulic scale model methods are discussed in the context of their use to simulate tsunami generation, deep-ocean propagation, interaction with islands or continental coastlines, and land inundation, and, most importantly, to evaluate the tsunami hazard in the United States. Tsunami hazard maps for the United States are included in Chapter 1.

Chapter 2 describes the effects of tsunamis on structures and facilities in the nearshore region. The water level depicted in the hazard maps of Chapter 1 can be used with force formulas presented in Chapter 2 to determine tsunami forces on structures. Examples are included to illustrate the concepts.

1. TSUNAMI HAZARD

1.1 Tsunamis

Cox (ref. 1) defined a tsunami as "a train of progressive long waves generated in the ocean by an impulsive disturbance." His definition of tsunami includes waves generated by abrupt bottom diplacement (caused, for example, by earthquakes), submarine or shoreline landslides, and volcanic or nuclear explosions.

Tsunamis can produce great destruction and loss of life. For example, the great Hoei Tokaido-Nankaido tsunami of Japan killed 30,000 people in 1707. In 1868, the great Peru tsunami caused 25,000 deaths, The great Meiji Sanriku tsunami of 1896 killed 27,122 persons in Japan and washed away over 10,000 houses (ref. 1).

Tsunamis have taken many lives in the United States, with more people having died since the end of World War II as a result of tsunamis than as a result of the direct effects of earthquakes. For example, the great Aleutian tsunami of 1946 killed 173 people in Hawaii and produced $26 million in property damage in the city of Hilo, Hawaii. The 1960 Chilean tsunami killed 61 people in Hawaii and caused $23 million in property damage (ref. 2). The most recent major tsunami to affect the United States, the 1964 Alaskan tsunami, killed 107 people in Alaska, 4 in Oregon, and 11 in Crescent City, California, and caused over $100 million in damage on the west coast of North America (ref. 3).

A major difference in the destructive characteristics of earthquakes and tsunamis is that earthquakes are locally destructive; whereas, tsunamis are destructive locally as well as at locations distant from the area of tsunami generation. For example, the 1960 Chilean earthquake caused destruction in Chile, but was unnoticed in the United States except for the recordings of seismographs. However, the tsunami generated off the coast of Chile by this earthquake not only killed more than 300 people in Chile and caused widespread devastation, but it also killed 61 people in Hawaii and produced widespread destruction in distant Japan where 199 people were killed, 5000 structures wrecked or washed away, and more than 7500 boats wrecked or lost (ref. 1).

Tsunamis are principally generated by undersea tectonic displacements produced by earthquakes of magnitudes greater than 6.5 on the Richter scale. The typical height of a tsunami in the deep ocean is less than a foot, and the wave period is 5 minutes to several hours. Tsunamis travel at the shallow-water wave velocity equal to the square root of the acceleration due to gravity times the water depth even in the deepest oceans because of their very long wavelengths. This speed of propagation can be in excess of 500 mph in the deep ocean.

When tsunamis approach a coastal region where the water depth decreases rapidly, wave refraction, shoaling, and bay or harbor resonance may result in significantly increased wave heights. The great period and wavelength of tsunami waves preclude their dissipating energy as a breaking surf; instead, they are apt to appear as rapidly rising water levels and only occasionally as bores.

1.1.1 Historical Tsunami Hazard in the United States

1.1.1.1 Atlantic and Gulf Coasts

The seismic activity of the Atlantic Ocean region is relatively low. In general, coasts bordering the Atlantic Ocean are not paralleled by lines of tectonic, seismic, or volcanic activity. They are rarely associated with structural discontinuities like those along the circum-Pacific seismic belt where about 80 percent of the world's earthquakes occur. Only about 10 percent of all reported tsunamis have originated in the Atlantic Ocean region.

The probability of significant water level elevations on the Atlantic or Gulf Coast of the United States produced by distantly generated tsunamis is thought to be very small. With the exception of the Portugal-Morocco region, the eartern Atlantic has a very low level of seismic activity. For example, the largest known shock for a thousand years in the area of Great Britain occurred in the North Sea in 1931 and had a magnitude of only 5-1/2 (4). The Atlantic Coast of France and all of the eastern coast of Africa south of Morocco have a similar low level of seismic activity. Large earthquakes do occur in certain areas of the midoceanic ridges. However, earthquakes that occur on crests of the mid-Atlantic ridge not associated with known fracture zones show either normal faulting (the tension axis being horizontal and perpendicular to the local strike of the ridge) or strike-slip motion of transform faulting. Earthquakes on the fracture zones of the mid-Atlantic ridge also are characterized by a predominance of strike-slip motion (ref. 5). Large tsunamis, however, are generated by vertical ground motion (ref. 6), and only small amounts of vertical motion may accompany strike-slip motion or normal

faulting with a horizontal tension axis. Consequently, although there have been many local tsunamis in the Azores Islands of the mid-Atlantic ridge, earthquakes there and elsewhere along the mid-Atlantic ridge have never produced a tsunami reported on any Atlantic coastline.

Large earthquakes have occurred in the Portugal-Morocco region (1356, 1531, 1597, 1722, 1755, 1761, 1773, 1926, 1960). The largest known Atlantic earthquake, and indeed one of the largest known earthquakes of historical times, occurred off the coast of Portugal on November 1, 1755. This earthquake generated the most destructive tsunami ever reported in the Atlantic. Tsunamis generated by this earthquake were reported in the West Indies. The sea rose 12 ft several times at Antigua, and every 5 minutes afterwards for 3 hours it rose 5 feet. The sea retired so far at St. Martin Island that a sloop riding at anchor in 15 feet of water was laid dry on her broadside. On the island of Saba, the sea rose 21 feet. At Martinique and most of the French Islands, the sea overflowed the lowland, returning quickly to its former limits (ref. 7). Reid (ref. 8), however, reported that there is little evidence that tsunamis generated by the 1755 earthquake were noticed on the coasts of the United States. The orientation of the fault along which this earthquake occurred is such that waves generated by a seismic event would be directed toward the West Indies and not the United States. Furthermore, the great continental shelf off the Atlantic and Gulf Coasts of the United States is likely to dissipate much of the energy of a tsunami. Part of the eastern coastline of Florida has a narrow continental shelf and is relatively close to the West Indies. However, the shelf off the Bahamas Islands probably shelters this area.

In the western Atlantic, the main tsunamigenic region is the subduction zone along the arc of the West Indies Islands. The many intense earthquakes of this area have had relatively short fault lengths and, therefore, small source areas for tsunami generation. There have been no reports of tsunamis generated in this area producing significant runup on any distant coast. The largest tsunami known to have been recorded on the Atlantic Coast of the United States was generated by an earthquake off the Burin Peninsula of Newfoundland on November 18, 1929. A tsunami from this Grand Banks earthquake moved up several inlets and obtained a maximum height of 50 feet. Several villiages were destroyed. Tide gages on the coast of New Jersey recorded the tsunami with a 1 feet elevation at Atlantic City, New Jersey.

The possibility of significant locally generated tsunamis on the Atlantic or the Gulf Coast of the United States appears to be remote. These coastlines do not have structural discontinuities associated with seismic activity. Crustal structures have been followed by geophysical and geological methods and appear to dip far under the ocean bottom without any break (10). Only one large earthquake has occurred on this coast in historical times. The Charleston, South Carolina, earthquake of 1886, which had an estimated magnitude of 7.5 was one of the largest earthquakes in the United States. There has been no earthquake in the Atlantic coastal plain of the United States having the same magnitude, before or since (ref. 9). Despite the large size of the Charleston earthquake, no tsunami was generated. McKinley (ref. 11) reported that "Except in the rivers the wave motion was not observed to have communicated to the water". Thus, the Charleston earthquake probably exhibited little of the vertical motion required to generate a significant tsunami. The complete lack of tsunamigenic activity on the eastern coast of the United States is probably

a result of not only a low level of seismic activity but also the lack of vertical motion.

The tsunami threat from both locally and distantly generated tsunamis is very small on the Atlantic and Gulf Coasts of the United States and, undoubtedly, less than the threat from hurricane or storms surges. However, this possible threat cannot be neglected when hazards are investigated for critical facilities such as nuclear power plants. For such a case, the effects of a tsunami, such as that generated in Portugal in 1755 or the occurrence of a locally generated tsunami such as the 1929 tsunami generated off the Burin Peninsula of Newfoundland, must be considered.

1.1.1.2 Puerto Rico and the Virgin Islands

Puerto Rico and the Virgin Islands lie along the subduction zone of the Lesser Antilles that forms the eastern boundary of the Caribbean tectonic plate. Earthquakes along this subduction zone generate important local tsunamis. Tsunamis were generated near the Virgin Islands in 1867 and 1868 (9). The 1867 tsunami swept the harbors of St. Thomas and St. Croix. A wall of water 20 feet high entered these harbors and broke over the lower parts of the towns. At St. Thomas, the water moved inland a distance of 250 feet. The tsunami also was large on adjacent islands and the east coast of Puerto Rico. The Alcalde of Yabucoa (southeastern Puerto Rico) reported that the sea retreated about 150 yards, then returned, and advanced an equal distance inland. The wave was noted as far as Fajardo (which is 20 miles to the northeast from the Alcalde of Yabucoa) and as far as 40 to 60 miles along the southern shore from the Alcalde of Yabucoa (ref. 12).

An earthquake and resulting tsunami in November 1918 killed 116 people in Puerto Rico and produced damage reported in excess of $4 million. During the tsunami, the ocean first withdrew exposing reefs and stretches of sea bottom that had not been visible before during the lowest tides. The water then returned reaching heights that were greatest near the northwest corner of Puerto Rico. At Point Borinquen, the tsunami reached an elevation of 15 feet, Near Point Agujereada, several hundred palm trees were uprooted by waves from 18 to 20 feet high. At Aguadilla, waves with heights from 8 to 11 feet were reported. The Columbus Monument, about 2-1/2 miles southwest of Aguadilla, was thrown down by waves at least 13 feet in height, and rectangular blocks of limestone weighing over a ton were washed inland distances as great as 250 feet. Heights of 4 feet were reported at Mayaguez, and heights of 3 feet at El Boqueron. The tsunami was noticeable at Ponce, Isabela, and Arecibo, but not at San Juan. Elevations of 13 feet were reported on the west coast of Mona Island (ref. 13).

The hazard in Puerto Rico and the Virgin Islands from distantly generated tsunamis is likely to be less than the hazard from locally generated tsunamis or hurricane surges. Houston et al. (ref. 14) demonstrated that a very large earthquake in the Portugal area similar to that of the 1755 earthquake will not produce a water level elevation in Puerto Rico greater than the elevations expected from locally generated tsunamis or hurricane surges.

1.1.1.3 Hawaiian Islands

As a result of their central location in the Pacific Ocean (where approximately 90 percent of all recorded tsunamis have occurred), the Hawaiian Islands have a history of destructive tsunamis. The earliest recorded tsunami in the Hawaiian Islands was the 1819 tsunami that was generated in Chile. Over 100 tsunamis have been recorded in the Hawaiian Islands, and 16 of these tsunamis have produced significant damage. Pararas-Carayannis (ref. 2) compiled a detailed catalog of historical observations of tsunamis in the Hawaiian Islands. Several corrections to the descriptive data and reported events in this catalog have been noted by Cox and Morgan (ref. 15). The distantly generated tsunamis that have produced destruction in the Hawaiian Islands have originated from the Aleutian Islands, Chile, the Kamchatka Peninsula of the Soviet Union, and Japan. More than one-half of all recorded tsunamis in the Hawaiian Islands were generated in the Kuril-Kamchatka-Aleutian regions of the north and northwestern Pacific, and one fourth were generated along the western coast of South America. Tsunamis generated in the Philippines, Indonesia, the New Hebrides, and the Tonga-Kermadec island arcs have been recorded in the Hawaiian Islands, but they have not been damaging.

Locally generated tsunamis also have produced destruction in the Hawaiian Islands. The 1868 tsunami that was generated on the southeastern coast of the big island of Hawaii produced severe destruction on the coast, Runup elevations perhaps as great as 60 feet were reported during this tsunami. A tsunami generated on November 29, 1975, along the same southeastern coast of the island of Hawaii, produced runup elevations as great as 45 feet. Loomis (ref. 16) presented a detailed description of the 1975 tsunami. Cox and

Morgan (ref. 15) compiled a detailed description of locally generated tsunamis in the Hawaiian Islands.

The tsunami hazard in the Hawaiian Islands is not uniform. For example, elevations are generally greater on the northern side of these islands as a result of the many tsunamis generated in the Kuril-Aleutian region. Runup elevations on a single island during a tsunami also may be large at one location and small at another, even at locations that are separated by short distances. Sometimes the reasons for these variations are known. For example, the extensive reefs in Kaneohe Bay on the island of Oahu protect the bay from tsunamis by strongly reflecting or dissipating energy. Often the reasons for these variations are not apparent as a result of the complex interactions that occur. Houston et al. (ref. 17) made predictions of elevations based upon historical data and numerical model calculations for the Hawaiian Islands. These predictions are discussed in Chapter IV.

1.1.1.4 Alaska

The Pacific and North American tectonic plates collide along the subduction zone of the Aleutian-Alaskan Trench. Boundaries between tectonic plates are highly seismic with almost 99 percent of all earthquakes occurring along these boundaries (ref. 18). The great seismicity of the region and vertical motions associated with the subduction zone make the Aleutian-Alaskan region highly tsunamigenic. The earliest recorded tsunami in this region occurred in 1788. Four major tsunamis have been generated since 1946. The 1946 tsunami was generated in the eastern Aleutian Islands, the 1957 tsunami in the central

Aleutian Islands, the 1964 tsunami in the Gulf of Alaska, and the 1965 tsunami in the western Aleutian Islands.

Figure 1 shows a map of Alaskan localities that have experienced tsunamis. These locations are concentrated along the boundary of the Pacific and North American plates. The remainder of Alaska has not had a reported tsunami. However, this region has a very low population density, and reporting may be quite poor. Cox and Pararas-Carayannis (ref. 19) published a catalog of reported tsunamis in Alaska. Locally generated tsunamis dominate the catalog.

The 1964 Alaskan tsunami demonstrated the tremendous destructive power of major locally generated tsunamis in Alaska. This tsunami produced over $80 million in damage and killed 107 people (ref. 3). In addition to the waves generated by the large-scale tectonic displacement, large waves were generated in many areas by submarine slides of thick sediments. The 1964 Alaskan tsunami is discussed in great detail in a report prepared by the National Academy of Sciences (ref. 20).

1.1.1.5 West Coast of the Continental United States

The hazard on the west coast of the United States due to distantly generated tsunamis has been demonstrated by tsunami activity since the end of World War II. For example, the 1946 Aleutian tsunami produced elevations (combined tsunami and astronomical tide) as great as 15 feet above mean lower low water (mllw) at Half Moon Bay, California; 13.4 feet above mllw at Muir Beach, California; 14 feet above mllw at Arena Cove, California; and 12.4 feet above mllw at Santa Cruz, California. One person in Santa Cruz was killed by this

tsunami. The 1960 Chilean tsunami produced a trough to crest height of 12 feet at Crescent City, California, and produced $30,000 in damage to the dock area and streets (ref. 21). The 1964 Alaskan tsunami produced elevations above mean high water (mhw) as great as 14.9 feet at Wreck Creek, 9.7 feet at Ocean Shores, and 12.5 feet at Seaview in the state of Washington. Elevations from 10 to 15 feet above mhw were produced along much of the coast of Oregon, and four people were killed. This tsunami reached an elevation of 20.7 feet above mllw at Crescent City, California. Crescent City sustained widespread destruction with $7.5 million in damage and 11 deaths (ref. 3).

Tsunamis generated in South America and the Aleutian-Alaskan region pose the greatest hazard (from distantly generated tsunamis) to the west coast of the United States. Historical records of tsunami occurrence in the Hawaiian Islands indicate that tsunamis generated in the Philippines, Indonesia, the New Hebrides, and the Tonga-Kermadec island arcs do not generate tsunamis that are significant at transoceanic distances. Tsunamis, such as the 1896 Great Meiji Sanriku tsunami and the 1933 Great Shorva Sanriku tsunami that were generated off the coast of Japan, have produced no significant elevations on the west coast of the United States. Kamchatkan tsunamis, such as the ones in 1923 and 1952 (which were the greatest from Kamchatka since at least 1837), did not cause damage on the west coast. The west coast of Canada lies along a strike-slip fault that has not historically produced tsunamis on the west coast of the United States. Tsunamis off the Pacific coast of Mexico have produced large local water level elevations, but they are generated by earthquakes covering areas that are apparently too small to cause significant elevations on the west coast of the United States.

The West Coast of the United States lies along the boundary of the Pacific and North American tectonic plates. However, this boundary is not a subduction zone. The Pacific and North American plates have a horizontal relative motion along this boundary, and earthquakes in the region exhibit strike-slip motion, which is not an efficient generator of tsunamis. For example, the great 1906 San Francisco earthquake (8.3 magnitude on Richter scale) produced waves with heights no greater than 2 inches (ref. 1).

The hazard of locally generated tsunamis on the west coast of the United States is probably much less than the hazard from distantly generated tsunamis. However, there have been reports of significant locally generated tsunamis on the west coast. For example, a recent publication of the California Division of Mines and Geology (ref. 22) mentions that Wood and Heck (ref. 23) reported that runup heights of a tsunami generated by the 1812 Santa Barbara earthquake reached 50 feet at Gaviota, 30-35 feet at Santa Barbara, and 15 feet or more at Ventura in California. However, an exhaustive study (ref. 24) of this event that included an investigation of the unpublished notes (cited by Wood and Heck) of the late Professor G. D. Louderback, University of California, Berkeley, has shown that the runup heights for this tsunami probably were not more than 10-12 feet at Gaviota and correspondingly lower at the other locations. A report of a tsunami at Santa Cruz, California, in 1840 also has been shown to be erroneous (ref. 24). The largest authenticated locally generated tsunami on the west coast was generated by the 1927 Point Arguello earthquake and produced runup elevations as great as 6 feet in the immediate vicinity. Although there is no solid evidence that locally generated tsunamis pose a great hazard on the west coast, the possibility of significant locally generated tsunamis cannot be

neglected when considering hazards to critical facilities such as nuclear power plants. There also is the possibility that locally generated tsunamis may produce greater runup elevations in areas protected from distantly generated tsunamis (Puget Sound, Washington, and parts of southern California) than are produced by distantly generated tsunamis.

1.1.1.6 Pacific Ocean island territories and possessions

Many of the island territories and possessions of the United States are parts of seamounts that rise abruptly from the ocean floor. As a result of the very short transition distance (relative to typical tsunami wavelengths in the deep ocean) from oceanic depths to the shoreline of these islands, distantly generated tsunamis do not produce large elevations on these islands. The maximum elevation produced on such Islands by distant tsunamis is on the order of 6 feet (elevation recorded at Johnston Island during the 1960 Chilean tsunami (ref. 25). Islands in this category include Wake Island, the Marshall Islands, Johnston Island, the Caroline Islands, the Mariana Islands, Howland Island, Baker Island, and Palmyra Island. The possibility of elevations on these islands greater than 6 feet being produced by distantly generated tsunamis cannot be neglected if the hazard to critical facilities is being considered. Detailed investigations of the response of different types of islands to tsunamis have not been performed. It is known that 20-foot elevations were recorded on Easter Island as a result of the 1960 Chilean tsunami (generated approximately 2000 miles away). This island is small and the surrounding seamount is fairly small. The exact transition between

seamounts too small to amplify tsunamis and those large enough to cause significant amplication is not known. Numerical models discussed in Chapter III can be used to determine the interaction of tsunamis with islands.

The Samoa Islands are subject to tsunami flooding. The 1960 Chilean tsunami had a trough to crest height of 15 to 16 feet at the head of Pago Pago harbor (crest elevation of 9.5 feet) in American Samoa (ref. 26). Property damage of $50,000 occurred in Pago Pago village during this tsunami. Local tsunamis also are destructive in the Samoa Islands. A destructive earthquake and 40-foot tsunami have been reported to have occurred in 1917 (ref. 9). Whether this elevation occurred on American Samoa or one of the other Samoan Islands is not known. However, the tsunami was destructive at Pago Pago, American Samoa. A catalog of tsunamis in the Samoan Island is presented in Reference 26.

1.1.2 Tsunami Characteristics

1.1.2.1 Generation and deep-ocean propagation

Most tsunamis are generated along the subduction zones bordering the Pacific Ocean. These zones are highly seislmic and earthquakes occurrig within these subduction zones often exhibit the vertical dip-slip motion that is required to produce significant tsunami elevations. Berg et al. (ref. 27) demonstrated that horizontal or strike-slip motion is a very inefficient menchanism for the generation of tsumanis.

Large tsunamis are associated with elliptically shaped generation areas that radiate energy preferentially in a direction perpendicular to the major axis. The major axis of the tsunami is approximately parallel to the oceanic trench or island arc that is the boundary between colliding tectonic plates. Momoi (ref. 28) developed a relationship between the tsunsmi wave height H_a in the direction of the major axis of a source of length a to the wave height H_b in the direction of the minor axis of length b for an instantaneously and uniformly elevated ellipitic source. This relationship is expressed by the equation $H_b/H_a = a/b$. Takahasi and Hatori (ref. 29) demonstrated that this equation was valid by performing laboratory tests using an elliptically shaped membrane. Hatori (ref. 30) showed that data from historical tsunamis indicated that this equation was reasonable.

The directional radiation of energy from the region of generation of a tsunamis is quite important. The ratio of the length of the major axis to the minor axis for large earthquakes, such as the 1964 Alaskan or the 1960 Chilean earthquake, can be approximately 4 to 6; thus, the waves radiated in the direction of the minor axis can be greater than those radiated in the direction of the major axis by a similar ratio. Therefore, the orientation of a tsunami source region relative to a distant area of interest is very important, and the runup at a distant site due to the generation of a tsunami at one location along a trench cannot be considered as being representative of all possible placements of the tsunami source along the trench region. For example, the 1957 Aleutian tsunami produced significant elevations in the Hawaiian Islands, but was fairly small on most of the west coast of the continental United States; whereas, the 1964 Alaskan tsunami was fairly small in the Hawaiian Islands and fairly large on the northern half of the west

coast. An earthquake generating a tsunami in an area southwest of the 1964 Alaskan tsunami will beam energy toward the southern half of the west coast of the United States.

The ground motion generating a large tsunami occurs over such a short time relative to the period of the tsunami that the motion can be considered to be instantaneous. Typical rise times (time from initiation of ground motion to attainment of permanent vertical displacement) are in the range of tens of seconds for earthquakes; whereas, tsunami periods are in the range of tens of minutes. Higher frequency oscillations superimposed upon the movement to a permanent displacement have periods in seconds. The time for the ground rupture to move the entire length of the source is a few minutes, Hammack (ref. 31) showed that for a large tsunami, such as the 1964 Alaskan tsunami, the actual time-displacement history of the ground motion is not important in determining far-field characteristics of the resulting tsunami. All time-diplacement histories reaching the same permanent vertical ground displacement will produce the same tsunami in the far field, Hammack (ref. 31) also showed that small-scale features of the permanent ground deformation produce waves that are not significant far from the source region. Thus, distantly generated tsunamis can be studied knowing only major features of the permanent ground displacement.

Tsunamis are generated along continental margins or island arcs and then propagate out into the deep ocean. The depth transition from the relatively shallow region of generation to the deep ocean occurs over a very short distance relative to typical tsunami wavelengths in the deep ocean that are in the order of hundreds of miles. In the deep ocean, tsunami wave heights are a

few feet at most. The wave steepness (ratio of wave height to wave length) is so small for tsunamis that they go unnoticed by ships in the deep ocean. Hammack and Segur (ref. 32) demonstrated that the propagation over transoceanic distances of the leading wave (or waves, since leading waves reflected off land areas may arrive at a distant location after the primary leading wave) of a large tsunami of consequence to distant areas is governed by the linear longwave equations. Hammack and Segur (ref. 32) also showed that eventually nonlinear and dispersive effects will become important in the propagation of a tsunami in the deep ocean, but that the propagation distance necessary for these effects to become significant for the leading wave of a large tsunami (such as the 1964 Alaskan tsunami) is large compared with the extent of the Pacific Ocean. The later smaller waves of a tsunami wave train have been shown to be [ipso facto] frequency dispersive (ref. 32).

1.1.2.2 Nearshore effects

When tsunamis approach a coastal region where the water depth decreases rapidly, wave refraction, shoaling, bay or harbor resonance, and other effects may result in significantly increased wave heights. The dramatic increase in heights of tsunamis often occurs over fairly short distances. For example, during the 1960 tsunami at Hilo, Hawaii, waves could be seen breaking over the water-front area of Hilo from a ship approximately 1 mile offshore, yet the personnel on the ship could not notice any disturbance passing by the ship. Tsunamis also can be quite large at one location and small at nearby locations (e.g., they may be large within a harbor as a result of resonance effects and small on the open coast.)

As tsunamis enter shallower water, their heights increase and their wavelengths decrease; therefore, nonlinear and frequency dispersion effects become more significant. However, Hammack and Segur (ref. 32) and Goring (ref. 33) showed that the linear long-wave equations are adequate to describe the propagation of a large tsunami, such as the 1964 Alaskan tsunami, from the deep ocean up onto the continental shelf.

Tsunamis usually appear at the shoreline in the form of rapidly rising water levels, but they occur occasionally in the form of bores. When they appear as bores, vertical accelerations are important in the region of the face of the bore and vertically integrated long-wave equations are not adequate to describe flow in this region. However, beyond the face of the bore the water surface has been described as being almost flat in appearance (ref. 34). Long-wave equations may adequately describe flows in this broad-crested region that probably governs the ultimate land inundation.

Even when a tsunami appears as a rapidly rising water level, there are many small-scale effects that develop that are highly nonlinear for which vertical accelerations are significant (e.g., small bores forming at the tsunami front during propagation over flatland and strong turbulence during flow past obstacles and areas of great roughness). However, there is substantial evidence that the main features of the extent of land inundation are governed by simple physical processes. Quite often the runup elevation (elevation of maximum inundation) is the same as the elevation near the shoreline and at other locations within the zone of inundation. Therefore, the water surface of the tsunami is fairly flat during flooding. For example, Magoon (ref. 21) reported flooding to about the 20-foot contour above mllw and elevations at

the shoreline of about 20 foot for the 1964 Alaskan tsunami at Crescent City, California. Wilson and Torum (ref. 3) report that the 20-foot (mllw) runup at Valdez, Alaska, for the 1964 tsunami checked "well for consistency with water-level measurements made on numerous buildings throughout the town". Similar comments were made by Brown (ref. 35) in reference to survey measurements of 30-foot (mllw) runup at Seward, Alaska, for the 1964 Alaskan tsunami. Runup elevations and elevations at the shoreline and in the inundation zone were similar at nine locations in Japan as recorded by Nasu (ref. 36) in surveys following the 1933 Sanriku tsunami. This tsunami had a short period (12 minutes) and reached an elevation as great as 90 feet at one survey location. The runup elevation and the elevation near the shoreline also were similar at Hilo, Hawaii, for the 1960 tsunami (borelike waves) (ref. 37). Differences are apparent, however, at locations where Eaton et al. (ref. 37) demonstrated that flow divergence is significant. Flow divergence and convergence, frictional effects, and time-dependent effects (that can limit the time available for complete flooding) are probably the major effects causing differences between runup elevations and elevations near shoreline.

1.2 Tsunami Modeling

1.2.1 Introduction

The scarcity of historical data of tsunami activity often makes it necessary to use hydraulic scale models, analytical methods, or numerical methods to model tsunamis in order to determine quantitatively the tsunami hazard. Even at locations with ample historical data, changes in land elevations and vegetation (thus changes in land roughness) as a result of development and the

building of protective structures may modify the tsunami hazard. Scale models, analytical methods, or numerical methods are required to determine the magnitude of this modification.

1.2.2 Hydraulic Scale Models

Although it would not be practical to use hydraulic scale models (with reasonable scales) to model tsunami propagation across transoceanic distances, these models have found some application in simulating tsunami propagation in nearshore regions and interaction with land areas. For example, hydraulic models have been used to study tsunami interaction with single islands that are reaslistically shaped and surrounded by variable bathymetry. Van Dorn (ref. 38) studied tsunami interaction with Wake Island using a 1:57,000 undistorted scale model. Jordaan and Adams (ref. 39) studied tsunami interaction with the island of Oahu in the Hawaiian Islands using a 1:20,000 distorted scale model. They found poor agreement between historical measurements of tsunami runup and the hydraulic model data. Scale effects (e.g. viscous effects) and the effects of the arbitrary boundaries that confine the hydraulic model probably account for the poor agreement. It is also difficult to measure tsunami elevations in such small-scale models. Jordaan and Adams (ref. 39) modeled the tsunami to a vertical scale of 1:2,000; thus, the waves had heights ten times the normal proportion. Even with this distortion, waves had heights of only a fraction of an inch in the model. The great expense required to build a hydraulic model of even a small island at a reasonable scale makes hydraulic models unattractive relative to numerical models as a means for modeling tsunamis.

Hydraulic models are sometimes useful in modeling complex tsunami propagation in small regions. For example, the 1960 tsunami at Hilo, Hawaii, formed a borelike wave in Hilo Bay. In addition, a phenomenon analogous to the Mach-reflection in acoustics may have developed along the cliffs north of the city (ref. 40). A Mach-stem wave may have entered Hilo and superposed upon an incident wave that came over and around the Hilo breakwater. Hydraulic models have been successfully used to model complex phenomena such as Mach-stem waves that developed during the 1960 tsunami in Hilo Bay (refs. 41, 42). Mach-stem waves also have been modeled numerically (ref. 43).

In general, hydraulic models are not suitable for modeling two-dimensional tsunami propagation even within small regions. Typical tsunami wavelengths (except perhaps when borelike waves are formed) are so long that wave makers in a hydraulic model are only a small fraction of a wavelength from the region to be studied. Thus, waves reflected by land are almost immediately reflected off the wave makers and back into the basin. Wave absorber screens in front of the wave makers are not very helpful because it is very difficult to absorb very long waves. The wave makers can be moved a few wavelengths from the region of interest by reducing the scale of the model; however, scale effects then become very significant. Hydraulic model tests by Grace (ref. 42) suffered the problem of trapping wave energy between the wave makers and the shoreline.

Hydraulic models have been used very successfully to study one-dimensional tsunami propagation. Hammack (ref. 31) studied tsunami generation and propagation using a hydraulic model and Goring (ref. 33) studied tsunami propagation up the continental slope to the nearshore region,

1.2.3 Analytical Methods

Analytical solutions have been used for a long time to study tsunamis. They are useful for simplified conditions (e.g., linear bottom slopes) rather than for general and arbitrary conditions. Analytical solutions for tsunami interactions with simple bathymetries are often used to verify numerical model solutions. For example, Omer and Hall's solution (ref. 44) for the diffraction pattern for long-wave scattering off a circular cylinder in water of constant depth can be used to verify a numerical model that calculates the interaction of tsunamis with an island in a constant depth ocean. Hom-ma's solution (ref. 45) for the diffraction pattern for long-wave scattering off a circular cylinder surrounded by a parabolic bathymetry can be used to verify a numerical model that calculates the interaction of tsunamis with an island in an ocean of variable depth. Analytical solutions also can provide insight into the important processes determining tsunami propagation. For example, Hammack and Segur (ref. 32) used analytical solutions to provide criteria for the modeling of tsunami propagation. Kajiura (ref. 46) described the propagation of the leading wave of a tsunami and Longuet-Higgins (ref. 47) considered the trapping of wave energy around islands.

Analytical solutions are often used in engineering practice to determine tsunami modification during propagation over simple bathymetric variations or interaction with simple shoreline configurations. Camfield (ref. 48) presented a description of many of the analytical solutions that have been used in engineering practice. These solutions are useful when time or cost constraints rule out the application of more general numerical models.

There are problems associated with use of analytical solutions to determine tsunami propagation for actual arbitrary conditions. Different phenomena, such as refraction, shoaling, reflection, and runup usually must all be solved separately if analytical solutions are used. Many techniques are used to solve each of these processes. The techniques often utilize different simplifying assumptions and, therefore, provide different answers. For example, Camfield (ref. 48) discussed several formulas that have been used to calculate tsunami runup. Some traditional techniques, such as simple refraction methods, also have been shown to be inadequate for most tsunami propagation problems (ref. 49).

1.2.4 Numerical Models

1.2.4.1 Generation and deep ocean propagation

Numerical models have been developed to generate tsunamis and to propagate them across the deep ocean (refs. 50, 51, 52). These models use finite difference methods to solve the linear long-wave equations on a spherical coordinate grid. One of the models (50) solves a nonlinear continuity equation, since the total water depth including the tsunami height is used. However, the tsunami height is so small compared with the water depth that this nonlinearity is inconsequential (and requires additional computational time). These models employ grids covering large sections of the Pacific Ocean. Transmission boundary conditions are used on open boundaries to allow waves to escape from the grid instead of reflecting back into the region of computation. Two of the models (refs. 51, 52) solve the equations of motion

with an explicit formulation. The model of Hwang et al. (ref. 50) uses an implicit - explicit formulation developed by Leendertse (ref. 53). A transmission boundary conditions is used in the model that requires the time step employed in the calculations to be limited by the stability constraint for explicit formulations. However, the implicit-explicit formulation requires more computational time than required by explicit formulations when the time step is limited by the same stability constraint.

These generation and deep-ocean propagation models use an initial condition that an uplift of water surface in the source region is identical to the permanent vertical ground displacement produced by the tsunamigenic earthquake. Hammack (ref. 31) demonstrated that it is this permanent vertical ground displacement, and not the transient motions that occur during the earthquake, that determines the far-field characteristics of the resulting tsunami. In addition, Hammack (ref. 31) showed that the small-scale details of the permanent ground deformation produce waves that are not significant far from the source region. Thus, distantly generated tsunamis can be studied when only the major features of the permanent ground deformation are known.

Hwang, et al. (ref. 50) used data of the permanent vertical ground displacement of the 1964 Alaskan tsunami collected by Plafker (ref. 54) in a simulation of the 1964 tsunami. Good agreement was demonstrated by Hwang et al. (ref. 50) between a recording of the 1964 tsunami (ref. 38) in relatively deep water off the coast of Wake Island and a simulation of this tsunami using a numerical model. Houston (ref. 55) used the model of Hwang et al. (ref. 50) and the model of Garcia (ref. 52) to generate the 1964 Alaskan and the 1960 Chilean tsunami, respectively. The data of the permanent vertical ground

displacement of the 1964 and 1960 earthquakes collected by Plafker (ref. 54) and Plafker and Savage (ref. 56) were used as initial conditions in these models. The deep-water wave forms calculated by these models were used by Houston (ref. 55) as input to a nearshore numerical model covering the Hawaiian Islands. Good agreement was shown between tide gage recordings of these tsunamis in the Hawaiian Islands and the numerical model calculations. Houston and Garcia (ref. 51) showed similar comparisons between tide gage recordings of the 1964 Alaskan tsunami on the west coast of the United States and numerical model calculations.

1.2.4.2 Tsunami interaction with islands

Tsunami destruction in the Hawaiian Islands has directed interest toward the development of numerical models to simulate the interaction of tsunamis with islands. Several numerical models have been developed in recent years. All of these models solve the linear long-wave equations, but different techniques are used in the solutions; therefore, the models have different capabilities.

Vastano and Reid (ref. 58) developed a numerical model to study the problem of determining the interaction of monochromatic plane waves of a tsunami period with a single island. A transformation of coordinates allowed a mapping of the arbitrary shoreline of an island into a circle in the image plane. The finite difference solution employed a grid that allowed greater resolution in the vicinity of the island than in the deep ocean. Such a variable grid is important since islands are usually small and surrounded by a very rapidly varying bathymetry. This numerical model can be applied only to a single island and not a multiple-island system.

Vastano and Bernard (ref. 59) extended the techniques developed by Vastano and Reid (ref. 58) to multiple-island systems. However, the transformation of coordinates technique allows high resolution only in the vicinity of one island of a multiple-island system. Thus, when Vastano and Bernard (ref. 59) applied their model to the three-island system of Kauai, Oahu, and Niihau in the Hawaiian Islands, the two islands of Oahu and Niihau had to be represented by cylinders with vertical walls whose cross sections were truncated wedges. Kauai was represented by a circular cylinder with the surrounding bathymetry increasing linearly in depth with distance radially from the island until a constant depth was attained. A single Gaussian-shaped plane wave composed of a broad band of wave frequencies was used as input to the model. No comparisons were made with historical tsunami data for the three islands. The model does allow the approximate effects of neighboring islands on a primary island of interest to be included in the calculations.

A finite difference model employing a grid covering the Hawaiian Island chain was used by Bernard and Vastano (ref. 60) to study the interaction of a plane Gaussian pulse with the Islands. The square grid cells were 3.3 miles on a side and close to the minimum feasible size for a constant-cell finite difference grid covering the major islands of Hawaii. However, historical data indicate that significant variations of tsunami elevations occur over distances much less than 3.3 km. The islands of Hawaii are relatively small and not well represented by a 3.3-mile grid. For example, Oahu has a diameter of only approximately 18 miles, and the land-water boundary of the island has characteristic direction changes that occur over distances of much less than 3.3 miles. The offshore bathymetry of the islands also varies rapidly with

depth changes of more than 4700 feet frequently occurring over distances of 3.3 miles. Furthermore, if a resolution of eight grid cells per wavelength is maintained for tsunami periods as low as 15 min, a 3.3-mile grid cannot be used for depths much below 950 feet. However, the processes that cause significant modifications and rapid variations of elevations along the coastlines, which are known to occur during historical tsunamis, probably occur in this region extending from water at a depth of 950 feet to the shoreline. This model allows all the islands of a multiple-island system to be included in the calculations and can determine the interaction of an arbitrary tsunami with the island system.

Lautenbacher (ref. 61) developed a numerical model that solved an integral equation. He applied it to an island with sloping sides surrounded by a constant depth ocean. An advantage of the model is that a wall or "no flow" condition is not required at the shoreline. However, the computational requirements of the model are extremely large since the matrix to be inverted is full. Thus, it is not feasible to apply the model to determine the interaction of tsunamis with actual islands surrounded by complex bathymetries. In addition, Mei (ref. 62) demonstrated that the integral equation method can have eigen solutions at certain frequencies and lead to ill-conditioned matrices.

A finite element numerical model based upon a model developed by Chen and Mei (ref. 63) for harbor oscillation studies was used by Houston (ref. 55) to calculate the interaction of tsunamis with the Hawaiian Islands. The model employed a finite element grid that telescoped from a large cell size in the deep ocean to a very small size in shallow coastal waters. The grid covered a

region that included the eight major islands of the Hawaiian Islands. Although time periodic motion was assumed in the solution, the interaction of an arbitrary tsunami waveform with the islands was easily determined within the framework of a linear theory by superposition. Houston (ref. 55) also demonstrated good agreement (major waves) between tide gage recordings of the 1960 Chilean and 1964 Alaskan tsunamis in the Hawaiian Islands and the numerical model simulations of these tsunamis. A generation and deep-ocean propagation numercial model was used to determine deep-ocean waveforms for these two tsunamis. These waveforms were used as input to the finite element numerical model. The advantages of this model include the flexibility of the finite element method that allows a telescoping grid so that extremely small elements can be placed in the nearshore region and the very small computational time required by the model as a result of the very tight bandedness of the matrix that is inverted. The model cannot be used to calculate the effects of local tsunamis generated within the Hawaiian Islands.

A time-stepping finite element numerical model developed by Sklarz et al. (ref. 64) has been used to investigate locally generated tsunamis near the big island of Hawaii. Large, locally generated tsunamis occurred on the southeast side of the island of Hawaii in 1868 and 1975. Sklarz et al. (ref. 64) attempted to simulate the 1975 tsunami by using a 5-foot uplift of the water surface in an elliptical area off the coast of the island of Hawaii as an initial condition in their numerical model. The finite element model solves the linear longwave equations. Reasonable general agreement was demonstrated between the numerical model calculations multiplied by a factor of 4 and measurements of runup for the 1975 tsunami. Sklarz et al. (ref. 64) also claimed that a factor of 4 will account for the difference between the

infinite wall at the shoreline used in their model and the amplification of a tsunami as it moves from the shoreline to the level of ultimate runup. The advantage of this model is that the flexibility of the finite element grid allows the shape of a land mass and a complex offshore bathymetry to be well represented. It is unlikely that it would be practical to include all of the Hawaiian Islands in detail in a grid used by this numerical model because a large matrix must be inverted at each time step. Thus, the cost of running the model for a large grid would be prohibitive. However, locally generated tsunamis have historically been important only on the single island nearest the uplift that generated the tsunami; thus, a grid containing a single island can be used to provide the information of practical concern for locally generated tsunamis.

1.2.4.3 Tsunami interaction with coastlines

Numerical models have been developed to calculate tsunami interaction with continental (or large islands such as the Japanese Islands) coastlines. Many of these models solve long-wave equations. Some of the models solve long-wave equations that include nonlinear advective and dissipative terms, and other solve the linear long-wave equations. According to Hammack and Segur (ref. 32), Goring (ref. 33), and Tuck (ref. 65), the propagation of large (long-period) tsunamis (at least the initial major waves), such as the 1964 Alaskan tsunami, from the deep ocean up onto the continental shelf is governed by the linear long-wave equations. Nonlinear and frequency dispersive effects are not important during this propagation since the transition from the deep ocean to the continental shelf occurs over such a short distance that there is not sufficient time for these effects to become significant. However, these terms

may become important during propagation from the edge of the continental shelf to the shoreline. The linear long-wave equations may govern tsunami interactions with islands (neglecting effects of reefs and occasional formation of bores) as a result of the very short shelf region of small islands in the Pacific Ocean.

One-dimensional numerical models that solve nonlinear equations and include frequency dispersion effects have been developed. Heitner and Housner (ref. 66) developed a one-dimensional finite element model that was used to calculate the runup of a solitary wave propagating up a linear slope. Mader (ref. 67) used a one-dimensional model to calculate the propagation of solitary waves and sinusoidal wave trains up linear slopes and past submerged barriers. Garcia (ref. 68) used a one-dimensional model to study short-period tsunamis that might be generated by horizontal motions of the Mendocino Escarpment off the western coast of the United States. These one-dimensional models are useful since they provide insight into the interaction of tsunamis with simple models of continental slopes. However, two-dimensional models are necessary to calculate tsunami propagation over realistic bathymetries and interaction with complex coastlines.

Aida (ref. 69) developed a two-dimensional finite difference numerical model with an explicit formulation to study tsunamis generated just off the coast of Japan. Various permanent vertical ground displacements for the 1964 Niigata and the 1968 Tokachi-oki tsunamis were used as initial conditions for this model that solved the linear long-wave equations. More recently Aida (ref. 70) applied a similar model to investigate tsunami generation and propagation for five tsunamis generated off the coast of Japan. A telescoping finite

difference grid was used so that grid cells could be made smaller in selected bays where there were historical measurements of these tsunamis. The tsunami source used in the calculations was a vertical displacement of the sea bottom derived from a seismic fault model for each earthquake. A crude general agreement was shown between the numerical model calculations and the historical tide gage recordings of the simulated tsunamis. Differences between the recorded and measured tsunamis are probably largely due to inaccuracies in the seismic fault model used to determine the vertical displacement of the sea bottom.

Houston and Garcia (ref. 71) employed a two-dimensional finite difference numerical model based upon the original formulation of a tidal hydraulic numerical model by Leendertse (ref. 53) to study tsunami interaction with the west coast of the United States. This model solves long-wave equations that include nonlinear and bottom friction terms. Leendertse's implicit-explicit multioperational method is employed in solving these equations. To verify the model, a generation and deep-ocean propagation numerical model (ref. 50) was used to generate the 1964 Alaskan tsunami and propagate it to the west coast of the United States. The resulting wave form was used as input to this nearshore numerical model that propagated the tsunami to the shoreline. Good agreement was shown between tide gage recordings of the 1964 Alaskan tsunami at Crescent City and Avila Beach, California, and the numerical model calculations. This numerical model does not employ a telescoping grid. However, the time step used by the model is not restricted by the stability critera for an explicit model. Therefore, it is practical to use fine grid cells and a grid covering a large area since a fairly large time step can be employed. Houston (ref. 72) employed a two-dimensional signal implicit finite

difference numerical model that used a uniformly varying computational grid to study tsunamis in Southern California. Comparisons of historical data and numerical computations were made of seven tide gage locations.

A time-stepping, two-dimensional finite element numerical model has been recently developed by Kawahara et al. (ref. 73). Unlike most finite element models that are implicit and require costly matrix inversions at each time step, this model uses a two-step explicit formulation. Thus, the computational time requirements of the model are modest and would compare favorably with explicit finite difference models. Although the finite difference formulation used by Houston and Garcia (ref. 71) allows a much larger time step than that permitted by this model, the flexibility of the finite element grid allows a region to be covered by fewer cells (as a result of the telescoping properties of the grid) and permits the shape of coastlines to be well represented. The model solves the linear long-wave equations in deep water and the long-wave equations including nonlinear advective terms in shallower water. A simulation of the 1968 Tokachi-oki tsunami is also performed by Kawahara et al. (ref. 73). A crude general agreement between tide gage recordings of this tsunami and the numerical model calculations are shown (with differences probably attributable to lack of knowledge concerning the ground displacement that generated the tsunami). Gray (ref. 74) demonstrated that the method used by Kawahara et al. (ref. 73) provides excessively dumped solutions that do not converge as the numerical time step is reduced.

Chen et al. (ref. 75) developed a two-dimensional finite difference model that solves Boussinesq-type equations. These higher order equations include the

effects of the nonlinear advective terms and frequency dispersion. Furthermore, Chen et al. (ref. 75) found that the third-order term accounting for frequency dispersion produced spurious high-frequency components that caused numerical difficulties. Thus, numerical filtering had to be used to suppress these components. The model was used to simulate a nearshore tsunami off the coast of Diablo Canyon, California. Chen et al. (ref. 75), also showed that a numerical model solving long-wave equations including nonlinear terms calculated a tsunami wave form almost identical (slightly greater amplitudes) to the waveform calculated by the model that solved the Boussinesq equations. Thus, frequency dispersion did not produce any significant effects, and Boussinesq equations were not found to be superior to long-wave equations. The slightly lower amplitudes calculated by the model that solved Boussinesq equations may have been caused by the numerical filtering which would tend to reduce amplitudes.

1.2.4.4 Tsunami inundation

The final phase of tsunami propagation involves the inundation of previously dry land. As discussed earlier, inundation patterns are often fairly simple. The tsunami appears as a rapidly rising water level, and inland flooding reaches an elevation similar to the tsunami elevation at the shoreline. However, flow divergence and convergence resulting from two-dimensional variations in topography (e.g., a narrowing canyon), frictional effects, and time-dependent effects (that can limit the time available for complete flooding) can change this simple pattern of inundation. Numerical models are required to determine inundation lines for actual tsunami propagation over complex topography.

Bretschneider and Wybro (ref. 76) developed a one-dimensional model to calculate tsunami inundation. Frictional effects, but not time-dependent effects, were included in the model calculations. Calculations can be performed for a series of constant ground slopes. This model is easy to apply and very economical. The main limitations of this approach are the one-dimensional and time-independent properties of the solution in addition to an assumption that the height of the tsunami decreases with the square of the velocity of the tsunami. This last assumption appears to contradict laboratory experiments performed by Cross (ref. 77).

Houston and Butler (ref. 78) described a two-dimensional and time-dependent numerical model that calculates land inundation of a tsunami. The model solves long-wave equations that include bottom friction terms. A coordinate transformation was used to allow the model to employ a smoothly varying grid that permits cells to be small in the inundation region and large in the ocean. The transformation is a piecewise reversible transformation that is used independently in the x and y directions to map the variable grid into a uniform grid for the computational space. A variable grid in real space is necessary since the extent of inundation has a spatial scale much smaller than a tsunami wavelength. An implicit formulation developed by Butler (ref. 79) is used in the finite difference model. The model was verified by simulating the 1964 Alaskan tsunami at Crescent City, California. This tsunami was very large at Crescent City (20 feet above mllw), and the Crescent City area is very complex. For example, the Crescent City harbor is protected by breakwaters, some of which were overtopped and others which were not. There is a developed city area, mud flats, and an extensive riverine floodplain.

Inland flooding was widespread in the floodplain area and extended as much as a mile inland. Sand dunes and elevated roads played a prominent role in limiting flooding in certain areas. Good agreement was demonstrated between historical measurements (ref. 21) and numerical model calculations for high-water marks, contours of tsunami elevations above the land during propagation over previously dry land, and the extent of inundation.

1.3 Tsunami Elevation Predictions

1.3.1 Predictions Based Upon Historical Data

A number of locations in the United States, such as Hilo, Hawaii, have sufficient historical data of tsunami activity to allow reasonable tsunami elevation predictions to be made based upon the available historical data. For such locations, the historical data can be ranked from the largest to the smallest recorded elevation (largest elevation with a rank equal to 1 and the second largest with a rank of 2). By dividing the rank by the total number of years of record plus one year, the frequency of occurrence of elevations equaling or exceeding a recorded elevation (mean exceedance frequency) can be defined.

Cox (ref. 80) found that the logarithm of the tsunami mean exceedance frequency was linearly related to tsunami elevations for the ten largest tsunamis occurring from 1837 to 1964 in Hilo, Hawaii. Earthquake intensity and the mean exceedance frequency have been similarly related by Gutenburg and Richter (ref. 4). Furthermore, Wiegel (ref. 81) found the same relationship between tsunami frequency of occurrence and measured elevations for tsunamis

at Hilo, Hawaii; San Francisco, California; and Crescent City, California; and Adams (ref. 82), for tsunamis at Kahuku Point, Oahu. Rascon and Villarreal (ref. 83) demonstrated that a linear relationahip between the logarithm of the mean exceedance frequency and recorded elevations held for historical tsunamis on the west coast of Mexico (data from 1732) and on the Pacific West Coast of America, excluding Mexico. Cox (ref. 80) showed that this linear relationship between the logarithm of the mean exceedance frequency and tsunami elevations at Hilo was valid for mean exceedance frequencies as high as approximately 0.1 per year (1-in-10-year tsunami) and that the relationship between mean exceedance frequency and elevation followed a power law for higher frequencies. Thus, the logarithmic distribution may not hold for small tsunamis. This distribution also must be invalid at some large tsunami elevations, since earthquakes reach certain maximum elevations as a result of the upper limit to the strain that can be supported by rock before fracture (ref. 4). Thus, tsunamis can be expected to have similar upper limits of intensity. The logarithmic distribution should be adequate (provided there is a sufficient length of historical record) to determine tsunami hazards at locations other than the sites of critical facilities such as nuclear power plants. At the site of a critical facility, the Probable Maximum Tsunami (ref. 84) must be predicted by deterministic and not probabilitic methods. Houston et al. (ref. 13) demonstrate this type of deterministic method.

Other mean exceedance frequency distributions can be applied to historical data of tsunami elevations. For example, the Gumbel distribution has been used in the past to study annual stream-flow extremes (ref. 85). Borgman and Resio (86) illustrated the use of this distribution to determine frequency curves for nonannual events in wave climatology. If the approach of Borgman

and Resio (ref. 86) is applied to the historical data of tsunami activity in Hilo, Hawaii (as compiled by Cox, (ref. 80)), a 1-in-100-year elevation of 28.8 ft is obtained. This compares with a 1-in-100-year elevation of 27.3 ft obtained using a logarithmic distribution. The frequency distribution governing tsunami activity at a location is not known a priori, and there is not sufficient historical data to determine a posteriori the governing distribution. However, the logarithmic distribution has been shown to provide a reasonable fit of historical data at several locations in the Pacific Ocean region.

Historical data of tsunami activity in the United States are available from several published sources. Iida et al. (ref. 1) and Soloviev and Go (ref. 87) presented catalogs of tsunami activity in the Pacific Ocean, Heck (ref. 9) listed the worldwide tsunamis covering the period from 479 BC to 1946 AD. Beringhausen (ref. 88) compiled a catalog of tsunamis in the Atlantic Ocean and also a separate catalog (ref. 89) of tsunamis reported from the west coast of South America (tsunamis generated in this region are of concern to areas in the western United States). Pararas-Carayannis (ref. 2) published a catalog of tsunami activity in Hawaii, and Cox and Pararas-Carayannis (ref. 19) a catalog of tsunami activity in Alaska. Cox and Morgan (ref. 15) described locally generated tsunamis in the Hawaiian Islands. A catalog of tsunamis in the Samoan Islands is presented in the report of Houston (ref. 26).

Detailed accounts of several major tsunamis in the United States are available. For Hawaii, Shepard et al. (ref. 90), described the 1946 tsunami; MacDonald and Wentworth (ref. 91), the 1952 tsunami; Fraser et al. (ref. 92), the 1957 tsunami; Eaton et al. (ref. 37) and USAE District, Honolulu (ref.

93), the 1960 tsunami; and loomis (ref. 16), the 1975 tsunami. Wilson and Torum (ref. 3), Brown (ref. 35), Berg et al, (ref. 27), and a report by the National Academy of Sciences (ref. 20) discussed the 1964 Alaskan tsunami. Magoon (ref. 21) presented the effects of the 1960 and 1964 tsunamis in northern California. Reid and Taber (refs. 12, 13) discussed the 1868 tsunami in the Virgin Island and the 1918 tsunami in Puerto Rico. Keys (ref. 94) described the 1960 tsunami in American Samoa. Symons and Zetler (ref. 25) and Spaeth and Berkman (ref. 94) presented tide gage recordings in the Pacific Ocean region of the 1960 and 1964 tsunamis. Tide gage records of several historical tsunamis in the Pacific Ocean are available from the World Data Center A for Solid Earth Geophysics, National Oceanographic and Atmospheric Administration, Boulder, Colorado.

1.3.2 Predictions Based Upon Historical Data and Numerical Models

Most of the coastlines of the United States have little or no data of tsunami activity. For example, most of the west coast of the United States has no quantitative data of tsunami elevations. Only a very few locations have data for tsunamis other than the 1964 Alaskan tsunami. The Hawaiian Islands have substantial data of tsunami elevations for tsunamis since 1946. However, the historical observations since 1946 are at discrete locations; therefore, elevations are not known along many stretches of coastline. Data of tsunami activity since 1837 is available in the Hawaiian Islands; however, historical observations prior to 1946 are concentrated in Hilo, Hawaii.

In addition to the general scarcity of historical data, those data that are available are for recent years when tsunami activity has apparently been

greater than the long-term trend. For example, in Hilo, Hawaii, the two largest and four of the ten largest tsunamis striking Hilo from 1837 through 1981 occurred during the 15-year period from 1946 through 1960. Two of the tsunamis from 1946 through 1960 originated in the Aleutian Islands, one in Kamchatka, and one in Chile. However, six of the ten largest tsunamis occurred during the 109-year period from 1837 through 1945 with three originating in Chile, two in Kamchatka, and one in Hawaii. Therefore, both the frequency of occurrence and the place of origin of tsunamis have been remarkably variable. The exceptionally frequent occurrence of major tsunamis in Hilo, Hawaii, during the period from 1946 to 1960 is a property of the unusual activity of tsunami generation areas and not of special properties of Hilo. Thus, any analysis of tsunami activity that only uses a short time span including the period from 1946 through 1960 will predict a significantly more frequent occurrence of large tsunamis than is warranted by historical data from 1837 through 1981.

From an analysis of tsunami data for Hilo, Hawaii, the errors introduced in frequency-of-occurrence calculations by consideration of a short-time period that includes the unrepresentative years from 1946 through 1960 are apparent. A 1-in-100-year elevation for Hilo, based upon data compiled by Cox (ref. 80) for the 10 largest tsunamis in Hilo from 1837 through 1976 and assuming a logarithmic distribution, is 27.3 ft. The 1-in-100-year elevation that is based just upon the large tsunamis druing the period of accurate survey measurements in Hilo from 1946 through 1976 is 44.2 ft. Since the largest elevation in Cox's data for the 140-year period from 1837 through 1976 was 28 ft (1960 Chilean tsunami), the 44.2-ft elevation for a 1-in-100-year tsunami is probably much too large. The choice of frequency distributions

does not change this conclusion. For example, use of a Gumbel distribution yields a 1-in-100-year elevation of 42.5 ft if the analysis is based only upon data for 1946. Of course, the quantitative accuracy of the data for tsunamis in Hilo from 1837 through 1945 may be somewhat questionable. However, there is little doubt that the recorded occurrence of large tsunamis is accurate (i.e., tsunamis noted as being significant were indeed so, and major tsunamis did not occur and go unrecorded). In addition, errors introduced by consideration of a short period that includes the years from 1946 through 1960 are greater than the errors resulting from possible obsevational inaccuracies of the 19th century in Hilo. For example, increasing by 50 percent the reported elevations for the five largest tsunamis recorded in Hilo during the 19th century (these five are included in the ten largest tsunamis recorded in Hilo) yields a 1-in-100-year elevation of 30.4 ft. This elevation is similar to the 27.3-ft elevation obtained using the reported elevations for the five largest tsunamis recorded during the 19th century.

The lack of historical data of tsunami activity in the United States covering reasonable periods of time makes it necessary to use various methods to expand the data base. For example, Rascon and Villarreal (ref. 83) predicted elevations at a site in Mexico by using historical data collected for the entire west coast of Mexico. A frequency distribution based upon data recorded at Hilo, Hawaii, and a Bayes estimation procedure are used to improve the estimate based upon the data for the west coast of Mexico. Such an approach is questionable since tsunamis at Hilo are primarily generated locally, in Kamchatka, in Chile, and in Alaska; whereas the tsunamis recorded on the west coast of Mexico are primarily locally generated. Therefore, there is no reason that the frequency distribution in Hilo should be related to the

distribution for the west coast of Mexico. In addition, elevation predictions for the specific site in Mexico are not based upon local effects that may amplify the tsunami. The following two sections describe studies that employ various techniques, including the use of numerical models to expand the data base, and thus allow elevation predictions at arbitrary locations within the study region.

1.3.2.1 Predictions for the Hawaiian Islands

Houston et al. (ref. 17) described in detail methods used to make tsunami elevation frequency of occurrence predictions for the Hawaiian Islands. In order to make these predictions it was necessary to use data of tsunami activity in Hilo, Hawaii, and to expand the data base at locations having recorded data of tsunami activity since 1946. In addition, Houston et al. used a numerical model to aid in developing predictions at locations not having complete data for tsunamis since 1946 or not having any data of tsunami activity.

To reconstruct elevations prior to 1946 at locations having historical data since 1946, Houston et al. (ref. 17) noted that tsunamis originatng near the the Aleutian Islands, Kamchatka, and Chile were recorded in the Hawaiian Islands from 1946 to 1964. Therefore, the response is known of many areas in the Hawaiian Islands to tsunamis originating in the three main locations where tsunamis of destructive power in these islands have historically been generated. They assumed that tsunamis generated in a single source region (Kamchatka or Chile, but not the Aleutians) approach the islands from approximately the same direction and have energy lying in the same band of

wave periods. The difference in wave elevations at the shoreline in the Hawaiian Islands produced by tsunamis generated at different times in the same region was attributed mainly to differences in deepwater wave amplitudes. For example, the 1841 tsunami from Kamchatka produced a wave elevation in Hilo, Hawaii, that was approximately 25 percent greater than that of the 1952 tsunami from Kamchatka. The same relative magnitudes of the two tsunamis were used for all of the islands to determine the elevations that must have occurred in 1841 at some locations, knowing the elevation occurred in 1952. Therefore, knowing the elevations of tsunamis from 1946 to 1960 at a location and the response of Hilo to tsunamis from 1837 to 1960 allowed a reconstruction of the elevations that occurred prior to 1946 at the location, but were not recorded (for tsunamis from Chile and Kamchatka). Data from 1837 at Hilo were used instead of data from 1837 at Honolulu (Hilo and Honolulu are the only two locations with substantial data since 1837) since data do not exist at Honolulu for the 1868 and 1877 tsunamis, and the 1837 and 1841 elevations given by Pararas-Carayannis (ref. 2) represented drops in the water level and not runup elevations.

The assumption that tsunamis generated in Kamchatka and Chile approach the Hawaiian Islands from nearly the same direction was justified by Houston et al, (ref. 17) by the small spatial extent of the known generation areas in Kamchatka and a study of tsunami propagation from Chile by Garcia (ref. 52) that indicated that directional effects for tsunamis originating along the Chilean coast are small in the Hawaiian Islands (probably because the generation areas in Chile subtend a relatively small angle with respect to the Hawaiian Islands). The position of the Aleutian-Alaskan Trench relative to the Hawaiian Islands does introduce important directional effects for tsunamis

generated in the Aleutian Alaskan area. However, these effects are known from historical observations for tsunamis generated in the western Aleutians (1957 tsunami), central Aleutians (1946), and eastern Alaskan area (1964).

Historical observations of tsunamis in Hawaii support the approach by Houston et al, (ref. 17) that estimates the elevations produced by tsunamis from Chile or Kamchatka prior to 1946 based upon data for tsunamis from these tsunamigenic regions recorded during the years of accurate survey measurements since 1946. Eaton et al. (ref. 37) noted that in the Hawaiian Islands "Tsunamis of diverse geographic origin are remarkably similar". Wybro (ref. 95) showed that even the distributions of normalized elevations (elevations normalized by the largest recorded elevation) produced in the Hawaiian Islands by different Aleutian-Alaskan tsunamis are nearly the same yet quite different from the distributions for tsunamis of other origins. Therefore, it is a reasonable assumption that tsunamis from the same geographic origin produce similar runup patterns in the Hawaiian Islands. Thus, the elevation of a pre-1946 tsunami at a location that has a recorded elevation for a post-1946 tsunami from the same geographic origin can be estimated using the ratio of recorded elevations of both tsunamis at Hilo, Hawaii.

There are many locations in the Hawaiian Islands that either do not have recordings of tsunami elevations since 1946 or only have recordings of some of these tsunamis. To reconstruct elevations at these locations, Houston et al. (ref. 17) used a finite element numerical model covering all of the Hawaiian Islands to simulate tsunami interactions with these islands. The numerical model calculations were then used to interpolate between recorded elevations and predict elevations at locations lacking historical observations. The

finite element model and the verification simulations of actual historical tsunamis in the Hawaiian Islands are described by Houston (ref. 55). The numerical model calculations allow predictions of tsunamis since 1946 to be made at any location in the Hawaiian Islands. The historical record at Hilo, Hawaii, can then be used to reconstruct elevations for tsunamis prior to 1946. Thus, a record of tsunami activity dating back to 1837 (beginning of Hilo record) can be reconstructed at any location and frequency of occurrence curves determined. Houston et al. (ref. 17) presented frequency of occurrence curves for all of the coastline of the Hawaiian Islands.

1.3.2.2 Predictions for the west coast of the United States

Unlike the Hawaiian islands, the west coast of the continental United States lacks sufficient data to allow tsunami elevation predictions to be made based upon local historical records of tsunami activity. Virtually all of the west coast is completely without data of tsunami occurrence, even for the prominent tsunami of 1964. Only a few locations have historical data for tsunamis other than the 1964 tsunami.

The lack of historical data of tsunami activity on the west coast of the United States necessitates the use of numerical models to predict runup elevations. Brandsma et al. (ref. 96) used a deep-ocean numerical model to predict probable maximum tsunami wave forms in water depths of 600 ft off the west coast of the United States. Houston and Garcia (ref. 97) used a numerical model to predict tsunami elevations in Puget Sound, San Francisco

Bay, and Monterey Bay; and Houston and Garcia (ref. 71), numerical models to predict tsunami elevations on all of the west coast of the United States outside of these regions.

In order to predict tsunami elevations on the west coast of the United States, it is necessary to base the analysis on historical data of tsunami generation in the tsunamigenic regions of the Pacific Ocean of concern to the west coast. Houston and Garcia (ref. 97) showed that the Aleutian-Alaskan area and the west coast of South America are the tsunamigenic regions that are of concern to the west coast. These regions have sufficient data on the generation of major tsunamis to allow a statistical investigation of tsunami generation. It is necessary to use historical data of tsunami occurrence in generation regions to determine occurrence probabilities of tsunamis rather than using data of earthquake occurrence to predict tsunami occurrence. Earthquake occurrence statistics are of little value since a satisfactory correlation between earthquake magnitude and tsunami intensity has never been demonstrated. Not all large earthquakes occurring in the ocean generate noticeable tsunamis. Furthermore, earthquake parameters of importance to tsunami generation, such as focal depth, rise time, and vertical ground motion, have only been determined in recent years for earthquakes.

Houston and Garcia (ref. 71) used the most recent and complete catalog (ref. 87) of tsunami occurrence in the Pacific Ocean to determine relationships between tsunami intensity and frequency of occurrence for the Aleutian-Alaskan and South American regions. The tsunami intensity scale used in the analysis is a modification by Soloviev and Go (ref. 87) of the standard Imamura-Iida tsunami intensity. Intensity is defined as

$$i = \log (2 H_{avg}) \qquad (1)$$

This definition in terms of an average runup H_{avg} (in meters) over a coast instead of a maximum runup elevation at a single location (used for the standard Imamura-Iida scale) tends to eliminate any spurious intensity magnitudes caused by anomalous responses (due, for example, to local resonances) of single isolated locations. Houston and Garcia (ref. 71) assumed that the logarithm of the tsunami frequency of occurrence was linearly related to the tsunami intensity and used linear regression of the historical data to determine the probability distributions of tsunami generation for these two tsunamigenic regions.

To relate the probability distributions of different intensity tsunamis to source characteristics, Houston and Garcia (ref. 71) assumed that the ratio of the source uplift heights producing two tsunamis of different intensities (as defined earlier) was equal to the ratio of the average runup heights produced on the coasts near these tsunami sources. This ratio is equal to $2(^{i}1-^{i}2)$ for two tsunamis having intensities i_1 and i_2.

The directional radiation of energy from tsunami source regions was described in an earlier section. The strong directional radiation from large tsunami sources makes the orientation of a tsunami source relative to a distant site where runup is to be determined very important. Thus, the runup at a distant site due to the generation of a tsunami at one location along a trench cannot be considered as being representative of all possible placements of the tsunami source in the entire region. In order to account for the effects of

directional radiation, Houston and Garcia (ref. 71) segmented the Aleutian and Peru-Chile Trenches and used a deep-ocean propagation model to generate tsunamis in each of the segments. The Aleutian Trench was segmented into 12 sections and the PeruChile Trench into 3 sections. The Aleutian Trench was segmented much finer than the Peru-Chile Trench since the Aleutian Trench is oriented relative to the west coast such that elevations produced on the west coast are very sensitive to the exact location of a source along the Trench. For example, the 1946 and 1957 Aleutian tsunamis did not produce large elevations on the west coast, whereas the 1964 Alaskan tsunami radiated waves toward the northern part of this coast where large elevations were recorded. Uplifts along the Peru-Chile Trench do not radiate energy directly toward the west coast regardless of their position along the trench. The Peru and Chile sections of the Peru-Chile Trench also have constant orientations relative to the west coast of the United States; therefore, elevations on the west coast of the United States are relatively insensitive to source location within these sections.

Houston and Garcia (ref. 71) used deep-ocean propagation numerical models to generate tsunamis having intensities from 2 to 5 in steps of one-half intensity increments in each of the segments of the two trench regions. Tsunamis with intensities less than 2 are too small to produce significant runup on the west coast. An upper limit of 5 was chosen because the greatest tsunami intensity ever reported was less than 5 (ref. 87). Perkins and McGarr (ref. 100) demonstrated that future earthquakes cannot have seismic moments (a measure of earthquake magnitude for great earthquakes) much larger than those of earthquakes that have occurred in recorded history. Since earthquakes only reach certain maximum magnitudes, tsunamis can be expected to have similar

upper limits to intensity. The tsunamis generated in the trench regions were propagated across the deep ocean using the deep-ocean propagation models.

As tsunamis approach the west coast of the United States their wavelengths decrease as a result of the decreasing water depths. The numerical grids used by Houston and Garcia (ref. 71) for deep-ocean propagation have too large a grid cell spacing to properly simulate tsunami propagation over the continental shelf of the west coast. Houston and Garcia (ref. 97) used an analytic solution to propagate tsunamis over the continental shelf to the shoreline. Houston and Garcia (ref. 71) used a numerical model that solved long-wave equations, including nonlinear and dissipative terms, and employed a very fine grid to propagate tsunamis over the continental shelf to the shoreline. Waveforms propagated to the west coast by the deep-ocean propagation models were the input to this nearshore numerical model. Each waveform was propagated from a water depth of 1570 feet to shore using the nearshore model. Numerical simulations of the 1964 tsunami at Crescent City and Avila Beach, California, were used to verify the numerical model. At each numerical grid location on the west coast, a group of 106 waveforms were determined by Houston and Garcia (ref. 71)--seven waveforms (for intensities from 2 to 5 in one-half intensity increments) for each segment of the Aleutian and Peru-Chile Trenches. Each of these waveforms had an associated probability equal to the probability that a certain intensity tsunami would be generated in a particular segment of a trench region.

The maximum "still-water" elevation produced during tsunami activity is the result of a superposition of tsunamis and tides. Therefore, the statistical effect of the astronomical tides on total tsunami runup must be included in a

predictive scheme. Houston and Garcia (ref. 97) used an analytical solution to determine combined tsunami and astronomical tide cumulative probability distributions. Houston and Garcia (ref. 71) also employed a direct numerical solution similar to that used by Petrauskas and Borgman (ref. 101) to determine combined tsunami and astronomical tide cumulative probability distributions. It was necessary to employ a numerical solution since the tsunami waveforms calculated by Houston and Garcia (ref. 66) using a nearshore numerical shore did not have a simple form (e.g., sinusoidal). Houston et al. (ref. 17) did not need to consider the effect of the astronomical tides in their elevation predictions for the Hawaiian Islands since the tidal range is quite small for these islands and the local historical data implicitly contained the effects of the astronomical tides.

In order to perform a convolution of tsunami and astronomical tides, Houston and Garcia (ref. 71) calculated tidal elevations for a year at locations all along the west coast using harmonic analysis methods (ref. 102). The year was then divided into 15-minute segments, and 24-hour tsunami waveforms were allowed to arrive at the beginning of each of these 15-minute segments and then superposed upon the astronomical tide for the 24-hour period. The maximum combined tsunami and astronomical tide elevation over the 24-hour period was determined for tsunamis arriving at each of these 15-minute starting times during a year. All of the maximum elevations had an associated probability equal to the probability that a certain intensity tsunami would be generated in a particular segment of the two trench regions and arrive during a particular 15-minute period of a year. These maximum elevations with associated probabilities were used by Houston and Garcia (ref. 71) to determine cumulative probability distributions of combined tsunami and

astronomical tide elevations. The 100- and 500-year elevations were determined for locations along the west coast of the United States using these cumulative probability distributions. Elevations for arbitrary return periods can be obtained by assuming that the 100- and 500-year elevation determined by Houston and Garcia (ref. 71) follow a logarithmic distribution.

1.3.2.3 Risk Calculation

The average frequency of occurrence F calculated by Houston et al. (ref. 17) and Houston and Garcia (ref. 71) is a mean exceedance frequency, i.e., an average frequency per year of tsunamis occurring and producing an equal or greater elevation. It also is possible to calculate the chance of a given elevation being exceeded during a particular period of time. Such a calculation is a risk calculation.

Tsunamis are usually caused by earthquakes, and earthquakes are often idealized as a generalized Poisson process (ref. 103). Many investigators have assumed that tsunamis also follow a stochastic process (refs. 81, 83). The probability that a tsunami with an average frequency of occurrence of F is exceeded in D years, assuming that tsunamis follow a Poisson process, is given by the following equation:

$$P = 1 - e^{-FD} \qquad (2)$$

For example, the probability that a 1-in-100-year elevation will occur in a 50-year period is

$$P = 1 - e^{-(0.01)(50)}$$
$$= 1 - e^{-0.5}$$
$$= 1 - 0.61$$
$$= 0.39$$

1.3.2.4 Tsunami Hazard Maps

Figure 1 is the general tsunami hazard map for the United States, and Figures 2 through 10 are the detailed maps (refs. 17, 71, 97, 98). Houston et al. (ref. 17) presented frequency curves of tsunami elevations for the Hawaiian Islands, and Houston and Garcia (refs. 71, 97), Garcia and Houston (ref. 98), and Houston (ref. 72) predicted 100- and 500-year elevations for the west coast of the continental United States. A tsunami elevation with a 90 percent probability of not being exceeded in 50 years represents a 475-year elevation. This is easily calculated from the previous section by setting D = 50 and P = 0.1 (10 percent probability of being exceeded) and solving for 1/F.

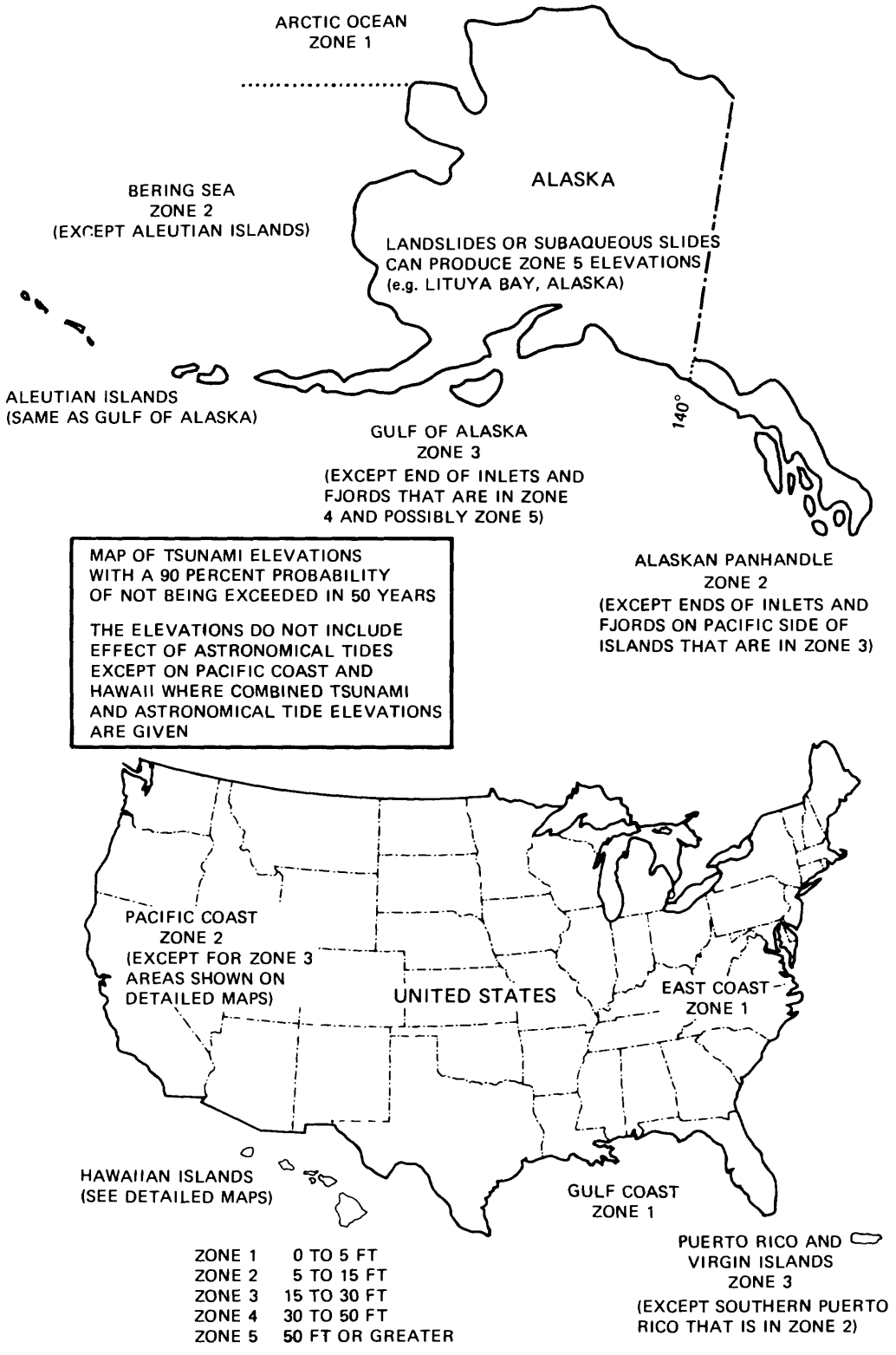

Figure 1. Tsunami hazard map

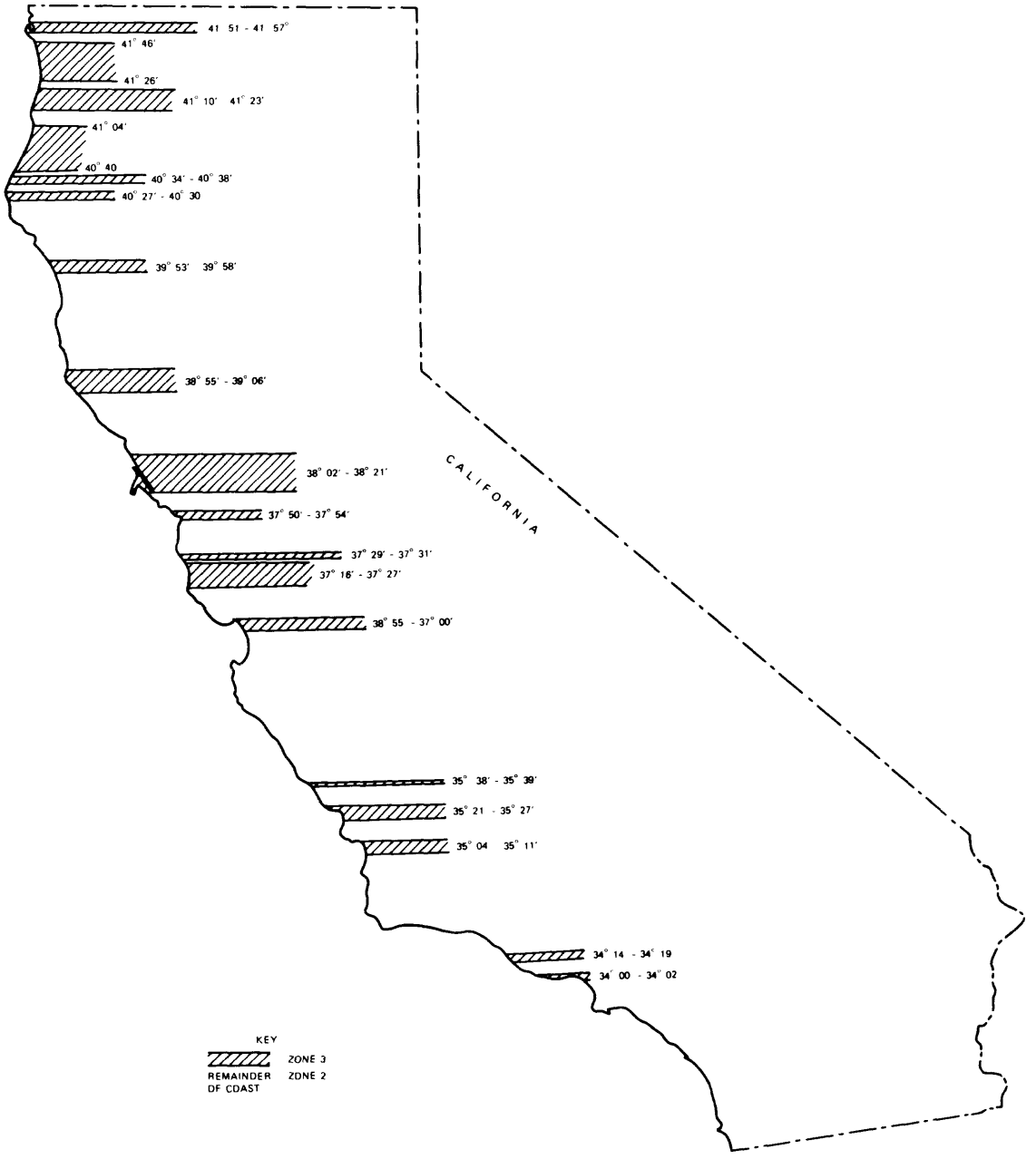

Figure 2. Tsunami hazard for California (adapted from Houston and Garcia, 1974 and 1978; Garcia and Houston, 1975)

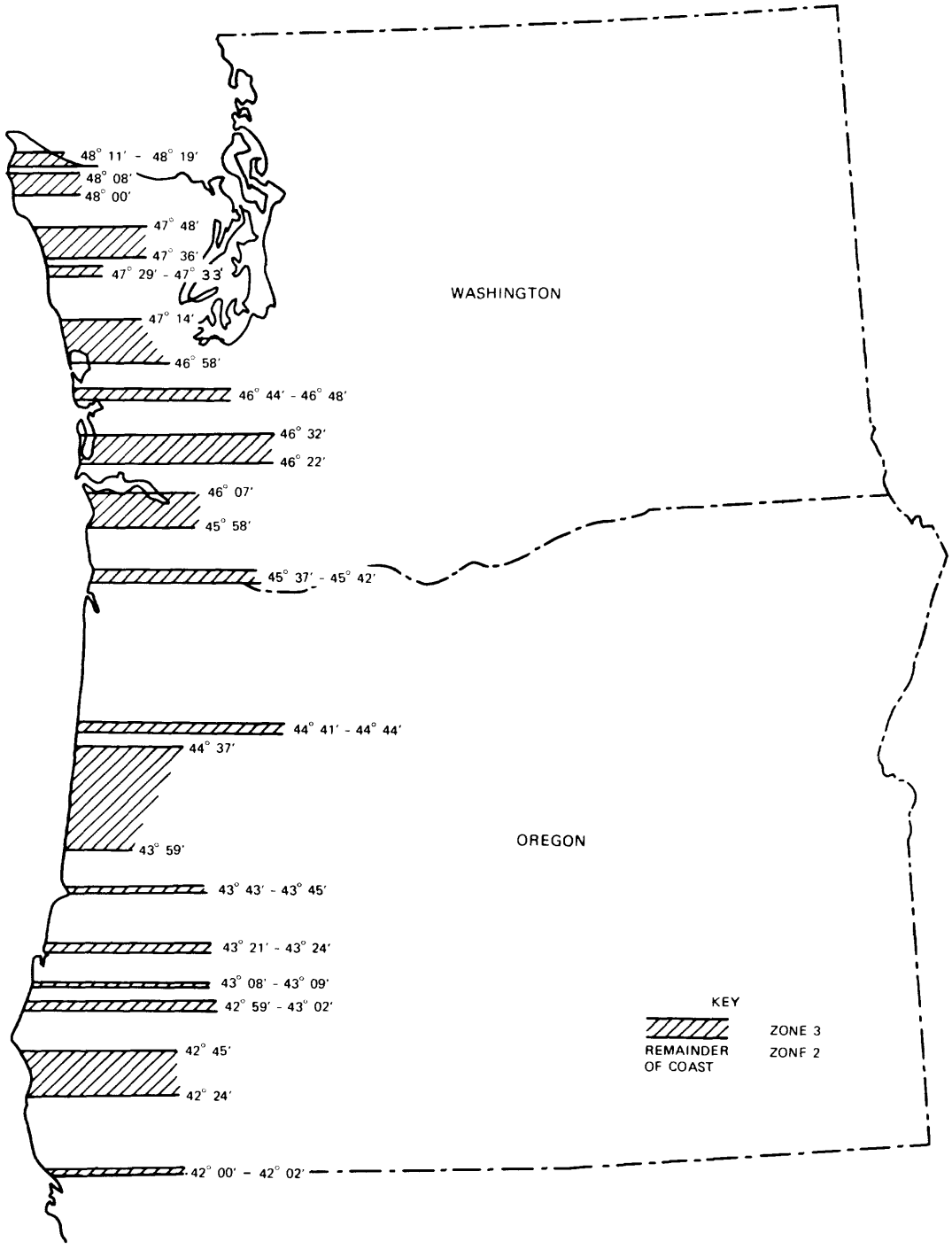

Figure 3. Tsunami hazard for Oregon and Washington (adapted from Houston and Garcia, 1978)

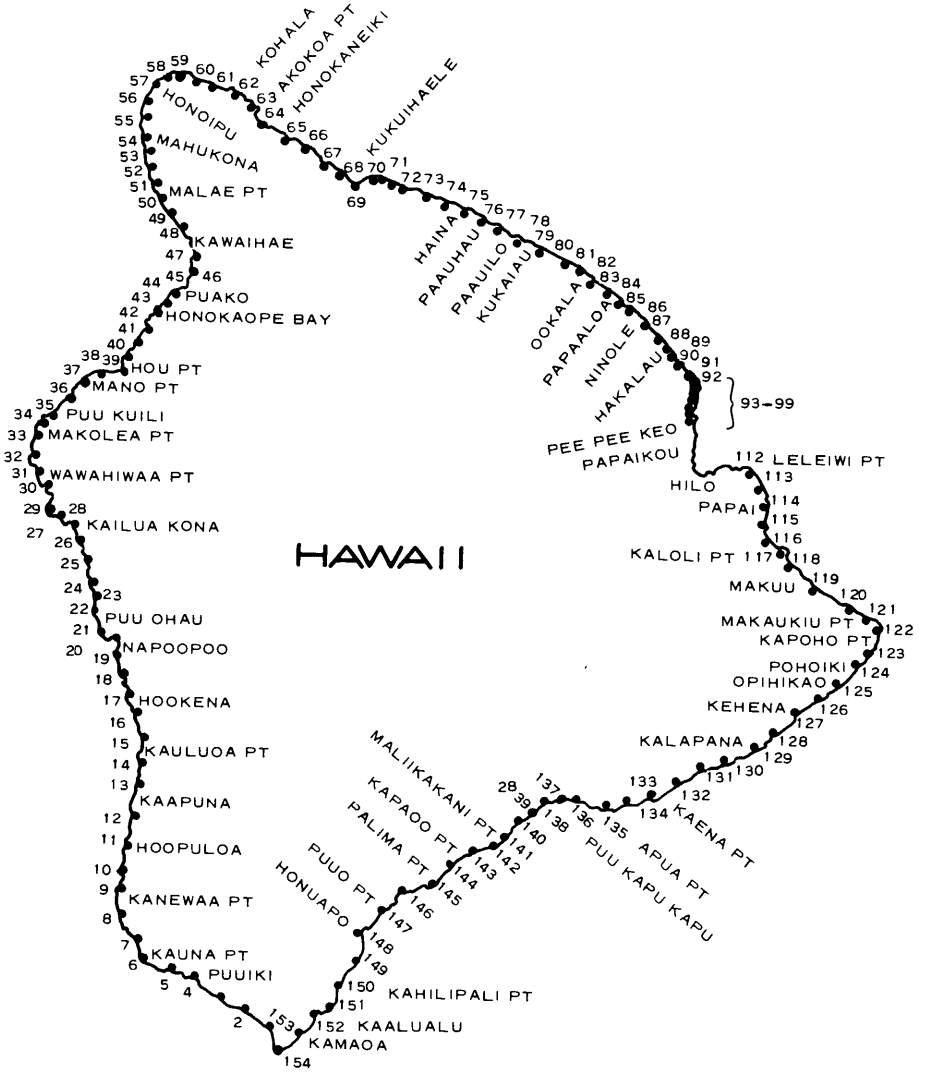

LOCATION NUMBER	ZONE
154 TO 4	3
4 TO 11	2
11 TO 13	3
13 TO 17	2
17 TO 19	3
19 TO 27	4
27 TO 31	3
31 TO 48	2
48 TO 61	3
61 TO 62	4
62 TO 64	5
64 TO 66	3
66 TO 69	4
69 TO 70	5
70 TO 77	4
77 TO 82	3
82 TO 110	4
110 TO 124	3
124 TO 127	4
127 TO 130	3
130 TO 134	4
134 TO 141	5
141 TO 154	4

Figure 4. Tsunami hazard map for Island of Hawaii (adapted from Houston et al., 1977)

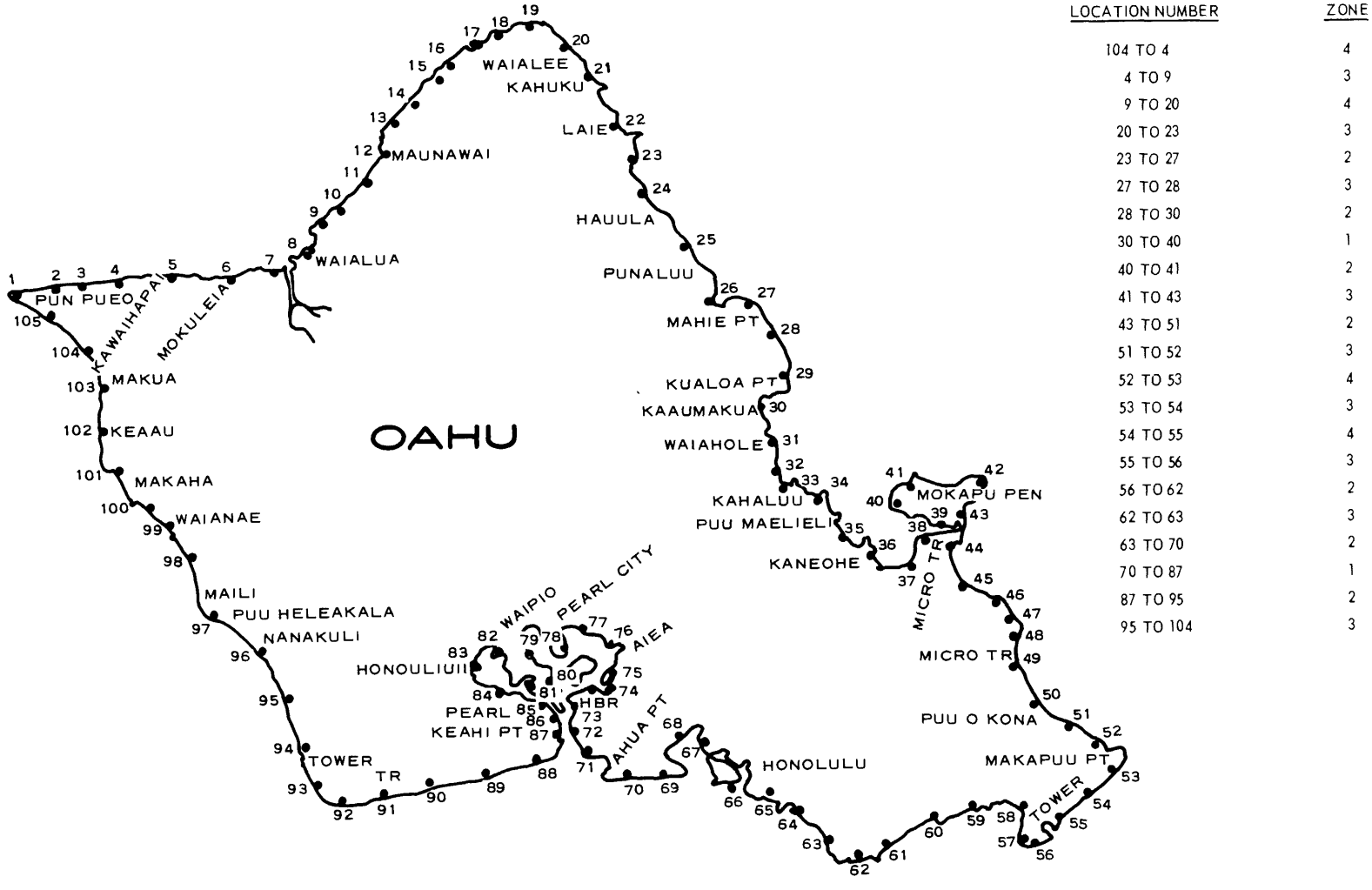

LOCATION NUMBER	ZONE
104 TO 4	4
4 TO 9	3
9 TO 20	4
20 TO 23	3
23 TO 27	2
27 TO 28	3
28 TO 30	2
30 TO 40	1
40 TO 41	2
41 TO 43	3
43 TO 51	2
51 TO 52	3
52 TO 53	4
53 TO 54	3
54 TO 55	4
55 TO 56	3
56 TO 62	2
62 TO 63	3
63 TO 70	2
70 TO 87	1
87 TO 95	2
95 TO 104	3

Figure 5. Tsunami hazard map for Oahu (adapted from Houston et al., 1977)

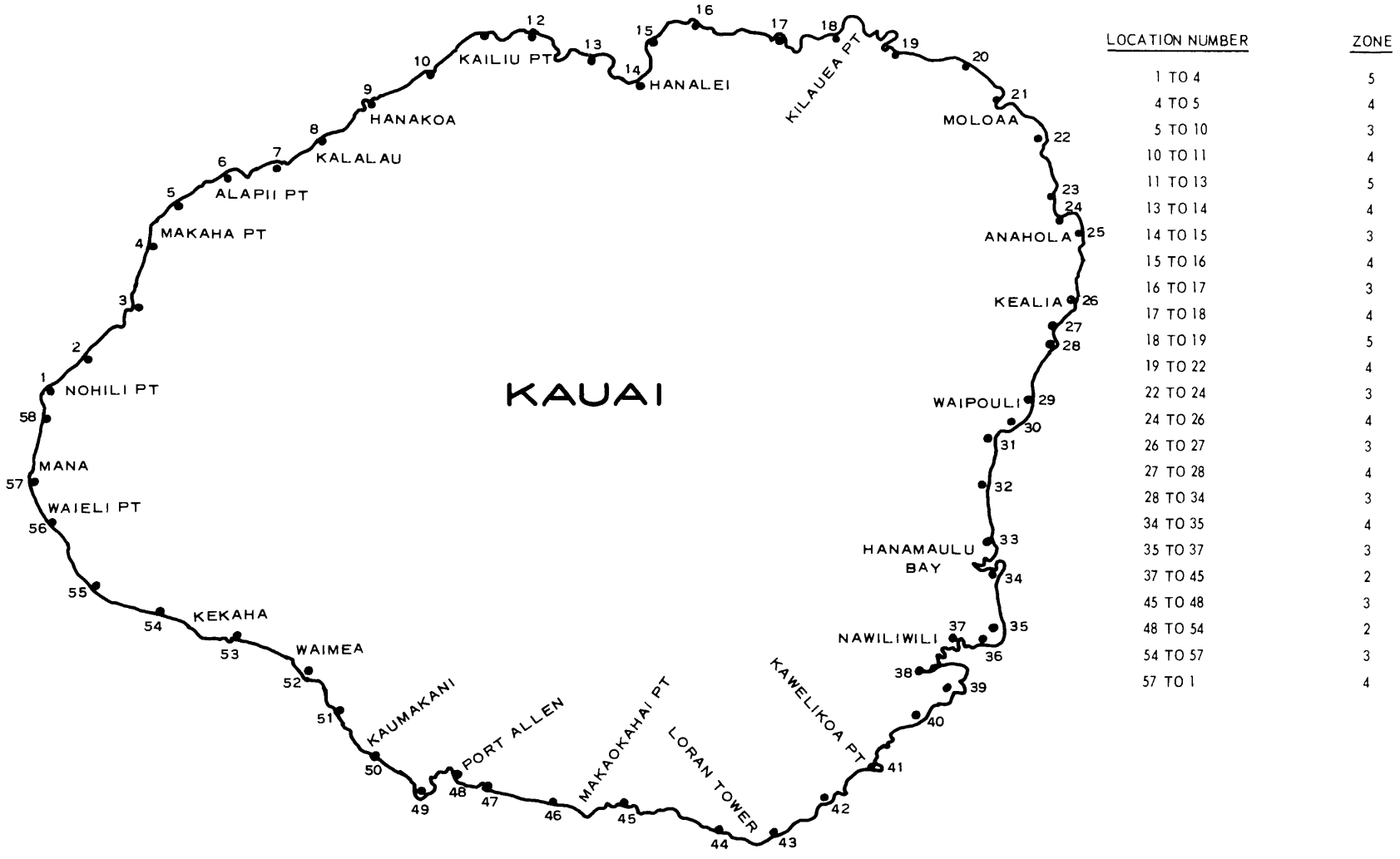

Figure 6. Tsunami hazard map for Kauai (adapted from Houston et al., 1977)

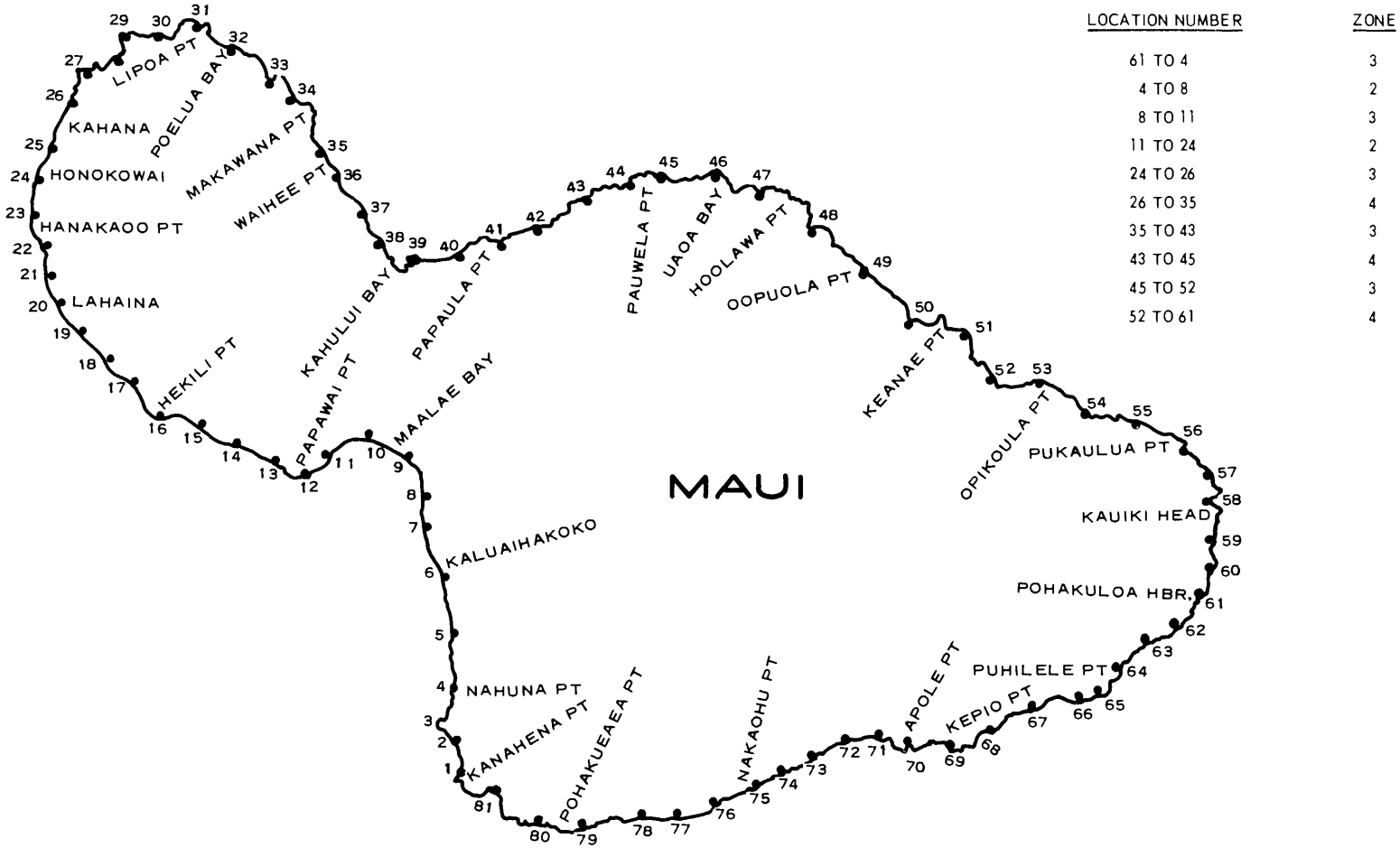

Figure 7. Tsunami hazard map for Maui (adapted from Houston et al., 1977)

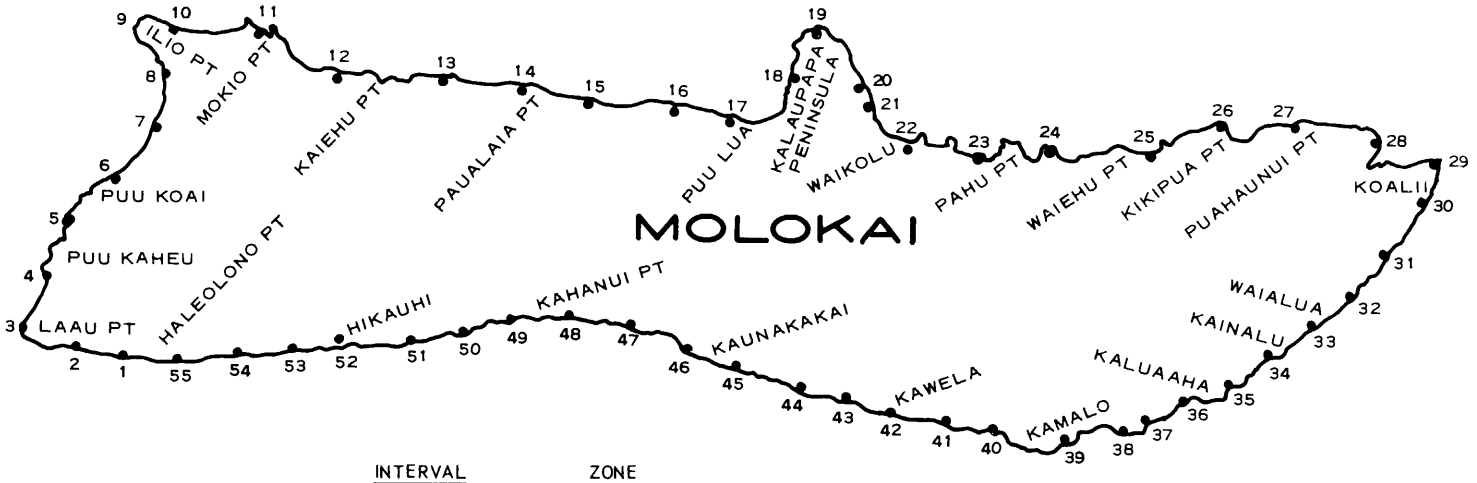

INTERVAL	ZONE
55 TO 2	3
3 TO 4	4
4 TO 5	3
5 TO 18	4
18 TO 21	3
21 TO 22	4
22 TO 26	5
26 TO 31	4
31 TO 32	3
32 TO 37	2
37 TO 52	1
52 TO 55	2

Figure 8. Tsunami hazard map for Molokai (adapted from Houston et al., 1977)

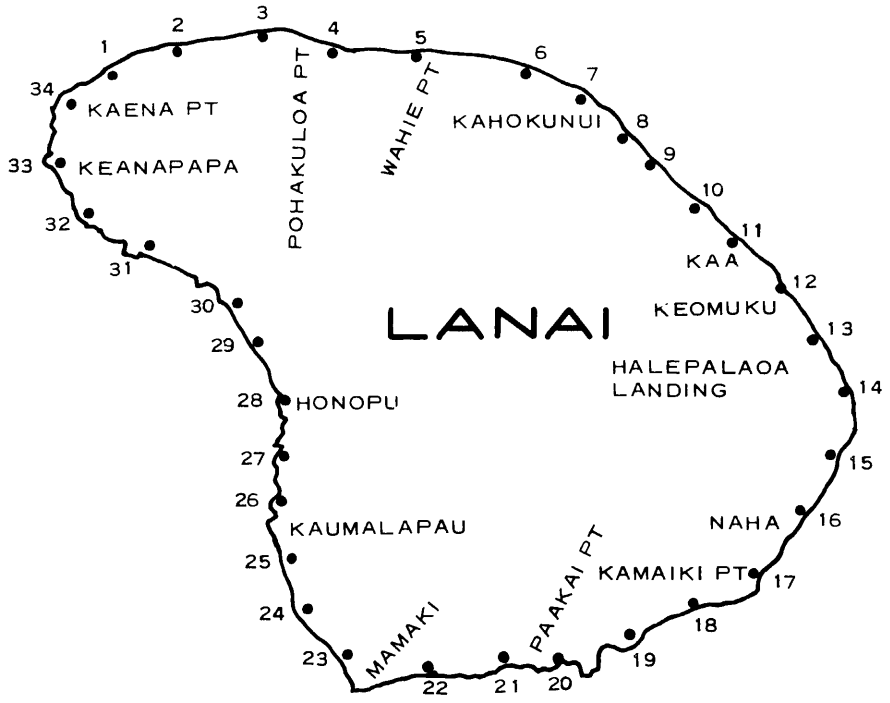

LOCATION NUMBER	ZONE
1 TO 6	3
6 TO 10	2
10 TO 14	3
14 TO 1	2

Figure 9. Tsunami hazard map for Lanai (adapted from Houston et al., 1977)

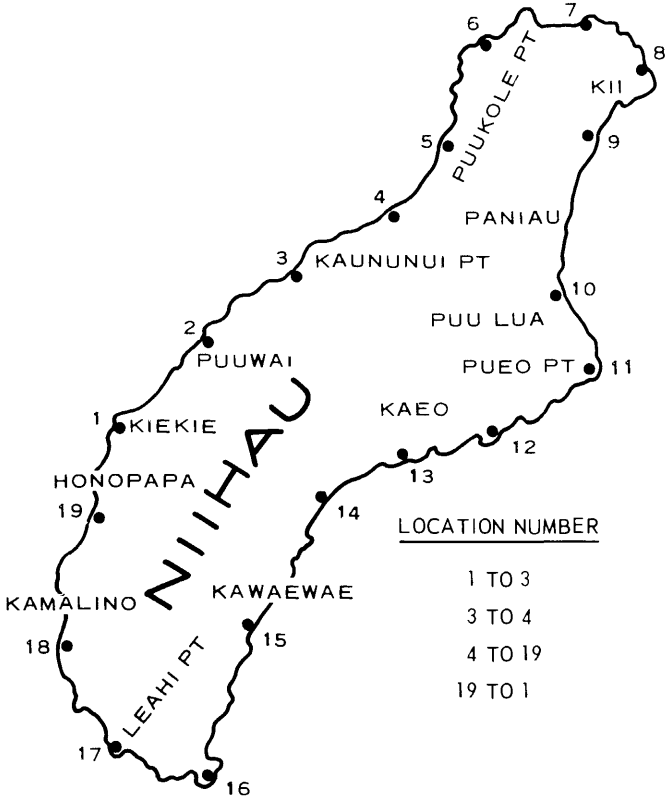

LOCATION NUMBER	ZONE
1 TO 3	3
3 TO 4	4
4 TO 19	3
19 TO 1	3

Figure 10. Tsunami hazard map of Niihau (adapted from Houston et al., 1977)

1.4 References

1. Iida, K., Cox, D. C., and Pararas-Carayannis, G., "Preliminary Catalog of Tsunamis Occurring in the Pacific Ocean," HIG-67-10, August 1967, Hawaii Institute of Geophysics, University of Hawaii, Honolulu, Hawaii.

2. Pararas-Carayannis, G., "Catalog of Tsunamis in Hawaii," Report SE-4, March 1978, World Data Center A for Solid Earth Geophysics, Boulder, Colorado.

3. Wilson, B. W. and Torum, A., "The Tsunami of the Alaskan Earthquake, 1964: Engineering Evaluation," Technical Memorandum No. 25, May 1968, Coastal Engineering Research Center, CE.

4. Gutenberg, B. and Richter, C. F., Seismicity of the Earth and Associated Phenomena, Hafner Publishing Co., New York, 1965.

5. Sykes, L. R., "Mechanics of Earthquake and Nature of Faulting on the MidOceanic Ridges," Journal of Geophysical Research, 1972, pp. 2131-2153.

6. Wiegel, R. L., Oceanographic Engineering, Prentice-Hall, Inc., New York, 1964.

7. Davidson, C., Great Earthquakes, T. Hurby and Co., London, 1936.

8. Reid, H. F., "The Lisbon Earthquake of November 1, 1755," Bulletin of the Seismological Society of America, Vol. 4, No. 2, 1914, pp. 53-80.

9. Heck, N. H., "List of Seismic Sea Waves," Bulletin of the Seismological Society of America, Vol. 37, No. 4, 1947, pp. 269-286.

10. Gutenberg, B. (ed), Internal Constitution of the Earth, Dover Publications, Inc., 1951.

11. McKinley, C., "A Descriptive Narrative of the Earthquake of August 31, 1886, with Notes of Scientific Investigations," City Year Book of 1886, Charleston, South Carolina, 1887.

12. Reid, H. F. and Taber, S., "The Virgin Islands Earthquakes of 1867-1868," Bulletin of the Seismological Society of America, Vol. 10, No. 1, 1920, pp. 9-30.

13. Reid, H. F. and Taber, S., "The Porto Rico Earthquakes of October-November, 1918," Bulletin of the Seismological Society of America, Vol, 9, No. 4 , 1919, pp. 103-123.

14. Houston, J. R., Butler, H. L., Whalin, R. W., and Raney, D., "Probable Maximum Tsunami Runup for Distant Seismic Events," NORCO-NP-1 PSAR, May 1975, Fugro, Inc., Long Beach, California, pp. 253.

15. Cox, D. C. and Morgan, J., "Local Tsunamis and Possible Local Tsunamis in Hawaii," HIG-77-14, November 1977, Hawaii Institute of Geophysics, University of Hawaii, Honolulu, Hawaii.

16. Loomis, H. G., "Tsunami Wave Runup Heights in Hawaii," HIG-76-5, May 1976, Hawaii Institute of Geophysics, University of Hawaii, Honolulu, Hawaii.

17. Houston, J. R., Carver, R. D., and Markle, D. G., "Tsunami-Wave ElevationFrequency of Occurrence for the Hawaiian Islands," Technical Report H-77-16 August 1977, U.S. Army Engineer Waterways Experiment Station, CE, Vicksburg, Mississippi.

18. Lomnitz, C., Global Tectonics and Earthquakes Risk, Elseview, Amsterdam, 1973.

19. Cox, D. C. and Pararas-Carayannis, G., "Catalog of Tsunamis in Alaska," Report SE-1, March 1976, World Data Center A for Solid Earth Geophysics, Boulder, Colorado.

20. National Academy of Sciences, 1972, "The Great Alaska Earthquake of 1964: Oceanography and Coastal Engineering," ISBN0-309-1605-3, Washington, D.C.

21. Magoon, O. T., "Structural Damage by Tsunamis,- Coastal Engineering Santa Barbara Specialty Conference of the Waterways and Harbors Division, American Society of Civil Engineers, October 1965, pp. 35-68.

22. Weber, H. F. and Kiessling, E. W., "Historic Earthquakes Effects in Ventura County," California Geology, May 1978, California Division of Mines and Geology, Vol. 31, No. 5, pp. 103-107.

23. Wood, H. O. and Heck, N. H., "Earthquake History of the United States, Part II, Stronger Earthquakes of California and Western Nevada," 1966, U.S, Coast and Geodetic Survey.

24. Marine Advisors, Inc., 1965, "An Examination of the Evidence for the Reported Santa Barbara Coast Tsunami of December 1812," unpublished report submitted to the Southern California Edison Company.

25. Davis, C. J., "The Tidal Wave of 23 May 1960," Memorandum, Resident Engineer Office, Johnston Island, U.S. Army Engineer District, Honolulu, May 1960.

26. Houston, J. R., "Tsunami Elevation Predictions for American Samoa;" Technical Report HL-80-16, September 1980, U.S. Army Engineer Waterways Experiment Station, CE, Vicksburg, Mississippi.

27. Berg, E., Cox, D. C., Furumoto, A. S., Kajiura, K., Kawasumi, H. and Shima, E., "Field Survey of the Tsunamis of 28 March 1964 in Alaska, and Conclusions as to the Origin of the Major Tsunami," Report No. HIG-70-2, January 1970, Hawaii Institute of Geophysics, Honolulu, Hawaii.

28. Momoi, T., "Some Remarks on Generation of Waves from Elliptical Wave Origin,- Bulletin of the Earthquake Research Institute, Tokyo University, Vol. 40, 1962, pp. 297-307.

29. Takahasi, R. and Hatori, T., "A Model Experiment on the Tsunami Generation from a Bottom Displacement Area of Elliptic Shape," Bulletin of the Earthquake Research Institute, Tokyo University, Vol, 40, 1962, pp. 873-883.

30. Hatori, T., "Directivity of Tsunamis," Bulletin of the Earthquake Research Institute, Tokoyo University, Vol. 41, 1963, pp. 61-81.

31. Hammack, J. L., "Tsunamis-A Model of their Generation and Propagation," Report No. KH-R-28, June 1972, California Institute of Technology, Pasadena, California.

32. Hammack, J. L. and Segur, H., "Modeling Criteria for Long Waves," Journal of Fluid Mechanics, Vol. 84, Pt. 2, January 1978.

33. Goring, D. G., "Tsunamis-The Progatation of Long Waves onto a Shelf," Report No. KH-R-38, November 1978, California Institute of Technology, Pasadena, California.

34. MacDonald, G. A., Shepard, F. P., and Cox, D. C., "The Tsunami of April 1, 1946, in the Hawaiian Islands," Pacific Science, Vol. 1, No. 1, January 1947, pp. 21-37.

35. Brown, D. L., "Tsunami Activity Accompanying the Alaskan Earthquake, 27 March 1964," April 1964, U.S. Army Engineer District, Alaska, CE, Anchorage, Alaska.

36. Nasu, N., "Heights of Tsunamis and Damage to Structures," Bulletin of the Earthquake Research Institute, Supplementary Vol, 1, Tokoyo Imperial University, 1934, pp. 218-235.

37. Eaton, J. P., Richter, D. H., and Ault, W. V., "The Tsunami of May 23, 1960, on the Island of Hawaii," Bulletin of the Seismological Society of America, Vol. 51, No. 2, April 1964, pp. 135-157.

38. Van Dorn, W. G., "Tsunami Response at Wake Island: A Model Study, "Journal of Marine Research, Vol, 28, 1970, pp. 336-344.

39. Jordaan, J. M. and Adams, W. M., "Tsunami Height, Oahu, Hawaii: Modeland Nature," Proceedings of the Eleventh Conference on Coastal Engineering, Institute of Civil Engineering and the American Society of Civil Engineering, 1968, pp. 1555-1574.

40. Wiegel, R. L., "Water Wave Equivalent to Mach-reflection," Proceedings of the Ninth Conference on Civil Engineering, ASCE, Lisbon, 1964, pp. 82-102.

41. Palmer, R. Q., Mulvihill, M. E., and Funasaki, G. T., "Hilo HarborTsunamis Model-Reflected Waves Superimposed," Coastal Engineering: Santa Barbara Specialty Conference, ASCE, 1964, pp. 24-31.

42. Grace, R. A., "Reef Runway Hydraulic Model Study, Honolulu International Airport, Three Dimensional Tsunami Study," Department of Transportation, State of Hawaii, 1969, Honolulu.

43. Hebenstreit, G. T. and Reid, R. D.," Reflection and refraction of solitary waves - a numerical investigation," Texas A&M University Technical Report 78-7-T, 1978.

44. Omer, G. C. and Hall, H. H., "The Scattering of Tsunamis by a Cylindrical Island," Bulletin of the Seismological Society of America, Vol. 39, 1949, pp. 257-260.

45. Hom-ma, S., "On the Behavior of Seismic Sea Waves Around a Circular Island," Geophysical Magazine, Vol. 21, 1950, pp. 199-208.

46. Kajiura, K., "The Leading Wave of a Tsunami," Bulletin, Earthquake Research Institute, Tokyo University, Vol. 41, 1963, pp. 535-571.

47. Longuet-Higgins, M. S., "On the trapping of wave energy round island," Journal of Fluid Mechanics, Vol. 29, 1967, pp. 781-821.

48. Camfield, F. E., "Tsunami Engineering," U. S. Army Coastal Engineering Research Center, Special Report No. 8, February 1980,

49. Jonsson, I. G., Skovgaard, O., and Brink-Kjaer, O., "Diffraction and Refraction Calculation for Waves Incident on an Island," Journal of Marine Research, Vol. 34, No. 3, 1976, pp. 469-496.

50. Hwang, L-S., Butler, H. L., and Divoky, H. L., "Tsunami Model: Generation and Open-Sea Characteristics," Bulletin of the Seismological Society of America, Vol. 62, No. 6, December 1972, pp. 1579-1594..

51. Chen, M. H. T., "Tsunami Propagation and Response to Coastal Areas," HI G-73-15, December 1973, Hawaii Institute of Geophysics, University of Hawaii, Honolulu, Hawaii.

52. Garcia, A. W., "Effect of Source Orientation and Location in the Peru-Chile Trench on Tsunami Amplitude Along the Pacific Coast of the Continental United States," Research Report H-76-2, September 1976, U.S. Army Engineer Waterways Experiment Station, CE, Vicksburg, Mississippi.

53. Leendertse, J. J., "Aspects of a Computational Model for Long-Period Water-Wave Propagation," RM-5294-PR, The Rand Corp., 1967.

54. Plafker, G., "Tectonics of the March 27, 1964, Alaska Earthquake," Geological Survey Professional Paper, 543-I, pp. 11-174.

55. Houston, J. R., "Interaction of Tsunamis with the Hawaiian Islands Calculated by a Finite-Element Numerical Model," Journal of Physical Oceanography, January 1978, Vol. 8, No. 1, pp. 93-101.

56. Plafker, G. and Savage, J. C., "Mechanics of the Chilean Earthquakes of May 21 and 22, 1960," Bulletin of the Geological Society of America, Vol. 81, 1970.

57. Houston, J. R. and Garcia, A. W., "Tsunami Elevation Predictions from Numerical Models," American Society of Civil Engineers Annual Convention, October 1977, San Francisco, California.

58. Vastano, A. C. and Reid, R. O., "Tsunami Response for Islands: Verification of a Numerical Procedure," Journal of Marine Research, Vol. 25, 1967, pp. 129-139.

59. Vastano, A. C. and Bernard, E. N., "Transient Long Wave Response for a Multiple Island System," Journal of Physical Oceanography, Vol. 3, 1973, pp. 406-418.

60. Bernard, E. N. and Vastano, A. C., "Numerical Computation of Tsunami Response for Island Systems," Journal of Physical Oceanography, Vol. 7, 1977, pp. 389-395.

61. Lautenbacher, C. C., "Gravity Wave Refraction by Islands," Journal of Fluid Mechanics, Vol. 41, 1970, pp. 655-672.

62. Mei, C. C., "Aspects of a Hybrid Element Method for Shallow Water Waves Near a Shore," Proceedings of the National Science Foundation Tsunami Workshore, May 1979, Coto de Caza, California.

63. Chen, H. S. and Mei, C. C., "Oscillations and Wave Forces in a Man-made Harbor in the Open Sea," Proceedings of the 11th Symposium on Naval Hydrodynamics, 1974, pp. 573-594.

64. Sklarz, M. A., Spielvogel, L. Q., and Loomis, H. G., "Numerical Simulation of the November 29, 1975, Island of Hawaii Tsunami by the Finite Element Method," JIMAR-78-0004, 1978, Joint Institute for Marine and Atmospheric Research, University of Hawaii, Honolulu, Hawaii.

65. Tuck, E. O., "Models for Predicting Tsunami Propagation," Proceedings of the National Science Foundation Tsunami Workshop, May 1979, Coto de Caza, California.

66. Heitner, K. L. and Housner, G. W., "Numerical Model for Tsunami Run-up," Journal of the Waterways, Harbors and Coastal Engineering Division, ASCE, No. WW3, August 1970, pp. 701-719.

67. Mader, C. L., "Numerical Simulation of Tsunamis," Journal of Physical Oceanography, Vol, 4, No. 1, January 1974, pp. 74-82.

68. Garcia, W. J., "A Study of Water Waves Generated by Tectonic Displacements," Report HEL 16-9, 1972, College of Engineering, University of California, Berkeley, California,

69. Aida, "Numerical Experiments for the Tsunami Propagation - the 1964 Niigata Tsunami and the 1968 Tokachi-oki Tsunami," Bulletin of the Earthquake Research Institute, Vol. 47, 1969, pp. 673-700.

70. Aida, I., "Reliability of a Tsunami Source Model Derived from Fault Parameters," Journal of the Physics of the Earth,- Vol, 26, 1978, pp. 57-73.

71. Houston, J. R. and Garcia, A. W., "Type 16 Flood Insurance Study: Tsunami Predictions for the West Coast of the Continental United States," Technical Report H-78-26, December 1978, U.S. Army Engineer Waterways Experiment Station, CE, Vicksburg, Mississippi.

72. Houston, J. R., "Type 19 Flood Insurance Study: Tsunami Predictions for Southern California," Technical Report HL-80-18, September 1980, U.S. Army Engineer Waterways Experiment Station, CE, Vicksburg, Mississippi.

73. Kawahara, M., Takeuchi, N., and Yoshida, T., "Two Step Explicit Finite Element Method for Tsunami Wave Propagation Analysis," International Journal for Numerical Methods in Engineering, Vol. 12, 1978, pp. 331-351.

74. Gray, W. G., "Do Finite Element Models Simulate Surface Flow," 3rd International Conference on Finite Elements in Water Resources, May 1980, Oxford, Mississippi.

75. Chen, M., Divoky, D., and Hwang, L. S., "Application of the Three-Dimensional Boussinesq Type Equations to Tsunami Modeling," Proceedings of the Symposium on Tsunamis, March 1977, Ensenada, Mexico, Published in the Manuscript Report Series No. 48, 1978, Department of Fisheries and the Environment, Ottawa, Canada.

76. Bretschneider, C. L. and Wybro, P. G., "Tsunami Inundation Prediction," Proceedings of the 15th Coastal Engineering Conference, American Society of Civil Engineers, pp. 1000-1024,

77. Cross, R. H., "Water Surge Forces on Coastal Structures," HEL-9-10, 1966, University of California, Berkeley, California.

78. Houston, J. R. and Butler, H. L., "A Numerical Model for Tsunami Inundation," Technical Report HL-79-2, February 1979, U.S. Army Engineer Waterways Experiment Station, CE, Vicksburg, Mississippi.

79. Butler, H. L., "Numerical Simulation of Coos Bay-South Slough Complex," Technical Report H-78-22, December 1978, U.S. Army Engineer Waterways Experiment Station, CE, Vicksburg, Mississippi.

80. Cox, D. C., "Tsunami Height-Frequency Relationship of Hilo," Unpublished Paper, November 1964, Hawaii Institute of Geophysics, University of Hawaii, Honolulu, Hawaii,

81. Wiegel, R. L., "Protection of Crescent City, California, from Tsunami Waves," March 1965, Redevelopment Agency of the City of Crescent City, Berkeley, California.

82. Adams, W. M., "Tsunami Effects and Risk at Kahuku Point, Oahu, Hawaii," Engineering Geology Case Histories, Geological Society of America, No. 8, 1970, pp. 63-70.

83. Rascon, O. A. and Villarreal, A. G., "On a Stochastic Model to Estimate Tsunami Risk," Journal, Hydraulic Research, Vol. 13, No. 4, 1975, pp. 383-403.

84. U. S. Nuclear Regulatory Commission, "Probable Maximum Tsunami Flooding," NUREG-751087, Section 2.4.6.

85. Gumbel, E. J., "The Calculated Risk in Flood Control," Applied Scientific Research, Section A, Vol. 5, 1955, pp. 273-280.

86. Borgman, L. E. and Resio, D. T., "External Prediction in Wave Climatology," Ports 77, 4th Annual Symposium of the Waterway, Port, Coastal, and Ocean Division, American Society of Civil Engineers, Vol. 1, March 1977, pp. 394-412,

87. Soloviev, S. L. and Go, Ch. N., "Catalog of Tsunamis in the Pacific (Main Data)," 1969, Union of Soviet Socialist Republics, Moscow.

88. Beringhausen, W. H., "Tsunamis and Seismic Seiches Reported from the Eastern Atlantic South of the Bay of Biscay," Bulletin of the Seismological Society of America, Vol. 54, No. 1, 1964, pp. 429-442.

89. Beringhausen, W, H., "Tsunamis Reported from the West Coast of South America, 1562-1960," Bulletin of the Seismological Society of America, Vol. 52, No. 4, 1962, pp. 915-921.

90. Shepard, F. P., MacDonald, G. A., and Cox, D. C., "The Tsunami of April 1, 1946," Bulletin of the Scripps Institution of Oceanography, Vol. 5, No. 6, 1950, University of California, La Jolla, California, pp. 391-528.

91. MacDonald, G. A. and Wentworth, C. K., "The Tsunami of November 4, 1952, on the Island of Hawaii, Bulletin of the Seismological Society of America, Vol. 44, No. 3, July 1954, pp. 463-469.

92. Fraser, G. D., Eaton, J. P., and Wentworth, C. K., "The Tsunami of March 9, 1957, on the Island of Hawaii," Bulletin of the Seismological Society of America, Vol. 49, No. 1, January 1959, pp. 79-90.

93. U.S. Army Engineer District, Honolulu, CE, "The Tsunami of 23 May 1960 in Hawaii," Final Post Flood Report, 25 April 1962, Honolulu, Hawaii.

94. Keys, J. G., "The Tsunami of 22 May 1960, In the Samoa and Cook Islands, "Bulletin of the Seismological Society of America, Vol. 53, No. 6, December 1963, pp. 1211-1227,

95. Wybro, P. G., "M. S. Plan B" (to be published), University of Hawaii, Honolulu, Hawaii.

96. Brandsma, M., Divoky, D., and Hwang, L. S., "Tsunami Atlas for the Coasts of the United States," Report No. TC-486, 1977, Tetra Tech, Inc., Pasadena, California.

97. Houston, J. R. and Garcia, A. W., "Type 16 Flood Insurance Study: Tsunami Predictions for Pacific Coastal Communities," Technical Report H74-3, May 1974, U. S. Army Engineer Waterways Experiment Station, CE, Vicksburg, Mississippi.

98. Garcia, A. W. and Houston, J. R., "Type 16 Flood Insurance Study: Tsunami Predictions for Monterey and San Francisco Bays and Puget Sound," Technical Report H-75-17, November 1975, U.S. Army Engineer Waterways Experiment Station, CE, Vicksburg, Mississippi.

99. Perkins, D., "The Search for Maximum Magnitude," National Oceanographic and Atmospheric Administration Earthquake Information Bulletin, July 1972, pp. 18-23.

100. McGarr, A., "Upper Limit to Earthquake Size," Nature, Vol. 262, No. 5567, July 1976, pp. 378-379.

101. Petrauskas, C. and Borgman, L. E., "Frequencies of Crest Heights for Random Combinations of.Astronomical Tides and Tsunamis Recorded at Crescent City, California," Technical Report HEL-16-8, 1971, University of California, Berkeley, California.

102. Shuremen, P., "Manual of Harmonic Analysis and Prediction of Tides," Special Publication 98, 1941, United States Department of Commerce, United States Coast and Geodetic Survey, Washington, D.C.

103. Newmark, N. M. and Rosenblueth, E., Fundamentals of Earthquake Engineering, Prentice-Hall, Englewood Cliffs, 1971.

2. Effects on Facilities

The effect of a tsunami on structures and other facilities will depend on the wave period, the height of the tsunami at the shoreline and subsequent runup, and the current velocity associated with the tsunami. The height of the tsunami will determine the buoyant force on structures and materials, and will also determine the magnitude of the current velocities. The height and period of the waves will determine the extent of flooding, and the current velocity will determine the magnitude of the hydrodynamic forces acting against structures and the velocity of material carried forward by the movement of the water.

The tsunami height and period may be determined using the methods described in chapter 1, "Tsunami Hazard." A maximum value of the current velocity for shoreline flooding can be obtained using the equation suggested by Keulegan (ref 1), which is given as

$$u = 2(gh)^{1/2} \qquad (3)$$

(1)

where u = the current velocity,

h = the tsunami height at any point on the shoreline,

g = the gravitation.al acceleration.

Approximate values of current velocities associated with tsunamis approaching the shoreline are discussed in the following section 2.1.4., "Impact forces and overtopping".

2.1 Shore Protection Structures

Breakwaters and seawalls may provide protection to coastal areas from tsunamis. Breakwaters may decrease the volume of water flowing into a harbor and onto the coastline when a tsunami occurs. Proper placement of breakwaters may also decrease wave heights by changing the natural period of an inlet. A sufficiently high seawall along a coastline may prevent flooding of the backshore areas. However, breakwaters may also affect the resonant period of a harbor so that wave heights are increased, and seawalls may reflect waves within a harbor. Also a tsunami may damage shore protection structures. Therefore, care must be exercised in the design of the structures.

A tsunami may damage shore protection structures by movement of stone or armor units, erosion at the base of the structure or erosion of backfill, overturning of the structure, or impact forces on the structure. In addition, water may overtop a structure, flooding the area the structure is designed to protect, and debris may be carried over the structure.

2.1.1 Movement of stone

There have been numerous instances of tsunamis damaging or destroying protective structures. The 1946 tsunami in Hawaii overtopped and breached the breakwater at Hilo, on the Island of Hawaii removing 8-foot stones to a depth

3 feet below the water surface along 9 sections of the breakwater crest with a total length of over 6,000 feet (ref. 2). Eaton, Richter, and Ault (ref. 3) found that the 1960 tsunami in Hawaii carried inland large rocks from a seawall, weighing up to 22 tons. Hydraulic model studies are required to determine tsunami effects on individual rubble structures, i.e., to determine if stone and armor units will be moved by tsunamis. An example of this type of study was carried out by Kamel (ref. 4) to study the repair of the breakwater at Hilo, Hawaii, after the breakwater was damaged by a tsunami.

2.1.2 Erosion

A number of examples can be found of damage caused by erosion. Matuo (ref. 5) refers to the case of an earthern embankment at Yosihama on the northeast coast of Honshu, Japan which had been constructed to protect a section of coastline. The 1933 Sanriku tsunami overtopped the embankment, and it was swept away flush with the original ground level.

Iwasaki and Horikawa (ref. 6) investigated areas along the northeast coast of the Island of Honshu, Japan. They indicate that a sea dike located on Kesennuma Bay, Japan failed during the 1960 tsunami because the water from the incident waves which had overtopped the dike caused extensive erosion receding at a gap in the dike. The receding water gradually widened the gap. They also note that a quay wall at Ofunato failed because of scouring of the backfilling and that a quay wall constructed of reinforced concrete sheet piles at Hachinohe collapsed due to a lack of interlocking strength after backfilling was washed away.

Iwasaki and Horikawa also indicate that receding water may seriously scour the seaward base of a revetment or seawall. The combination of this scouring, and the increased hydrostatic pressure from initial overtopping, may cause failure. The concrete seawall along a highway between Hadenya and Mitobe on Shizukawa Bay, Japan collapsed seaward.

Similar failures occurred along a highway on Onagawa Bay and a quay wall at Kamaishi, Japan. Magoon (ref. 7) noted that 6 to 7 feet of sand was scoured at the seaward toe of a steel pile retaining wall at Crescent City, California in 1960, contributing to its partial failure. Also, a wood pile mooring dolphin was destroyed as a result of the loss of sand at its base. Matuo (ref. 5) mentions a concrete retaining wall which was overturned seaward by the 1933 Sanriku tsunami.

The erosive force of a tsunami can be seen from the fact that the 1960 tsunami in Hawaii washed out concrete seawalls 3 feet high. Also a gully 10 feet deep and 90 feet wide was washed into a highway along the shoreline at Hilo, extending inland 60 feet. Shepard, et al., (ref. 8) mentions a case where water overtopping sand dunes cut a channel 100 feet wide and 15 feet deep.

Protection must be provided against scour damage at structures. The ground surface behind seawalls or revetments, and the ground surface adjace to buildings, may be protected by paving or vegetation. The U.S. Army Engineer Division, Pacific Ocean (ref. 9) lists trees, shrubs, and ground covers which are found in Hawaii, and which are suitable for protection against tsunamis. Similar types of landscaping can be used in other locations where favorable climatic conditions exist..

2.1.3 Overturning

A tsunami may produce large forces against a structure which cause overturning of the structure. Matuo (ref. 5) reports on a dynamometer located on a breakwater at Hatinohe Harbor, Japan during the 1933 Sanriku tsunami. The dynamometer was located 2.4 feet below the level of water surface at the time of arrival of the tsunami. The recorded maximum pressure was 800 lbs/foot^2 for a wave with a height of about 10 feet and a period of 6 minutes. As noted in Section 2.1.2, "Erosion," these forces may also combine with erosion to cause failure of a structure.

Nasu (ref. 10) developed some empirical criteria for the stability of breakwaters based on the geometric shape of the breakwater. For a breakwater with a seaward slope of 1:2.5 and a landward slooe of 1:2, he gives

$$u^2 < \frac{h_v + 0.89b}{0.0358} \qquad (2)$$

where u = the current velocity in meters/second,

h_v = the height in meters of the vertical segment of the face of the breakwater against which the current acts,

b = the top width of the breakwater in meters,

for the condition of geometric stability.

2.1.4 Impact forces and overtopping

Impact forces against a shore protection structure may result either from debris in the water, or storm waves riding on top of the longer period tsunami. Water and debris may be carried over the structure either by runup and overtopping of the structure, or by the flow of water resulting from a tsunami having a higher height than the structure.

As a tsunami acts as a shallow water wave, the maximum current velocity, u, associated with the tsunami for a non-breaking (non-bore) type tsunami, treated as a small amplitude wave, is

$$u = \frac{a}{d}\sqrt{gd} \tag{3}$$

where a = the amplitude of the tsunami above the still water level,

d = the still water depth

as noted by Camfield (ref. 11). Where the tsunami forms a surge approaching the shoreline through shallow water (not over a dry bed), the surge velocity, c, can be taken from Keulegan (ref. 1) as

$$c = \sqrt{gd}\left[\frac{d+a}{2d}\left(\frac{d+a}{d}+1\right)\right]^{\frac{1}{2}} \tag{4}$$

The current velocity, u, associated with the surge is

$$u = c\left(1 - \frac{d}{d + a}\right) \tag{5}$$

Equations 3 and 5 describe the velocity at which debris might be carried forward into the structure. The momentum, M_o, of a piece of debris hitting the structure is given as

$$M_o = um \tag{6}$$

where m = the mass of the piece of debris.

Impact of storm waves hitting a structure is given by the U.S. Army, Coastal Engineering Research Center (ref. 12). For a wave breaking against a vertical wall, the force, F, is given as

$$F = 100\gamma \frac{H_b^2}{3L_D} \frac{d_s}{D}\left(D + d_s\right) \tag{7}$$

where = the unit weight of the water,

Hb = the breaker height

D = the depth one wavelength in front of the wall,

LD = the wavelength in water of depth

ds = the depth at the toe of the wall (including the added depth resulting from the tsunami).

The force, F, given by equation 7 is assumed to act at the waterline. In addition to this force, there is a hydrostatic force including that from the increased water level due to the tsunami plus the breaking wave (that is, a total water level against the face of the wall of ds + 0.5 Hb).

For a broken wave hitting the all the force, F, is given as

$$F = 0.39 \ \gamma \ d_b H_b \tag{8}$$

and is assumed to act at a distance $0.39H_b$ above the waterline. The hydrostatic force assumes a total water level against the face of the wall of $d_s + 0.78H_b$, where d_s again includes the tsunami height. A further, detailed discussion of wave forces is given by the U.S. Army, Coastal Engineering Research Center (ref. 12).

The volume of water overtopping a wall is discussed by Wiegel (ref. 13). Wiegel gives the following empirical equation for overtopping volume, V, in cubic meter length of wall

$$V = 0.287 \int_{t_1}^{t_2} \left(\tfrac{1}{2} h_s \cos \frac{2\pi t}{T} - h_w \right)^{3/2} dt \tag{2.9}$$

where h_s = the total wave height in meters (crest to trough) of the wave at the shoreline,

T = the wave period

t_1 = the point in time where overtopping begins,

t2 = the time when overtopping ends.

As the wall height, h_w, in meters is measured from the sea level at the time the tsunami occurs, it varies, but would have its lowest value (that is, the greatest overtopping would occur) when the sea level is at the highest tidal stage. Values for overtopping are shown in Figure 11.

2.2 Other Structures Located at the Shoreline

In addition to the effects on shore protection structures, tsunamis may damage other structures located at the shoreline, or along river and navigation channels near the shoreline which are affected by the tsunami. These structures may include docks and bridges. Failure of the structures may result from scouring at the foundations, or from hydrodynamic forces on the structure leading to direct structural failure.

2.2.1 Scouring at foundations

Scouring at structure foundations was discussed in the previous report section 2.1.3, "Erosion." An example of this effect on bridges is shown by Iwasaki and Horikawa for a bridge support at Mangoku, Japan. The bridge support slumped 2.38 feet due to heavy scouring of the channel bottom.

The current velocities associated with the tsunami are given in equations 3 and 5. For a tsunami, the horizontal current velocities are assumed to be uniform from the water surface to the channel bottom or sea bottom. An investigation of the material near the foundations is required for individual structures to determine the susceptibility to erosion.

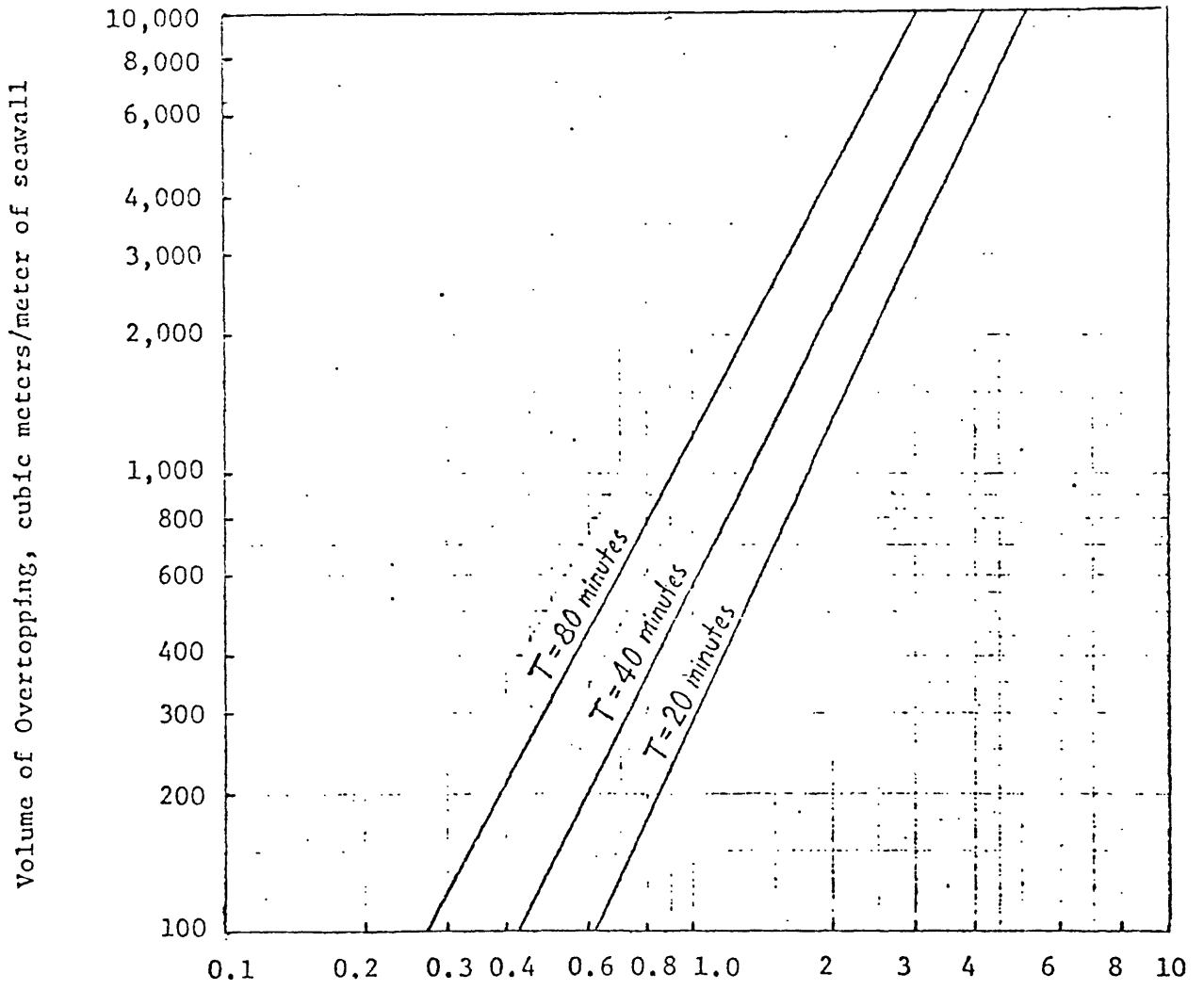

Figure 11. Elevation of tsunami crest above seawall, meters overtopping volumes (ref. 13)

2.2.2 Structural Failure

Examples of structural failure caused by a tsunami are illustrated in Shepard, et al. (ref. 8). The 1964 tsunami, which originated in Alaska, caused a tsunami surge at Seaside, Oregon that destroyed a bridge over the Necanicum River and a railroad trestle over Neawanna Creek.

For a tsunami flowing past a structure, the velocity will be slowly varying, and the force can be taken as a drag force, that is, acceleration is assumed to be negligible and inertia forces are neglected. The drag force, F_D, is defined as

$$F_D = C_D A \frac{u^2}{2} \qquad (10)$$

where = the density of seawater,

C_D = a coefficient of drag, depending on the structure, given in Table 2.1,

A = the projected area of the structure normal to the direction of flow,

u = the current velocity of the water.

Tabulated values of drag coefficients are generally not available for free surface flow at high Reynolds numbers. It is therefore necessary to use existing tables of drag coefficients, and establish maximum coefficients to ensure safe design. Table 1 gives examples of drag coefficients.

Hallermeier (ref. 14) discusses the importance of the parameter, $u^2/(gd)$, where d is the projected horizontal dimension of the structure transverse to the direction of flow, Where this parameter approaches unity there are strong unidirectional free-surface flow effects. In that case, it would be expected that the coefficients of drag, C_D, given in Table 1 may be too low. Individual model tests would be required to determine a more exact interaction between the tsunami and the structure.

For cases where flow does not overtop a structure, and where there is no underflow, the flow may be treated as flow around an "infinitely long" structure where the ground and the free surface define the boundaries of a layer of fluid. For example, flow around a vertical cylindrical column would be treated as flow around an infinitely long cylinder in order to obtain a drag coefficient.

In cases where there is overtopping and underflow, a determination should be made of the ratio of length to width for the structure. This ratio should then be used for determining the coefficient of drag.

TABLE 1
Drag Coefficients

Object	l/d	Reynolds Number	C_D
Circular Cylinder 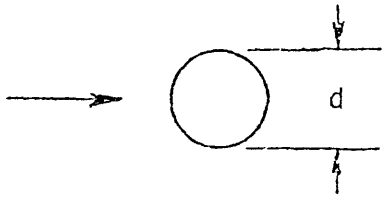	1	10^5	0.63
	5	10^5	0.74
	∞	10^5	1.20
	∞	$>5 \times 10^5$	0.33
Square Cylinder 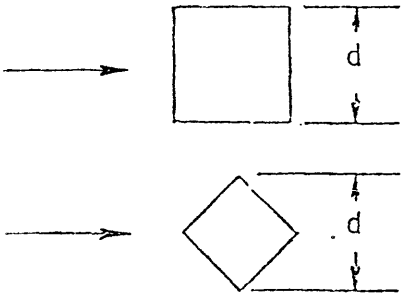	∞	3.5×10^4	2.0
	∞	10^4 to 10^5	1.6
Rectangular Flat Plate (totally submerged) 	1	$>10^3$	1.1
	5	$>10^3$	1.2
	20	$>10^3$	1.5
	∞	$>10^3$	2.0

L = The height of a submerged cylinder, or the length of the flat plate
d = The projected dimension shown, or the width of the flat plate

For a situation in which there is either overflow or underflow, the coefficient of drag can be determined by making use of an approximation. Assume that the depth of flow around the structure is twice the actual depth, and that the height of the structure is twice the actual depth, and that the height of the structure is equal to twice the wetted height. Then obtain a coefficient of drag as if there was both underflow and overflow (see Fig. 12). An example of this type of calculation follows:

**********EXAMPLE PROBLEM 1 **********

GIVEN: A Flat sided structure is 14 meters (45.9 feet) wide, and is normal to the direction of flow. The structure is 3.5 meters (11.5 feet) high, but is supported on columns so that there is a 1.5 meter (4.9 feet) high open space under the base of the structure. The tsunami surge has depth of 2.5 meters (8.2 feet), giving a wetted height on the structure equal to 1.0 meters (3.3 feet).

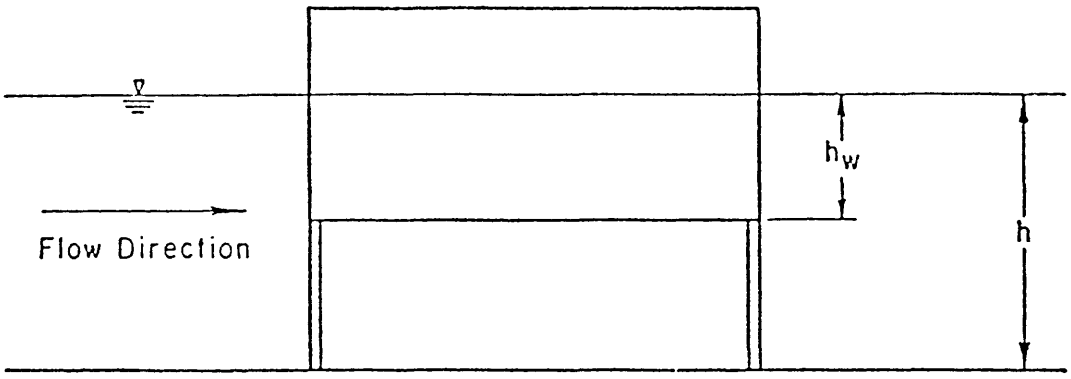

Tsunami surge flowing past elevated structure

h = surge height

h_w = wetted height on structure

L = length measured perpendicular to the sections shown above and below

$L/d = L/(2h_w)$

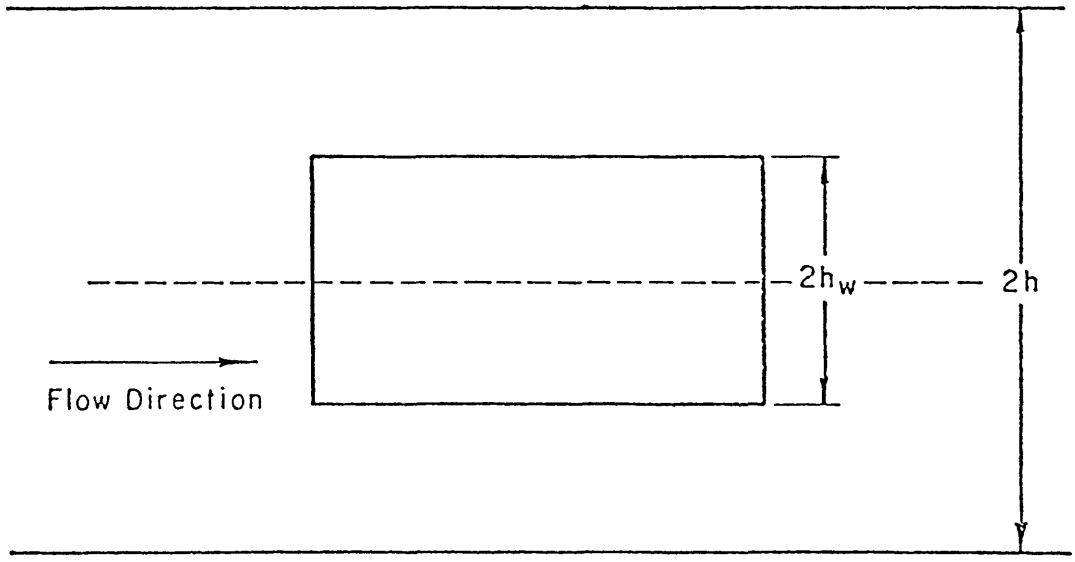

Equivalent body used for determining coefficient of Drag C_D
Flow is assumed symmetrical about the dashline

Figure 12. Determination of C_D when flow passes under a structure.

FIND:

(a) the coefficient of drag of the structure; and

(b) the coefficient of drag of a similar structure located at level with no underflow.

Tsunami surge flowing past elevated structure

h = surge height

h_w = wetted height on structure

L = length measured perpendicular to the sections shown above and below

$L/d = L/(2h_w)$

Equivalent body used for determining coefficient of Drag C_D

Flow is assumed symmetrical about the dashline

SOLUTION:

(a) It can be assumed, for purposes of determining the coefficient of drag, that the structure is equivalent to a structure 14 meters wide and 2.0 meters high with both underflow and overflow (see Figure 2.6). From Table 1, for a flat plate normal to the flow direction where L/d = 7, the coefficient of drag C_D 1.25.

(b) The structure is higher than the depth of flow so that, in this case, there would be neither underflow or overflow. This corresponds to an infinitely high structure where L/d = . From Table 1 $D_D = 2.0$.

****

The following example problem illustrates the calculation of forces on structural columns.

**********EXAMPLE PROBLEM 2**********

GIVEN: A structure, 3 meters (9.84 feet) above a channel bottom, is supported by square columns having 14 cm x 14 cm (5.5 inch x 5.5 inch) cross sections. The still water depth is 1 meter (3.24 feet). A tsunami creates a surge giving a water depth of 2.44 meters (8 feet) under the platform. The surge acts normal to the sides of the columns, which are rigidly fixed at ground level.

FIND: The moment of the surge force about the base of a column.

SOLUTION: To determine the coefficient of drag, the columns may be considered as infinitely long columns, and from Table 1, we have that $C_D = 2.0$. From equations 4 and 5.

$$u = \sqrt{gd}\left[\frac{d+a}{2d}\left(\frac{d+a}{d}+1\right)\right]^{\frac{1}{2}}\left(1-\frac{d}{d+a}\right)$$

$$u = \sqrt{9.81 \times 1}\left[\frac{2.44}{2}\left(2.44+1\right)\right]^{\frac{1}{2}}\left(1-\frac{1}{2.44}\right)$$

$u = 3.79$ meters/sec (12.42 ft/sec)

The drag force on a column is given by Equation 2.10 as

$$F_D = \rho\ C_D\ A\ \frac{u^2}{2} = 1026(2)\ (2.44)\ (0.14)\ \frac{(3.79)^2}{2}$$

$$F_D = 5.03 \times 10^3 \text{ newtons}$$

The velocity is assumed to be equal over the 2.44 meter depth so that the resultant drag force acts 1.22 meters (4 feet) above ground level. The moment is then

$M = 5.03 \times 10^3\ (1.22) = 6.14 \times 10^3$ newton-meters (4.39×10^3 ft/lbs) on each of the columns.

****

Wilson and Torum (ref. 14) discuss another means of tsunami damage to docks. In 1964, a dock at Crescent City, California was damaged when the water elevation increased to a level of 2 meters (6.5 feet) above the deck elevation, uplifting a large lumber barge moored to the dock. As a tsunami lifts a vessel upwards, the mooring lines prevent the vessel from rising as high as the increase in water level. This results in additional submergence of the vessel, and a corresponding increase in the buoyant force, which causes a strain in the mooring lines. The additional buoyant force is transmitted

through the mooring lines to the dock structure, with the result that a dock may be pulled apart if a large vessel is moored at the dock during a large increase in water level accompanying a tsunami.

2.3 Onshore Structures and Facilities

The tsunami height at any point on the shoreline can be determined using the methods outlined in chapter 1, "Tsunami Hazard." After the runup height of a tsunami has been established, it is necessary to determine the effects of this runup on structures and other objects located near the shoreline. When the tsunami acts as a rapidly rising tide, the resulting incident current velocities are relatively low, and most initial damage will result from buoyant and hydrostatic forces and the effects of flooding. Shepard, et al., (ref. 8) noted that in many instances the withdrawal of the water occurred much more rapidly than the runup and flooding. In some instances, damage may result from the higher current velocities associated with the withdrawal. These velocities would be on the order of those normally associated with an incident surge. More concern is therefore given to a tsunami which approaches the shoreline as a bore.

When the tsunami forms a borelike wave, the runup on the shoreline has the form of a surge on dry ground. This surge should not be confused with the bore approaching the shoreline, as different equations govern the motion and profile of the surge. Miller (ref. 16) noted, from laboratory observations, that a bore approaching a shoreline exhibits a relative steepening of the bore face just before reaching the shoreline, and that this is followed by a flattening of the face of the surge on the dry slope. The current velocities

associated with the surge are proportional to the squareroot of the surge height, and approximations of the current velocities can be obtained from Equation 2.1. As an example, for a surge height approaching 5 meters (16.4 feet), the estimated current velocity would be on the order of 14 meters/second (46 feet/second). When the tsunami runup acts as a high velocity surge of water across the ground, five types of forces may result from the surging water. Buoyant forces are caused by partial or total submergence of a structure, the buoyant force will tend to lift the structure from its foundations. Vehicles and other large items may also be lifted up into the surging water.

Surge forces are caused by the leading edge of the surge impinging on a structure. As the leading edge of the surge has the appearance of an elongated wedge, the force of the surge on a structure gradually increases as a function of the increase in surge height. The buoyant force also increases as a function of surge height, so that a structure may be carried forward by the leading edge of the surge, or may be destroyed in place if the surge force is sufficiently high and the buoyant force is not sufficient to lift the structure from its foundation.

Drag forces are caused by the high velocity of the surging water flowing around a structure, where the water level is relatively constant. These forces will displace buildings or other items in the direction of the current, and the high velocity flow may cause severe erosion of the ground and damage structures by scouring material at the base of the structure.

Impact forces are caused by buildings, boats, or other material carried forward by the surging water. These forces may either destroy other structures on impact, or create momentum which, when added to other forces, will move a structure in the direction of the current. Impact forces may also be the result of short period waves riding on top of the tsunami.

Hydrostatic forces are caused by partial or total submergence of structures by by the tsunami. This can result in cracking or collapse of a structure or wall.

2.3.1 Flooding and Water Damage

The tsunami inundation level determined using the methods outlined in Section 1, "Tsunami Hazard," gives the extent of flooding which will cause water damage to structures and facilities. Flooding and water damage may result when water intrudes into building, washes over open storage areas, flows through power substations, or flows into freshwater supplies. Inundation may also render utility service lines inoperable.

The U.S. Army Engineer Division, Pacific Ocean (ref. 9) discusses means of floodproofing structures and facilities including flood shields and watertight seals, berm or wall construction, and elevating structures. They also discuss placement of damageable property within a structure. Watertight, lightweight aluminum or steel flood shield may be used to cover doorways and windows. Sealants may be applied to the exterior walls of a structure to reduce seepage.

Floodwalls may be constructed of concrete, brick, or stone, and must be capable of resisting floodwater pressures and the effects of erosion. Flood shields can be used to close access openings in floodwalls. Earthern berms can be used, but they may be subject to erosion from high velocity currents (see Section 2.1.2 "Erosion"). The elevation of structures on posts or columns, or the use of elevated platforms for facilities may substantially reduce damage from flooding.

2.3.2 Buoyant Forces

Buoyant forces are defined by the weight of the displaced water when objects are partially or totally submerged. For saltwater, taking the density 1.026 grams/centimeter^3 (1.99 lb-sec^2/feet^4), the buoyant force is

$$F_B = g\ V \tag{11}$$

where V = the displaced volume of water. This assumes water intrudes under the structure but not within the structure.

**********EXAMPLE PROBLEM 3**********

GIVEN: A house occupies a floor area of 225 square meters (2,422 square feet). Calculations to predict tsunami runup have indicated a probable surge depth of 2 meters (6.56 feet) at that location. It is assumed that the flow of water will be at a constant depth around the house.

FIND: The buoyant force on the house.

SOLUTION: The buoyant force is given by

$F_B = g\ V$

$F_B = 1026$ kilograms/meter^3 (9.81 meters/second^2) (225 meters^2) (2 meters)

$F_B = 4.53 \times 10^6$ newtons (1.02×10^6 pounds)

**********EXAMPLE PROBLEM 4**********

GIVEN: An oil storage tank is 3 meters (9.84 feet) high and 6.1 meters (20 feet) in diameter, Assume that the tank (empty) has a mass of 3180 kilograms (7000 lbs-mass), and that it is filled to a depth fo 2.5 meters (8.2 feet) with oil having a specific gravity of 9.88 (density = 880 kilograms/meter^3). The tsunami water depth is 1.8 meters (5.91 feet).

FIND:

(a) the buoyant force on the tank; and

(b) the force holding the tank in place,

SOLUTION:

(a) The buoyant force is given by

$F_B = \rho g\ V$

$F_B = 1026(9.81)(\frac{\Pi}{4})(6.1^2)(1.8) = 5.29 \times 10^5$ kilogram-meters/second^2

$F_B = 5.29 \times 10^5$ newtons (1.19×10^5 pounds)

(b) The force holding the tank in place is the mass, M, of the empty tank multiplied by its density and g, so that

$$F = Mg + \rho g V$$

$$F = 3180\ (9.81) + 880\ (9.81)\ (\tfrac{\pi}{4})\ (6.1^2)(2.5)$$

$$F = 6.62 \times 10^5 \text{ newtons } (1.49 \times 10^5 \text{ pounds})$$

It can be seen that very little reserve force remains to resist drag forces from the surge. With a lower level of oil in the tank, the buoyant force could overcome the mass of the tank and the oil plus the strength of any structural anchorages.

****

Shepard, et al., (ref. 8) discuss some of the effects of the tsunami of April 1, 1946 in Hawaii. A house at Kawela Bay on Oahu was floated off its foundation and deposited in a cane field 200 feet inland, leaving breakfast cooking on the stove and dishes intact on shelves. Many other homes were also gently floated from their foundations, and some homes could be moved back to their original foundations with very little repair work required. Damage caused by buoyant forces was the result of buildings being deposited on uneven ground, the fact that some buildings had weak structures and broke apart when lifted from their foundations, and minor damage from the breaking of water pipes and electric lines.

2.3.3 Surge Forces

Cross (ref. 17) investigated the case of a surge traveling across dry ground and impinging normally on a vertical wall. The general shape of a surge over dry ground is shown in Figure 13. For the assumption shown in the figure that is small, Cross shows that the force, F, of the surge at any point is given as

$$F = \frac{1}{2}\rho g h^2 + \left[\left(\frac{4gn^2}{h^{1/3}}\right)^{1.2} + 1\right]\rho u^2 h \qquad (11.12)$$

where u = the surge velocity,

n = the Manning roughness coefficient,

h = the surge height at the wall at that point in time.

The surge velocity is taken from equation 1, using the total height of the surge. An illustration of the application of this equation is given in Example 2.5.

**********EXAMPLE PROBLEM 5**********

GIVEN: A surge with a maximum height of 2.5 meters (8.2 feet) impacts normally against the vertical side of a building. The Manning roughness coefficient n = 0.1, and it is assumed that the surge velocity, u = 2 gh, remains relatively constant and that the surge profile remains constant.

FIND: The surge force per meter of building width as a function of surge height.

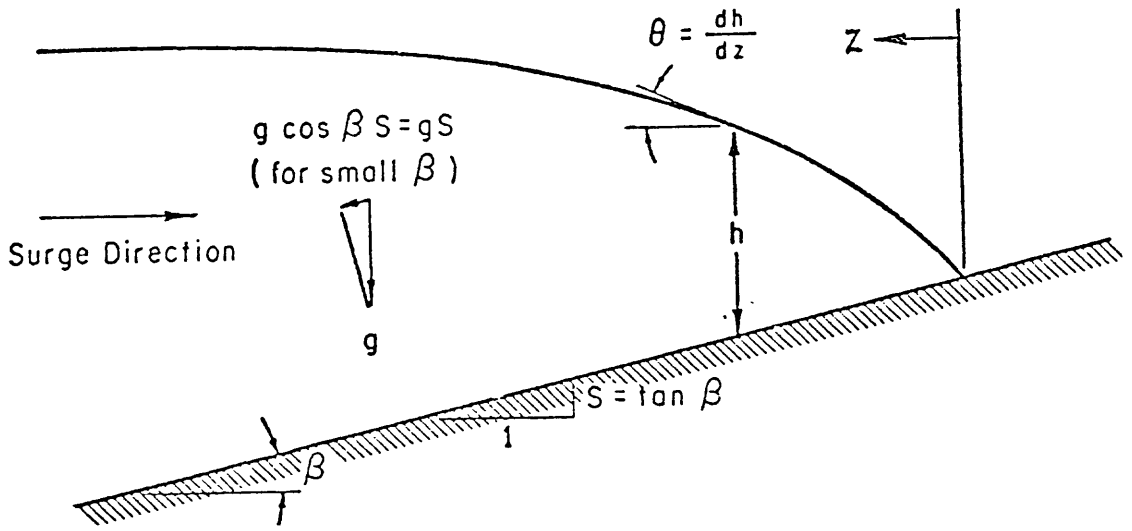

Figure 13. Definition sketch of a surge on a dry bed (hydrostatic forces included).

SOLUTION: The surge velocity is determined from the maximum surge height, so that

$$u = 2\sqrt{gh} = 2\sqrt{9.81\ (2.5)} = 9.9 \text{ meters/sec}$$

The surge force is given by equation 12 as

$$F = \frac{1}{2}\rho g h^2 + \left[\left(\frac{4gn^2}{h^{1/3}}\right)^{1.2} + 1\right]\rho u^2 h$$

$$F = \frac{1}{2}(1026)(9.81)h^2 + \left[\left(\frac{4(9.81)(0.1)^2}{h^{1/3}}\right)^{1.2} + 1\right] 1026\ (9.9)^2 h$$

$$F = 5033\ h^2 + \left[\left(\frac{0.392}{h^{1/3}}\right)^{1/2} + 1\right] 100{,}560\ h$$

For various values of h, the force, F, is tabulated below.

h, meters	0.5	1.0	1.5	2.0	2.5
F, Newtons/meter	73,100	138,300	203,900	270,800	339,500

Note: Calculations will show that $C_F > 1$ at the maximum surge height (where the rate of change of surge height $\rightarrow 0$). This indicates that the calculated value is conservative for design purposes.

****

As indicated by example problem 5, and as shown in Figure 13 there is a gradual rise in water level at the front of the surge, although this change in water level appears to occur rapidly with respect to time because of the forward velocity of the surge. It may be noted in laboratory tests that a bore approaching a shoreline has a much steeper front than the surge running up the dry bed. The buoyant force of the leading edge of the surge will tend to lift objects into the surging water, and the force of the surge will then carry these objects forward.

Wilson and Torum (ref. 15) report on the case at Seward, Alaska of a tsunami surge overtaking a pickup truck being driven from the shoreline. The truck was swept up by the surge and carried forward like a surfboard into nearby woods.

As the water velocity near the leading edge of a surge is relatively high, and the height of the leading edge is relatively low (that is, the buoyant force is low), it is possible that the surge force may destroy a structure before the buoyant force lifts it into the flow.

2.3.4 Drag Forces

For a tsunami surge over dry ground, the associated current velocities are given by equation 1, and the drag force resulting from flow around a structure can be determined using equation 10 and the methods previously described in Section 2.2.2, "Structural Failure." The effect of drag forces is illustrated in example problem 6 below.

**********EXAMPLE PROBLEM 6**********

(This example is taken from an actual situation which occurred at Seward, Alaska in 1964; (ref. 15).

GIVEN: A 104.5 metric ton (230,000 pound) railroad locomotive was overturned by a tsunami surge. The surge was assumed to have a depth of 1.83 meters (6 feet). The clear space under the locomotive was approximately 0.91 meters (3 feet) and the length of the locomotive body was 12.5 meters (41 feet). The width between the rails was 1.52 meters (5 feet) and the width of the locomotive body was 3.05 meters (10 feet), The surge was assumed to act normal to the side of the locomotive.

FIND: The overturning force on the locomotive.

SOLUTION: The buoyant force is given by equation 11 as

$F_B = \rho g V = 1026\ (9.81)(1.83-0.91)(3.05)(12.5)$

$F_B = 3.53 \times 10^5$ newtons (78,700 pounds)

As indicated previously, the coefficient of drag can be determined by doubling the wetted height and assuming both underflow and overflow for a flat surface 2.1 for a flat plate for L/D = 6.8, gives

$$C_D = 1.24$$

The velocity can be obtained from equation 1 so that for

$$h = 1.83$$

$$u = 2\sqrt{gh} = 2\sqrt{9.81(1.83)} = 8.47 \text{ meters/second}$$

From equation 10, the drag force is

$$F_D = \rho\, C_D\, A\, \frac{u^2}{2}$$

$$F_D = 1026\ (1.24)\ (1.83-0.91)(12.5)\ \frac{(8.47)^2}{2}$$

$$F_D = 5.24 \times 10^5 \text{ newtons } (1.17 \times 10^5 \text{ pounds}).$$

which will act against the side of the locomotive at a distance, Z, above the ground, given as

$$Z = 0.91 + \frac{(1.83-0.91)}{2}$$

$Z = 1.37$ meters (4.5 feet)

The downward force from the mass of the locomotive is the mass, m, times gravitational acceleration, g, or

$F = mg = 104{,}500$ kilograms (9.81 meters/second^2)

$F = 1.025 \times 10^6$ newtons (2.3×10^5 pounds)

Taking overturning moments about a rail, the center of mass of the locomotive is equidistant from the two rails, or 0.76 meters (2.5 feet) from the rail. The buoyancy and drag forces produce overturning moments (+) and the mass of the locomotive a restraining force (-). Summing moments

$M = F_B\ (0.76) + F_D Z - F\ (0.76)$

$M = 3.53 \times 10^5\ (0.76) + 5.24 \times 10^5\ (1.37) - 1.025 \times 10^6\ (0.76)$

$M = 2.07 \times 10^5$ newton-meters (1.48×10^5 ft-lbs)

indicating that the overturning moments are greater than the restraining moment. Therefore the locomotive will be overturned.

****

As indicated in example problem 6, drag forces and surge forces can act in conjunction with buoyant forces. Buildings can be seriously damaged when the buoyant forces lift them from their foundations, and the surge or drag forces slam them into such things as trees or other structures. When a building is firmly attached to its foundation to resist the buoyant forces, it must also have sufficient structural strength to withstand the drag forces acting against it. The drag forces can be lessened by constructing a building on an elevated platform some distance above the ground. In some instances, the first floor of a building may be designed so that it will be carried away by the tsunami, thereby reducing the forces on the building and protecting the higher floors, although this may be an expensive solution and has the undesirable feature of adding debris to the water.

The high velocity of a tsunami surge can also damage structures of facilities by scouring material. Shepard, et al. (ref. 8), note that at Kalaupapa, Molokai, the backwash from the tsunami undermined a road.

Other instances of erosion are also discussed. They noted that dense stands of grass prevented or greatly diminished ground erosion. The U.S. Army Engineer Division, Pacific Ocean provides a listing in Table 2 of landscaping material that can be used in the State of Hawaii to prevent erosion and provide protection from tsunami surge.

2.3.5 Impact Forces

The high velocity of a tsunami surge will sweep large quantities of material forward with the surge. This material may include automobiles, trees, oil

tanks, buildings and pieces of buildings, or any other material in the path of the surge. In higher latitudes, when tsunamis occur during the winter, the material may include large quantities of broken ice.

Impact forces from material carried forward by the current are not as easily analyzed as other forces. The drag force will initially accelerate material which is swept up into the current. The velocity of forward motion of such material is dependent upon the distance the material has moved, the ratio of the drag force to the actual mass of the object in motion and the resistance created by the object dragging against the ground or impacting and grinding against other objects.

Analyzing the effects of a structure impacting with another structure also requires knowledge of the rigidity of the structures and the angle of impact. If the flat side of one structure impacts with the flat side of a second structure, the impact force is spread over a wide area. However, if a corner of the first structure impacts with the flat side of the second structure, the force is concentrated and there will be a greater tendency to crush the impacting structures. It should be remembered that if a structure is partially flooded, the water within the structure becomes a portion of the mass of the structure.

Considering an object being swept forward from a stationary position by a moving fluid such as tsunami surge, the velocity of the fluid, u, with respect second structure, the impact force is spread over a wide area. However, if a corner of the first structure impacts with the flat side of the second structure, the force is concentrated and there will be a greater tendency to

Table 2. Landscaping Material

SEACOAST	Botanical Name	Common Name
Trees:	Hibiscus tiliaceus	Hau
	Casuarina equisetifolia	Ironwood
	Terminalia catappa	False Kamani
	Calophyllum inophyllum	True Kamani
	Coccoloba unifera	Sea Grape
	Cocoa nucifera	Coconut plam
	Thespesia populnea	Milo
	Brassaia actinophylla	Octopus Tree
	Conocarpus erectus	Silver Buttonwood
	Tamarix asphylla	Tamarisk
	Noronhia emarginata	Madagascar Olive
Shrubs:	Neriuim oleander	Oleander
	Scaelola frutescens	Naupaka
	Carissa grandiflora	Natal Plum
	Pittosporum tobira	Pittosporum
Ground Covers:	Cynodon dactylon	Common Bermuda
	Cynodon dactylon hybrid	Hybrid Bermuda

INLAND	Botanical Name	Common Name
Trees:	Erythrina sandwicensis	Wili Wili
	Eucaluptus sideroxylon rosea	Red Ironbark
	Euclyptus saligna	Sydney Blue Gum
	Ficus benjamina	Weeping Banyan
	Ficus retusa Chinese Banyan	
	Melaleuca leucadendron	Paper Bark Tree
	Samanea Saman	Monkeypod
	Acacia koa Koa	
	Aleurites moluccana	Kukui
	Tristania conferta	Brisbane Box
	Mangifera indica	Mango
	Urevillea robusta	Silk Oak
	Aravcaria excelsa	Norfolk Island Pine
Shrubs:	Northopanaz guilfoylei	Panax
	Ligustrum texanum	Texas Privet
	Hibiscus chinensis	Hibiscus
Ground Covers:	Lippia oanescens	Lippia Grass
	Wedelia trilobata	Wedelia
	Ficus tikoua	Waipahu Fig

crush the impacting structures. It should be remembered that if a structure is partially flooded, the water within the structure becomes a portion of the mass of the structure.

Considering an object being swept forward from a stationary position by a moving fluid such as tsunami surge, the velocity of the fluid, u, with respect to the ground is assumed to be constant, and the velocity of the object, u_b, with respect to the ground varies as the object is accelerated. The velocity, u_b, of the object approaches the velocity, u, of the fluid after the object has moved over some distance (that is, the velocity of the object approaches some terminal velocity). The force accelerating the body is a combination of drag forces and inertia forces. The velocity, u_b, of the object moving forward in the flow, at any time, t, after initiation of motion is given by Camfield (ref. 11).

as

$$u_b = u - \frac{u}{\alpha u t + 1} \tag{13}$$

where

$$\alpha = \frac{C_D A}{2V(1 + C_M)} \tag{14}$$

and A is the submerged cross-sectional area of the object transverse to the direction of motion, C_M is the inertia or mass coefficient, and V is the volume of water displaced by the object. Brater, McNown, and Stair (ref. 18) give examples of C_M as developed by Riabouchinski (ref. 19). These are shown in Figure 14.

The relationship between distance moved, x, an time, t, is given by Camfield (ref. 11) as

$$x = ut - \frac{1}{\alpha} \ln (\alpha ut + 1) \tag{15}$$

and the force, F, accelerating the object is given as

$$F = \rho V \alpha (u - u_b)^2 \tag{16}$$

Typical drag coefficients are given in Table 1. The coefficient of added mass, C_M, can be estimated for a rectangular structure by using the results shown in Figure 14. It should be noted that the values given in Figure 14 are for irrotational flow without separation. The formation of a wake behind the structure would be expected to modify these values. To obtain exact values, individual model tests would be required. Example solutions of equation 15 are shown in Figure 15.

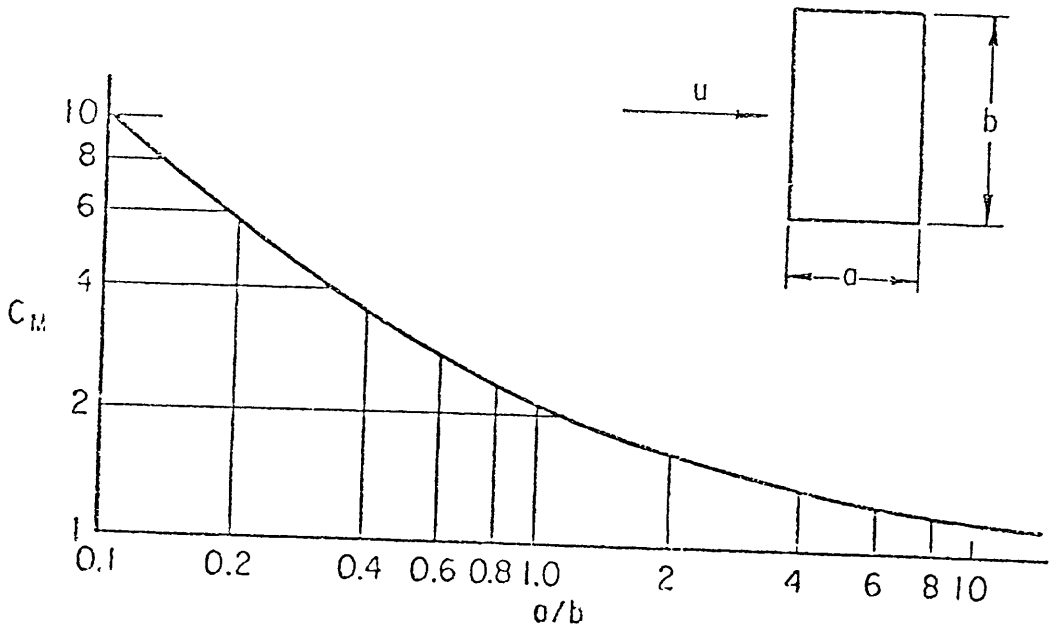

Figure 14. C_M **for two-dimensional flow past rectangular bodies (ref. 18).**

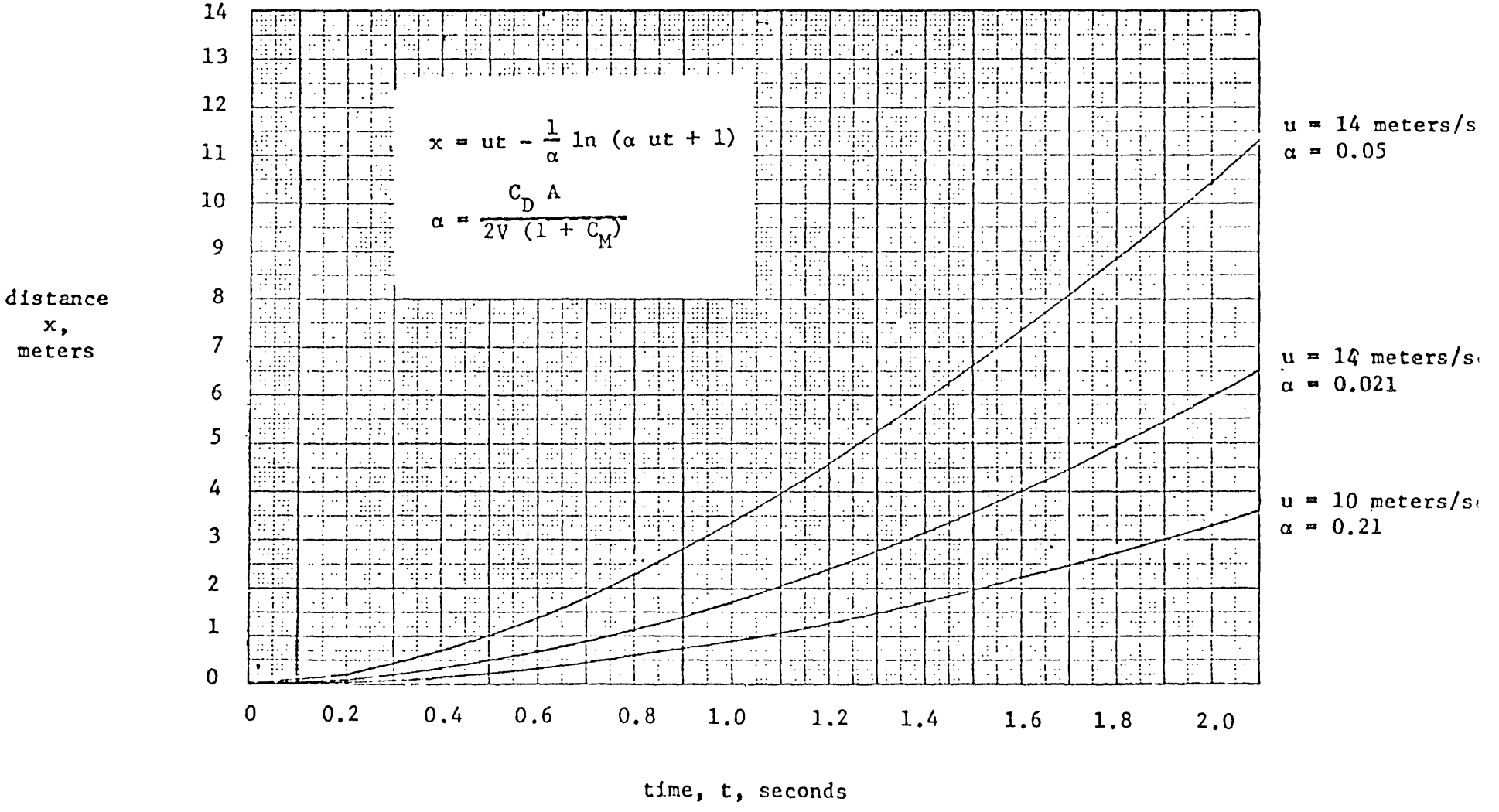

Figure 15. Example plots of x vs t for objects moved by tsunami surge

**********EXAMPLE PROBLEM 7**********

GIVEN: A tsunami surge is 5 meters (16.4 feet) high at the shoreline. A building located at the shoreline is swept forward a distance of 6.1 meters (20 feet), and impacts with another building. The building is rectangular, 12 meters (39.4 feet) wide and 6 meters (19.7 feet) deep in the direction of the flow, and is submerged to a depth of 3 meters (9.8 feet) as it is carried forward as shown in Figure 16. The velocity of the surge is approximated as u = 14 meters/second.

FIND:

(a) the time required for the building to impact with the other building;
(b) the force accelerating the building at the moment of impaact; and
(c) the momentum of the building at the moment of impact.

SOLUTION:

(a) The submerged cross sectional area of the building, transverse to the direction of the.surge, is given as

A = width x submerged depth = 12.0 x 3.0 = 36 meters^2 and the submerged volume (the displaced water) is

V = width x length x depth = 12.0 x 6.0 x 3.0 = 216 meters^3

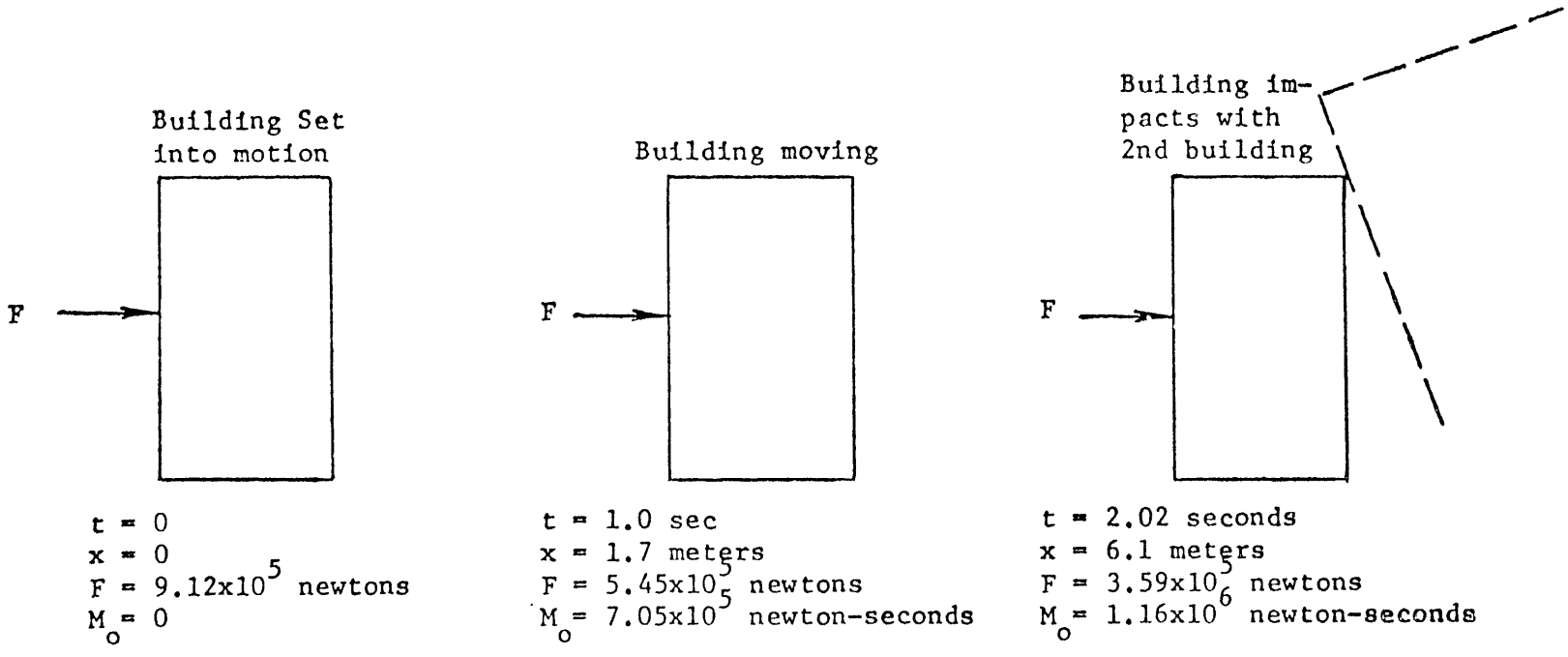

u = 14 meters/second
C_D = 1.13
C_M = 3.5
A = 36 meters^2
V = 216 meters^3

Figure 16. Building moved by tsunami surge

The coefficient of drag can be approximated by assuming the side of the building is a flat plate. To determine an equivalent flat plate using Table 1 assume that the submerged depth for underflow and overflow (a totally submerged plate) is twice the depth of the building, or

$$\frac{L}{d} = \frac{12.0}{2 \times 3.0} = 2.0$$

and from Table 1,

$$C_D \simeq 1.13$$

From Figure 14, where

$$\frac{a}{b} = \frac{6.0}{12.0} = 0.5$$

we have

$$C_M = 3.5$$

and equation 14 gives

$$\alpha = \frac{C_D A}{2V\ (1 + C_M)} = \frac{1.13 \times 36}{2 \times 216\ (1 + 3.5)} = 0.021$$

The relationship between distance and time is shown on Figure 15, which gives, for x = 6.1 meters,

$t = 2.02$ seconds

(b) From equation 13

$$u_b = u - \frac{u}{\alpha u t + 1} = 14 - \frac{14}{(0.021 \times 14 \times 2.02) + 1}$$

$u_b = 5.22$ meters/sec (17.1 feet/sec).

From equation 16

$$F = \rho V \alpha (u - u_b)^2$$

$$F = 1026 \times 216 \times 0.021 (14 - 5.22)^2 = 3.59 \times 10^5 \text{ kilograms-meters/sec}^2$$

$F = 3.59 \times 10^5$ newtons (8.1×10^4 lbs)

(c) Momentum, M_o, at impact is

$M_o = u_b \times$ mass

taking the mass of the building equal to the mass of the displaced water for a partially submerged building which is floating (the mass includes water within the building),

mass = ρV = 1026 kilograms/meter^3 x 216 meters^3

and the momentum is

$M_o = u_b$ x mass = 5.22 x 1026 x 216 = 1.16 x 10^6 kilograms-meters/sec

(2.56 x 10^5 lb-sec)

****

Magoon (ref. 7) indicates that substantial damage occurred during the 1964 tsunami at Crescent City as a result of debris impacting on structures. This debris included logs, automobiles, and baled lumber. The impact forces either destroyed the load carrying capacity of walls, or caused bending or breaking of light columns.

Wilson and Torum (ref. 15) discuss some instances of impact damage in Alaska which resulted from the 1964 tsunami, including the damage which occurred at the Union Oil Company tank farm at Whittier. Buildings and larger tanks were able to withstand the force of the tsunami. However, smaller tanks were carried forward by the surge and impacted with other tanks. Some of the larger tanks were apparently set into motion by the impact, and almost all of the tanks were ruptured. A resulting fire destroyed the tank farm.

Wilson and Torum also mention the problem of a small boat harbor located immediately in front of a developed shoreline. At Kodiak City, Alaska, the boat harbor contained a large number of fishing boats and yachts. The 1964

tsunami carried these boats into the adjacent waterfront business area adding substantially to the damage. Van Dorn (ref. 20) notes that harbor regulations could be instituted requiring ships large enough to damage harbor structures to stand clear of a harbor in the event of a tsunami warning. In the case at Kodiak City there was insufficient time between the tsunami warning and the arrival of the tsunami. However, when tsunamis are generated from distant sources there might be sufficient time to clear harbors of shipping.

An interesting example of impact forces is reported by Wilson and Torum (ref. 15). During the 1964 tsunami a house was washed out to sea near Point Whiteshed. The house was swept along the shoreline, carried into the harbor at Cordova, and rammed the dock, knocking down the end of the dock.

Impact forces can also result from short period waves riding on top of the tsunami. These wave impact forces are discussed in Section 2.1.4, "Impact forces and overtopping."

2.3.6 Hydrostatic Forces

Hydrostatic forces are normally relatively small compared to surge and drag forces. The hydrostatic force on a wall, per foot width of wall, for a water depth h is

$$F = \frac{1}{2} \rho g h^2 \qquad (17)$$

Once the initial surge has passed a structure, if it is assumed that water levels are equal on all sides of the structure, the hydrostatic force will not contribute to the motion or potential motion of the structure. However, this force can cause cracking of exterior walls and interior flooding of the structure.

Magoon (ref. 7) indicates that the flooding caused by a tsunami can saturate the fill behind a retaining wall. Combined with the large drawdown of the water level which may occur at the seaward toe of a wall during the withdrawal of a tsunami wave, large hydrostatic forces may result on the wall. It is believed that this contributed to the partial failure of a retaining wall at Crescent City, California.

There was an unusual occurrence at the abandoned Kahuku Airfield on Oahu (ref. 8). Blocks of pavement were titled in circular areas 3 to 5 feet across, apparently as a result of hydraulic pressure from water penetrating into the sand under the pavement when the tsunami flooded the area. The higher pressure under the pavement has not been explained, but could have resulted from water trapped in the sand during a rapid withdrawal of the tsunami.

2.3.7 Debris

Debris may cause damage by impacting against structures and facilities, by piling up against structures and adding to the hydrodynamic loads, and by contamination. The impacting of debris against structures is discussed in Section 2.3.5, "Impact forces."

Debris piling against a structure can increase the cross sectional area. As an example, where a structure is supported on columns the debris may pile up against the columns so that it acts as wall. Rather than a lower force acting against the individual columns (see Example Problem 2.2), a much higher force would be distributed against the columns and the structure might be destroyed.

A wide variety of debris carried in the water may result in both chemical and bacterial contamination. Stored goods may be damaged or rendered unfit for use. Fresh water supplies may also be contaminated. In addition, chemical and bacterial hazards may necessitate decontamination of an area before normal services and activities can be restored.

2.4 REFERENCES

1. KEULEGAN, C.H., "Wave Motion," Chapter 11, Engineering Hydraulics, Proceedings of the Fourth Hydraulics Conference, John Wiley and Sons, New York, New York, 1950.

2. U.S. Army Engineer District, Honolulu, "Hilo Harbor, Hawaii, Report on Survey for Tidal Wave Protection and Navigation," Nov. 14, 1960.

3. EATON, J.P., D.H. RICHTER, AND W.U. AULT, "The Tsunami of May 23, 1960, on the Island of Hawaii," Bulletin of the Seismological Society of America. Volume 51, No. 2, pages 135-157, April 1961.

4. KAMEL, A.M., "Stability of Rubble-Mound Tsunami Barrier Hilo Harbor, Hawaii," U.S. Army Engineer Waterways Experiment Station, Technical Report No. 2-792, August 1967.

5. MATUO, HARUO, "Estimation of Energy of Tsunami and Protection of Coasts," Bulletin of the Earthquake Research Institute, Tokyo Imperial University, Supplementary Volume I, pages 55-64, 1 plate, March 1934.

6. IWASAKI, TOSHIO, AND KIYOSHI HORIKAWA, "Tsunami Caused by Chile Earthquake in May 1960 and Outline of Disasters in Northeastern Coasts of Japan," Coastal Engineering in Japan, Volume 3, pages 33-48, 1960.

7. MAGOON, ORVILLE T., "The Tsunami of May 1960 as It Affected Northern California," Presented at the ASCE Hydraulics Division Conference, Davis, California, August 1962 (unpublished).

8. SHEPARD, F.P., G.A. MACDONALD, AND D.C. COX, "The Tsunami of April 1, 1946," Bulletin of the Scripps Institution of Oceanography, Volume 5, No. 6, pages 391-528, 1950.

9. U.S. Army Engineer Division, Pacific Ocean, "Residential Construction Practices Handbook for Flood Prone Areas in the State of Hawaii," in preparation 1979.

10. NASU, NOBUJI, "Local Phenomena of Tsunami, Part 2," Bulletin of the Earthquake Research Institute, Tokyo University, Volume 26, Nos. 1-4, pages 27-35, 1948.

11. CAMFIELD, FREDERICK E., "Tsunami Engineering," U.S. Army Coastal Engineering Research Center, Special Report No. 8, February 1980.

12. U.S. Army Coastal Engineering Research Center, "Shore Protection Manual," U.S. Government Printing Office, 1977.

13. WIEGEL, ROBERT L., "Tsunamis," Chapter II, Earthquake Engineering, Prentice Hall, Englewood Cliffs, New Jersey, 1970.

14. HALLERMEIER, ROBERT J., "Nonlinear Flow of Wave Crests Past a Thin Pile," Journal of the Waterways, Harbors, and Coastal Engineering Division, ASCE, Volume 102, No. WW4, pages 365-377, November 1976.

15. WILSON, BASIL W., ALF TORUM, "The Tsunami of the Alaskan Earthquake, 1964: Engineering Evaluation," TM No. 25 U.S. Army Coastal Engineering Research Center, May 1968.

16. MILLER, ROBERT L., "Experimental Determination of Runup of Undular and Fully Developed Bores and an Examination of Transition Modes and Internal Structure," Technical Report No. 8, Department of Geophysical Sciences, University of Chicago, June 1968.

17. CROSS, RALPH H., "Tsunami Surge Force," Journal of the Waterways,Harbors, and Coastal Engineering Division, ASCE, Volume 93, WW4, November 1967.

18. BRATER, ERNEST F., JOHN S. MCNOWN, AND LESLIE D. STAIR, "Wave Forces on Submerged Structures," Journal of the Hydraulics Division, ASCE, Volume 84, HY6, November 1958.

19. RIABOUCHINSKI, D., "Sur la Resistance des Fluides," International Congress of Mathematics, Pages 568-585, Strasburg, 1920.

20. VAN DORN, WILLIAM G., "Tsunamis," Advances in Hydroscience, Vol. 2, Academic Press, 1965 (Also published as Scripps Institution of Oceanography Report, Federal Clearing house No. AD457729, 26 January 1965).

GLOSSARY OF THE TERMS USED IN EARTHQUAKE HAZARDS ASSESSMENTS

Accelerogram. The record from an accelerometer showing acceleration as a function of time. The peak acceleration is the largest value of acceleration on the accelerogram.

Acceptable Risk. A probability of occurrences of social or economic consequences due to earthquakes that is sufficiently low (for example in comparison to other natural or manmade risks) as to be judged by authorities to represent a realistic basis for determining design requirements for engineered structures, or for taking certain social or economic actions.

Active fault. A fault is active if, because of its present tectonic setting, it can undergo movement from time to time in the immediate geologic future. This active state exists independently of the geologists' ability to recognize it. Geologists have used a number of characteristics to identify active faults, such as historic seismicity or surface faulting, geologically recent displacement inferred from topography or stratigraphy, or physical connection with an active fault. However, not enough is known of the behavior of faults to assure identification of all active faults by such characteristics. Selection of the criteria used to identify active faults for a particular purpose must be influenced by the consequences of fault movement on the engineering structures involved.

Attenuation. A decrease in seismic signal strength with distance which depends on geometrical spreading and the physical characteristics of the transmitting medium that cause absorption and scattering.

Attenuation law. A description of the average behavior of one or more characteristics of earthquake ground motion as a function of distance from the source of energy.

b-value. A parameter indicating the relative frequency of earthquakes of different sizes derived from historical seismicity data.

Capable fault. A capable fault is a fault whose geological history is taken into account in evaluating the fault's potential for causing vibratory ground motion and/or surface faulting.

Design earthquake. A specification of the ground motion at a site based on integrated studies of historic seismicity and structural geology and used for the earthquake-resistant design of a structure.

Design spectra. Spectra used in earthquake-resistant design which correlate with design earthquake ground motion values. A design spectrum is typically a broad band specturm having broad frequency content. The design spectrum can be either site-independent or site-dependent. The site-dependent spectrum tends to be less broad band as it depends at least in part on local site conditions.

Design time history. One of a family of time histories used in earthquake-resistant design which produces a response spectrum enveloping the smooth design spectrum, for a selected value of damping.

Duration. A description of the length of time during which ground motion at a site exhibits certain characteristics such as being equal to or exceeding a specified level of acceleration such as 0.05g.

Earthquake hazards. Natural events accompanying an earthquake such as ground shaking, ground failure, surface faulting, tectonic deformation, and inundation which may cause damage and loss of life during a specified exposure time. See earthquake risk.

Earthquake risk. The probability that social or economic consequences of earthquakes, expressed in dollars or casualties, will equal or exceed specified values at a site during a specified exposure time.

Earthquake waves. Elastic waves (P, S, Love, Rayleigh) propagating in the Earth, set in motion by faulting of a portion of the Earth.

Effective peak acceleration. The value of peak ground acceleration considered to be of engineering significance. It can be used to scale design spectra and is often determined by filterng the ground-motion record to remove the very high frequencies that may have little or no influence upon structural response.

Epicenter. The point on the Earth's surface vertically above the point where the first fault rupture and the first earthquake motion occur.

Exceedence probability. The probability (for example, 10 percent) over some exposure time that an earthquake will generate a level of ground shaking greater than some specified level.

Exposure time. The period of time (for example, 50 years) that a structure or facility is exposed to earthquake hazards. The exposure time is sometimes related to the design lifetime of the structure and is used in seismic risk calculations.

Fault. A fracture or fracture zone in the Earth along which displacement of the two sides relative to one another has occurred parallel to the fracture. See Active and Capable faults.

Focal depth. The vertical distance between the earthquake hypocenter and the Earth's surface.

Ground motion. A general term including all aspects of motion; for example, particle acceleration, velocity, or displacement; stress and strain; duration; and spectral content generated by an earthquake, a nuclear explosion, or another energy source.

Intensity. A numerical index describing the effects of an earthquake on the Earth's surface, on man, and on structures built by him. The scale in common use in the United States today is the Modified Mercalli scale of 1931 with intensity values indicated by Roman numerals from I to XII. The narrative descriptions of each intensity value are summarized below.

I. Not felt--or, except rarely under specially favorable circumstances. Under certain conditions, at and outside the boundary of the area in which a great shock is felt: sometimes birds and animals reported

uneasy or disturbed; sometimes dizziness or nausea experienced; sometimes trees, structures, liquids, bodies of water, may sway--doors may swing, very slowly.

II. Felt indoors by few, especially on upper floors, or by sensitive, or nervous persons. Also, as in grade I, but often more noticeably: sometimes hanging objects may swing, especially when delicately suspended; sometimes trees, structures, liquids, bodies of water, may sway, doors may swing, very slowly; sometimes birds and animals reported uneasy or disturbed; sometimes dizziness or nausea experienced.

III. Felt indoors by several, motion usually rapid vibration. Sometimes not recognized to be an earthquake at first. Duration estimated in some cases. Vibration like that due to passing of light, or lightly loaded trucks, or heavy trucks some distance away. Hanging objects may swing slightly. Movements may be appreciable on upper levels of tall structures. Rocked standing motor cars slightly.

IV. Felt indoors by many, outdoors by few. Awakened few, especially light sleepers. Frightened no one, unless apprehensive from previous experience. Vibration like that due to passing of heavy or heavily loaded trucks. Sensation like heavy body of striking building or falling of heavy objects inside. Rattling of dishes, windows, doors; glassware and crockery clink or clash. Creaking of walls, frame, especially in the upper range of this grade. Hanging objects swung, in numerous instances. Disturbed liquids in open vessels slightly. Rocked standing motor cars noticeably.

V. Felt indoors by practially all, outdoors by many or most; outdoors direction estimated. Awakened many or most. Frightened few--slight excitement, a few ran outdoors. Buildings trembled throughout. Broke dishes and glassware to some extent. Cracked windows--in some cases, but not generally. Overturned vases, small or unstable objects, in many instances, with occasional fall. Hanging objects, doors, swing generally or considerably. Knocked pictures against walls, or swung them out of place. Opened, or closed, doors and shutters abruptly. Pendulum clocks stopped, started or ran fast, or slow. Move small objects, furnishings, the latter to slight extent. Spilled liquids in small amounts from well-filled open containers. Trees and bushes shaken slightly.

VI. Felt by all, indoors and outdoors. Frightened many, excitement general, some alarm, many ran outdoors. Awakened all. Persons made to move unsteadily. Trees and bushes shaken slightly to moderately. Liquid set in strong motion. Small bells rang--church, chapel, school, etc. Damage slight in poorly built buildings. Fall of plaster in small amount. Cracked plaster somewhat, especially fine cracks chimneys in some instances. Broke dishes, glassware, in considerable quantity, also some windows. Fall of knickknacks, books, pictures. Overturned furniture in many instances. Move furnishings of moderately heavy kind.

VII. Frightened all--general alarm, all ran outdoors. Some, or many, found it difficult to stand. Noticed by persons driving motor cars. Trees and bushes shaken moderately to strongly. Waves on ponds, lakes, and

running water. Water turbid from mud stirred up. Incaving to some extent of sand or gravel stream banks. Rang large church bells, etc. Suspended objects made to quiver. Damage negligible in buildings of good design and construction, slight to moderate in well-built ordinary buildings, considerable in poorly built or badly designed buildings, adobe houses, old walls (especially where laid up without mortar), spires, etc. Cracked chimneys to considerable extent, walls to some extent. Fall of plaster in considerable to large amount, also some stucco. Broke numerous windows and furniture to some extent. Shook down loosened brickwork and tiles. Broke weak chimneys at the roof-line (sometimes damaging roofs). Fall of cornices from towers and high buildings. Dislodged bricks and stones. Overturned heavy furniture, with damage from breaking. Damage considerable to concrete irrigation ditches.

VIII. Fright general--alarm approaches panic. Disturbed persons driving motor cars. Trees shaken strongly--branches and trunks broken off, especially palm trees. Ejected sand and mud in small amounts. Changes: temporary, permanent; in flow of springs and wells; dry wells renewed flow; in temperature of spring and well waters. Damage slight in structures (brick) built especially to withstand earthquakes. Considerable in ordinary substantial buildings, partial collapse, racked, tumbled down, wooden houses in some cases; threw out panel walls in frame structures, broke off decayed piling. Fall of walls, cracked, broke, solid stone walls seriously. Wet ground to some extent, also ground on steep slopes. Twisting, fall, of chimneys, columns,

monuments, also factory stacks, towers. Moved conspicuously, overturned, very heavy furniture.

IX. Panic general. Cracked ground conspicuously. Damage considerable in (masonry) buildings, some collapse in large part; or wholly shifted frame buildings off foundations, racked frames; serious to reservoirs; underground pipes sometimes broken.

X. Cracked ground, especially when loose and wet, up to widths of several inches; fissures up to a yard in width ran parallel to canal and stream banks. Landslides considerable from river banks and steep coasts. Shifted sand and mud horizontally on beaches and flat land. Changes level of water in wells. Threw water on banks of canals, lakes, rivers, etc. Damage serious to dams, dikes, embankments. Severe to well-built wooden structures and bridges, some destroyed. Developed dangerous cracks in excellent brick walls. Destroyed most masonry and frame structures, also their foundations. Bent railroad rails slightly. Tore apart, or crushed endwise, pipelines buried in earth. Open cracks and broad wavy folds in cement pavements and asphalt road surfaces.

XI. Disturbances in ground many and widespread, varying with ground material. Broad fissures, earth slumps, and land slips in soft, wet ground. Ejected water in large amounts charged with sand and mud. Caused sea-waves ("tidal" waves) of significant magnitude. Damage severe to wood-frame structures, especially near shock centers. Great to dams, dikes, embankments often for long distances. Few, if any

(masonry) structures, remained standing. Destroyed large well-built bridges by the wrecking of supporting piers or pillars. Affected yielding wooden bridges less. Bent railroad rails greatly, and thrust them endwise. Put pipelines buried in each completely out of service.

XII. Damage total--practically all works of construction damaged greatly or destroyed. Disturbances in ground great and varied, numerous shearing cracks. Landslides, falls of rock of significant character, slumping of river banks, etc., numerous and extensive. Wrenched loose, tore off, large rock masses. Fault slips in firm rock, with notable horizontal and vertical offset displacements. Water channels, surface and underground, disturbed and modified greatly. Dammed lakes, produced waterfalls, deflected rivers, etc. Waves seen on ground surfaces (actually seen, probably, in some cases). Distorted lines of sight and level. Threw objects upward into the air.

Liquefaction. The primary factors used to judge the potential for liquefaction, the tranformation of unconsolidated materials into a fluid mass, are: grain size, soil density, soil structure, age of soil deposit, and depth to ground water. Fine sands tend to be more susceptible to liquefaction than silts and gravel. Behavior of soil deposits during historic earthquakes in many parts of the world show that, in general, liquefaction susceptibility of sandy soils decreases with increasing age of the soil deposit and increasing depth to ground water. Liquefaction has the potential of occurring when seismic shear waves having high acceleration and long duration pass through a saturated sandy soil, distorting its granular structure and causing some of

the void spaces to collapse. The pressure of the pore water between and around the grains increases until it equals or exceeds the confining pressure. At this point, the water moves upward and may emerge at the surface. The liquefied soil then behaves like a fluid for a short time rather than as a soild.

Magnitude. A quantity characteristic of the total energy released by an earthquake, as contrasted to intensity that describes its effects at a particular place. Professor C. F. Richter devised the logarithmic scale for local magnitude (M_L) in 1935. Magnitude is expressed in terms of the motion that would be measured by a standard type of seismograph located 100 km from the epicenter of an earthquake. Several other magnitude scales in addition to M_L are in use; for example, body-wave magnitude (m_b) and surface-wave magnitude (M_s), which utilize body waves and surface waves, and local magnitude (M_L). The scale is theoretically open ended, but the largest known earthquakes have had M_s magnitudes near 8.9.

Region. A geographical area, surrounding and including the construction site, which is sufficiently large to contain all the geologic features related to the evaluation of earthquake hazards at the site.

Response spectrum. The peak response of a series of simple harmonic oscillators having different natural periods when subjected mathematically to a particular earthquake ground motion. The response spectrum may be plotted as a curve on tripartite logarithmic graph paper showing the variations of the peak spectral acceleration, displacement, and velocity of the oscillators as a function of vibration period and damping.

Return period. For ground shaking, return period denotes the average period of time or recurrence interval between events causing ground shaking that exceeds a particular level at a site; the reciprocal of annual probability of exceedance. A return period of 475 years means that, on the average, a particular level of ground motion will be exceeded once in 475 years.

Risk. See earthquake risk.

Rock. Any solid naturally occurring, hard, consolidated material, located either at the surface or underlying soil. Rocks have a shear-wave velocity of at least 2,500 ft/sec (765 m/s) at small (0.0001 percent) levels of strain.

Seismic Microzoning. The division of a region into geographic areas having a similar relative response to a particular earthquake hazard (for example, ground shaking, surface fault rupture, etc.). Microzoning requires an integrated study of: 1) the frequency of earthquake occurrence in the region, 2) the source parameters and mechanics of faulting for historical and recent earthquakes affecting the region, 3) the filtering characteristics of the crust and mantle along the regional paths along which the seismic waves travel, and 4) the filtering characteristics of the near-surface column of rock and soil.

Seismic zone. A generally large area within which seismic design requirements for structures are uniform.

Seismotectonic province. A geographic area characterized by similarity of geological structure and earthquake characteristics. The tectonic processes causing earthquakes are believed to be similar in a given seismotectonic province.

Source. The source of energy release causing an earthquake. The source is characterized by one or more variables, for example, magnitude, stress drop, seismic moment. Regions can be divided into areas having spatially homogeneous source characteristics.

Strong motion. Ground motion of sufficient amplitude to be of engineering interest in the evaluation of damage due to earthquakes or in earthquake-resistant design of structures.